Lawrence Berkeley National Laboratory
Recent Work

Title
ELECTROCHEMICAL STUDIES OF THE NiO-,CoO-,Fe0.95O-Na2Si2 O5 GLASS SYSTEMS

Permalink
https://escholarship.org/uc/item/9g09f4qd

Author
Lacy, Alton Monroe.

Publication Date
1969-09-01

eScholarship.org Powered by the California Digital Library
University of California

UCRL-19078

ey. 2

RECEIVED
LAWRENCE
RADIATION LABORATORY

OCT 16 1969

LIBRARY AND
DOCUMENTS SECTION

ELECTROCHEMICAL STUDIES OF THE NiO-, CoO-, $Fe_{0.95}O$-$Na_2Si_2O_5$ GLASS SYSTEMS

Alton Monroe Lacy
(Ph. D. Thesis)

September 1969

AEC Contract No. W-7405-eng-48

TWO-WEEK LOAN COPY

This is a Library Circulating Copy which may be borrowed for two weeks. For a personal retention copy, call Tech. Info. Division, Ext. 5545

LAWRENCE RADIATION LABORATORY
UNIVERSITY of CALIFORNIA BERKELEY

UCRL-19078

ey. 2

DISCLAIMER

This document was prepared as an account of work sponsored by the United States Government. While this document is believed to contain correct information, neither the United States Government nor any agency thereof, nor the Regents of the University of California, nor any of their employees, makes any warranty, express or implied, or assumes any legal responsibility for the accuracy, completeness, or usefulness of any information, apparatus, product, or process disclosed, or represents that its use would not infringe privately owned rights. Reference herein to any specific commercial product, process, or service by its trade name, trademark, manufacturer, or otherwise, does not necessarily constitute or imply its endorsement, recommendation, or favoring by the United States Government or any agency thereof, or the Regents of the University of California. The views and opinions of authors expressed herein do not necessarily state or reflect those of the United States Government or any agency thereof or the Regents of the University of California.

ELECTROCHEMICAL STUDIES OF THE
NiO-, CoO-, $Fe_{0.95}O$-$Na_2Si_2O_5$ GLASS SYSTEMS

Contents

ELECTROCHEMICAL STUDIES OF THE NiO-, CoO-, $Fe_{0.950}$-$Na_2Si_2O_5$ GLASS SYSTEMS

Alton Monroe Lacy

Inorganic Materials Research Division, Lawrence Radiation Laboratory,
and Department of Materials Science and Engineering,
College of Engineering, University of California
Berkeley, California

ABSTRACT

A high temperature galvanic cell of the type

$$Ni/NiO \,||\, electrolyte \,||\, Me/MeO + NS_2(glass)$$

(in which the electrolyte was calcia stabilized zirconia and where Me = Fe, Co, or Ni) has been developed for the measurement of activities and other thermodynamic properties of $Fe_{.950}$, CoO and NiO in sodium disilicate glass over the temperature range 700° to 1100°C. The results indicate that these three oxides show increasing negative deviations from Raoult's Law in the order NiO, CoO, $Fe_{.950}$. The solubility limits of each oxide in sodium disilicate glass have been measured by this technique and presented as liquidus lines on proposed phase diagrams for the binary systems $Fe_{.950}$-, CoO-, NiO-$Na_2Si_2O_5$. Activities of sodium disilicate have been calculated as a function of composition and temperature by integration of the Gibbs-Duhem equation; and sodium disilicate liquidus lines have been determined by equating the calculated activities with the activity of the pure solid sodium disilicate relative to the supercooled liquid. The calculated freezing point depression of sodium disilicate by $Fe_{.950}$ was not coincident with phase diagram data published in the literature, but agreement could be achieved by proposing the existence of at least one previously unreported compound in the ternary

system $FeO-Na_2O-SiO_2$. Partial molar free energies, entropies and enthalpies, as well as free energies, entropies and enthalpies of mixing for the metal oxides and sodium disilicate glass have also been determined.

I. INTRODUCTION

An understanding of the thermodynamics of oxide-silicate systems is necessary for any fundamental interpretation of the physical chemistry of these systems. Some areas of investigation where this need has been clearly demonstrated are:

Bonding. In the development of a glass-metal bond, Pask, Fulrath, Borom, et al.[1-4] have demonstrated that two types of bonds may be formed as the product of chemical reaction--a mechanical bond established by corrosion of the metal substrate with subsequent formation of dendritic precipitates on or near the interface; and a chemical bond formed by the establishment of a thermodynamically continuous structure across the glass-metal interface. They have shown that the condition for formation of the latter is the saturation of the glass (at the interface) with the lowest oxide of substrate metal. When this occurs, an oxygen activity balance exists and strongest bonding of the chemical type occurs. This is, however, a limiting condition, since the theory does not account in a quantitative way for any variation in the bond strength with varying degrees of saturation.

If the degree of chemical bonding is to be related to the imbalance in activity between the oxide of the interfacial metal and that dissolved in the glass, then the need for a thorough knowledge of the activity variation of the oxide in the glass solution as functions of composition, temperature and pressure is obvious.

Similarly, if one is concerned with the redox reactions between glass and metal, predictions of their free energies can only be made if one knows the activities of the components involved. To date, little

effort toward this end has been made in complex silicate systems.

Wetting. Aksay[5] has related the degree of wetting in high temperature MgO-silicate liquid reactions to the activities of components of phases in physical contact. He states, "If the liquid and the solid are not at a thermodynamic equilibrium, a redistribution of the components between the liquid and the solid will take place. An equilibrium contact angle will form only after this thermodynamic equilibrium is achieved..." Humenik and Kingery,[6] as well as Gaidos and Pask,[2] have similarly related changes in interfacial energy to interfacial reactions.

Stability. The stability of glasses with respect to their environment is also greatly affected by the activities of the component oxides. Glasses containing oxides with small free energies of formation become very susceptible to decomposition at low oxygen pressure, high temperatures, or when exposed to reducing atmospheres of other gases. Since many of these glasses have properties of special interest (e.g., coatings, composites, electronics), it is particularly important to define carefully and accurately the limits of chemical stability as functions of composition and environment.

Solid-Liquid Phase Equilibria. Many phase relations within glass-forming systems can also be inferred from thermodynamic activity measurements of the components. Such data can be used to calculate or predict liquidus lines, as well as thermodynamic properties of pure components.

Structure. Structure and bonding are also related to thermodynamic properties of solutions. For example, strong positive deviations from Raoult's Law are associated with a tendency for like atomic or molecular species to associate, tending toward immiscibility; whereas

negative deviations often represent formation of complex molecular or ionic species and tendencies toward compound formation. Knowledge of activities in glass may assist one in inferring possible structural models for these systems, which can be valuable in supporting other theories of structure based upon different type of experimental observations.

Kinetics. The kinetics of reactions in glasses may also be controlled by the activities of the components. For example, the rates of those processes that are diffusion-controlled, such as dissolution of many pure oxides by glass,[7,8] will be dictated not by composition gradients per se, but rather by activity gradients, which, in the case of non-ideal solutions, may be quite different from the former.

It is therefore apparent that a lack of specific knowledge of the thermodynamics of glass systems seriously limits one's ability to predict reactions, confirm theories related to chemical equilibrium, or control rate processes. Every study toward overcoming this void in our knowledge will be small relative to the total need, but valuable toward solving some of the present problems and in building the foundation for further work. It is to this end that the present study has been directed.

This work is specifically motivated by the need to obtain the necessary thermodynamic data to define the activity-composition-temperature relations in the systems NiO-, CoO-, and FeO-$Na_2Si_2O_5$.* Sodium disilicate

---

* FeO will be used throughout the text to represent that iron oxide composition in thermodynamic equilibrium with Fe metal at the temperature of consideration. That is, over the temperature range 700°-1100°C, "FeO" $\cong$ $Fe_{.950}O$.

was initially chosen because it is a glass composed of one glass-forming and one glass-modifying ion, thus facilitating structural interpretations based on O/Si ratios.

These systems have been used in this laboratory for the past decade in studies of bonding, wetting, and diffusion. Therefore, clarification of questions raised in those investigations would require the same systems for this work.

In addition, the heat capacities, entropies and enthalpies of $Na_2Si_2O_5$ (solid and liquid) have been measured by Kelley and King[9,10] and a phase diagram for the binary system FeO-NS_2* is published in the literature.[11]

Those activity measurements on molten silicates reported in the literature have been made principally on binary metal oxide-silica systems and on multicomponent slags. Most of these have been carried out by gas equilibration techniques. The electrochemical method is, however, often preferable to the gas equilibration method because of the wider range of oxygen potentials capable of being measured accurately. (Oxygen pressures in the range of 10^{-20} atm require CO/CO_2 ratios of ~1000/1 at 1000C. This ratio is near the limit of detection for general experimental measurement but the same O_2 pressure is readily and accurately detected with solid oxygen conducting electrolytic cells.) In spite of these advantages, the number of electrochemical studies reported on liquid silicate systems is relatively small.

---

* The following abbreviations will be used throughout this text: N=Na_2O, F=FeO, S=SiO_2, and C=CoO. (That is, NS_2=$Na_2Si_2O_5$.)

Herring[12] and Didtshenko and Rochow[13] have used concentration cells of the type O_2(Pt)/liquid I :: liquid II/O_2(Pt) in order to determine the activities of Na_2O in soda-silica glasses and Na_2O, K_2O and Li_2O in PbO-SiO_2 glasses respectively. In both cases, the cells appeared to function properly (i.e., they were reversible and stable), but there has been no independent verification of the data. This type of cell is generally not suitable for such measurements because of the possibility of errors in emf measurements arising from unknown thermoelectric emfs, liquid junction potentials, poorly defined cell reactions, and indeterminant transference numbers of the conducting species.

Simple formation cells of the type M/MO(in solution)/O_2 are theoretically possible for activity determination in liquid silicates, but practically infeasible because of the unknown magnitude of electronic conductance in most silicate systems at high temperatures. (If not quantitatively accounted for, any electronic transference will short the cell internally, reducing the external emf, and result in erroneous output for activity determination.) This may be particularly true for glasses containing multivalent ions that impart a tendency for semiconduction. Esin[14] has constructed such a cell to measure the activities of FeO in complex silicate melts. The procedure he used was technically difficult and the reversibility of the cells is not known.

Solid electrolytes in which the transference number, (t), of an ion which can take part in the cell reaction is known (preferably 1.0) appear the most feasible for high temperature thermodynamic studies in glasses. Stabilized ZrO_2 and ThO_2 are oxygen ion conductors ($t_{O^{2-}} = 1.0$),

they are inert to corrosion by many liquid silicates, and have been successfully used since 1957[15] for a variety of high temperature thermodynamic investigations on metals and oxides. The reader is referred to Steele[16*] for further reference to these works. A search of the literature has indicated that Matsushita and Goto,[17] H. S. Ray,[18] and Charette and Flengas[19] have carried out the only previous studies of glasses with solid electrolyte cells. Matsushita and Goto, and Charette and Flengas have both investigated the activity of PbO and SiO_2 in binary PbO-SiO_2 glasses at 900-1100°C using a cell of the type Ni/NiO ‖ CSZ[**] ‖ Pb/PbO-SiO_2. Their data corresponds well with that of Richardson and Webb,[20] obtained by other methods. Ray has studied (concurrently with this investigation) activities of Cu_2O, NiO, CoO and Fe_xO in ternary Na_2O-K_2O-SiO_2 solvents; his study apparently has not been published, and only an abstracted summary was available to the writer.

---

* Steel has presented a very concise survey of the development and application of solid electrolytes and high temperature galvanic cells, together with a complete bibliography referring to their uses. Even though such solid electrolyte cells have not been previously used to study complex glass systems, Steele's article is still relevant to this work. Inclusion of any of his material here, however, would simply be repetitious.

** CSZ will be used throughout this thesis to designate "calcia-stabilized zirconia."

II. THEORETICAL

A. General Cell Theory

The method developed for activity determinations utilized a variation of the oxygen concentration cell containing a CSZ electrolyte, similar in principle to those developed first by Kiukolla and Wagner.[15]

$$O_2(p_A) \,\|\, CSZ \,\|\, O_2(p_B) \tag{1}$$

where p_A and p_B represent the oxygen pressures in compartments A and B respectively, and $p_A > p_B$.

Since CSZ is a pure oxygen conductor from p = 1 atm to p = 10^{-20} atm, we may represent the process of electrochemical oxygen transfer as follows:

Compartment A: $$\frac{1}{2}\, O_2(p_A) + 2e^- = O_A^{2-} \tag{2}$$

In electrolyte: $$O_A^{2-} \rightarrow O_B^{2-} \tag{3}$$

Compartment B: $$O_B^{2-} = \frac{1}{2}\, O_2(p_B) + 2e^- \tag{4}$$

The overall cell reaction thus becomes: $\frac{1}{2}\, O_2(p_A) = \frac{1}{2}\, O_2(p_B)$.

The free energy for transfer of one mole of oxygen from p_A to p_B may be expressed as

$$\Delta F = RT \ln \frac{p_B^{1/2}}{p_A^{1/2}} \tag{5}$$

From the relation

$$\Delta F = nF\varepsilon \tag{6}$$

where n = the number of electrons transferred

F = Faraday's Constant - 23011 cal/volt

ε = measured cell output voltage,

we may relate the cell voltage to the oxygen pressures by:

$$\varepsilon_{measured} = \frac{-RT}{2nF} \ln \frac{p_B}{p_A} . \tag{7}$$

If in either compartment we fix the oxygen pressure either directly or by equilibration of a metal and its oxide, the unknown pressure may be determined by Eq. (7).

When a mixture of solid metal A and its oxide AO are placed in compartment A, an equilibrium oxygen pressure is established, which is related to the standard free energy of formation of AO, according to reaction (8).

$$A(s) + \frac{1}{2} O_2 = AO(s) \tag{8}$$

The free energy for this reaction may be written

$$\Delta F_{AO} = \Delta F^{\circ}_{AO} + RT \left(\ln a_{AO} - \ln p_A^{1/2}(O_2)\right); \tag{9}$$

at equilibrium $\Delta F_{AO} = 0$, and

$$-\Delta F_{AO} + RT \ln p_A^{1/2}(O_2) = RT \ln a_{AO}. \tag{10}$$

In compartment B, we place a mixture of metal B and its oxide BO. The half cell reaction for this compartment may be expressed as

$$BO(s) = B(s) + \frac{1}{2} O_2 \tag{11}$$

and

$$\Delta F_{BO} = \Delta F^\circ_{BO} + RT \left(\ln p_B^{1/2}(O_2) - \ln a_{BO}\right). \tag{12}$$

At equilibrium $\Delta F_{BO} = 0$, and

$$-\Delta F^\circ_{BO} - RT \ln p_B^{1/2}(O_2) = -RT \ln a_{BO}\ . \tag{13}$$

The overall cell reaction may be expressed as

$$A + BO = AO + B; \tag{14}$$

summing (10) and (13)

$$-(\Delta F^\circ_{AO} + F^\circ_{BO}) + RT \ln \frac{p_A^{1/2}(O_2)}{p_B^{1/2}(O_2)} = RT \ln \frac{a_{AO}}{a_{BO}} \tag{15}$$

If $a_{BO} = 1$, we find from (5), (6) and (7),

$$-nF\ (\varepsilon^\circ - \varepsilon_{cell}) = RT \ln a_{AO}. \tag{16}$$

In the event that A and B are the same metal, Eq. (16) reduces to

$$-nF\varepsilon_{cell} = RT \ln a_{AO} \ . \tag{16b}$$

The emf output of the cell will give directly the activity of the AO in solution, relative to the solid standard state, by the application of Eq. (16b).

$$a_{AO} = \exp\left(\frac{-nF}{RT} \varepsilon_{cell}\right) \ . \tag{17}$$

B. Calculation of the Activity of a Second Binary Component When the Activity of One is Known

In a two-component system, the activity of the second component (BO) can now be determined by calculating the activity coefficient, γ_{BO} (where $\gamma_{BO} \equiv a_{BO}/N_{BO}$), from integration of the Gibbs-Duhem equation

$$N_{AO} \ d \ln \gamma_{AO} + N_{BO} \ d \ln \gamma_{BO} = 0 \ . \tag{18}$$

The $\ln \gamma_{BO}$ can be directly determined from the integration

$$\ln \gamma_{BO} = - \int_{N_{BO}=1}^{N_{BO}=N_{BO}} \frac{N_{AO}}{N_{BO}} \ d \ln \gamma_{AO} \tag{19}$$

Darken and Gurry have provided an alternate integration by defining a function,

$$\alpha_{AO} = \frac{\ln \gamma_{AO}}{N_{BO}^2} \tag{20}$$

Differentiation of $\ln \gamma_{AO} = \alpha_{AO} N_{BO}^2$ and substitution into (18) results in the expression

$$\ln \gamma_{BO} = -\alpha_{AO} N_{AO} N_{BO} - \int_{N_{BO}=1}^{N_{BO}=N_{BO}} dN_{BO} \tag{21}$$

This may be evaluated graphically.

C. Partial Molar and Integral Thermodynamic Functions

If the cell reaction is written

$$AO(\text{solid})_{a=1} \rightarrow AO(\text{glass})_{a<1} \tag{22}$$

the free energy of this reaction (ΔF_{rxn}) may be expressed

$$\Delta F_{rxn} = RT \ln a_{AO(\text{glass})}. \tag{16c}$$

The free energy expressed in Eq. (16c) is recognized as the partial molar free energy ($\overline{\Delta F}_{AO}$) of the oxide in solution. Similarly, having obtained a_{BO} from either Eqs. (19) or (21), the partial molar free energy for the second component may be found from

$$\overline{\Delta F}_{BO} = RT \ln a_{BO}. \tag{16d}$$

The integral free energy of mixing (or formation) of the solution from its components according to the reaction

$$AO + BO \rightarrow ABO_2(\text{glass}) \tag{23}$$

may be obtained from

$$\Delta F_{mix} = N_{AO}\,\overline{\Delta F}_{AO} + N_{BO}\,\overline{\Delta F}_{BO} \; . \tag{24}$$

The partial molar entropies may be calculated from the relation

$$dF = - SdT + VdP \tag{25}$$

where, at constant pressure

$$\left(\frac{\partial \overline{\Delta F}}{\partial T}\right)_p = - \overline{\Delta S} \; . \tag{26}$$

The partial molar entropies for component AO (Eq. (22)) may then be obtained from the slope of the cell voltage vs. temperature according to Eqs. (16b), (16d), and (26).

$$-nF\left(\frac{\partial \varepsilon}{\partial T}\right)_p = - \overline{\Delta S}_{AO} \equiv - \Delta S_{\text{cell reaction}} \; . \tag{27}$$

The partial molar enthalpy of component AO is simply the heat of the cell reation (22), and may be found by either of the following relations:

$$\overline{\Delta H}_{AO} = \overline{\Delta F}_{AO} + T\overline{\Delta S}_{AO} = - nF \left[\varepsilon - T\left(\frac{\partial \varepsilon}{\partial T}\right)_p\right] \tag{28a}$$

or

$$\frac{\partial\left(\frac{\overline{\Delta F}_{AO}}{T}\right)_p}{\partial\left(\frac{1}{T}\right)} = \overline{\Delta H}_{AO}, \text{ assuming } \overline{\Delta S}_{AO} \text{ constant} \tag{29a}$$

with temperature. The integral entropy of mixing may be found by applying the equation

$$\Delta S_{mix} = N_{AO}\overline{\Delta S}_{AO} + N_{BO}\overline{\Delta S}_{BO}, \tag{30}$$

where $\overline{\Delta S}_{BO}$ has been calculated from (16d) and (26).

The integral enthalpy is readily determined from

$$\Delta H_{mix} = \Delta F_{mix} + T\Delta S_{mix} , \tag{31}$$

$$\frac{\partial\left(\frac{\Delta F_{mix}}{T}\right)_p}{\partial\left(\frac{1}{T}\right)} = \Delta H_{mix} \tag{29b}$$

or

$$\Delta H_{mix} = N_{AO}\,\overline{\Delta H}_{AO} + N_{BO}\,\overline{\Delta H}_{BO} . \tag{28b}$$

D. Activities Referred to Pure Supercooled Liquid Standard State

If one wishes to compare calculated partial and integral molar functions with these same quantities for ideal molecular solutions, the activities of AO in solution must be referred to the pure supercooled liquid AO, by adding the appropriate thermodynamic quantities for Eq. (32).

$$AO\ (\text{supercooled liquid}) \rightarrow AO\ (\text{solid})_{a<1} \qquad (32)$$

to those same quantities for Eq. (22). By comparison of the resulting sum with the same functions for ideal solutions, excess quantities may be readily determined.

If the heat capacities of both the pure solid and the supercooled liquid are known, as well as the heat of fusion, the free energy for reaction (32) at any temperature may be found by integration of

$$\frac{\Delta F}{T} = -\int_{T_1}^{T_2} \frac{\int_{T_1}^{T_2} \Delta C_p dT}{T_2}\, dT = -R \ln \frac{a_{solid}}{a_{liquid} \equiv 1} = -R \ln K \qquad (33)$$

from which the activity of the pure solid relative to the pure supercooled liquid, (K), may be found.

If heat capacity data are not available, K_{AO} may be related to the heat of fusion (ΔH_F) of AO by the relation

$$-\ln K_{AO} = \frac{\Delta H_F}{RT}\left(1 - \frac{T}{T_F}\right) \qquad (34)$$

where T_F = the melting temperature (°K) of pure AO. This assumes that the heat capacities of the pure solid and supercooled liquid are equal below T_F. This is generally a good first approximation. (See appendix D).

The solubility limits of both components AO and BO may be found by the points of intersection of plots of the measured activities and the activities of the pure solid (when both are referred to the same standard state) vs. temperature.

III. EXPERIMENTAL PROCEDURE

A. Glass Production

The NiO glass was prepared by mechanically mixing weighed quantities of Baker's analyzed NiO with sodium disilicate glass* obtained from the Philadelphia Quartz Company. Each mixture was then heated in a Pt crucible at 1200°C for 12 hours in air to insure homogeneity. The CoO-NS_2 glass was prepared in a similar fashion, the CoO being prepared before mixing from vacuum decomposition of chemically pure Co_3O_4 powder at 1000°C.

The $Fe_{0.95}O$-NS_2 glasses were prepared by adding Fe_2O_3 + Fe in the proper ratio to give hypothetically stoichiometric FeO. This three-component mixture (Fe + Fe_2O_3 + NS_2) was packed in Fe crucibles and placed in a vacuum quench furnace. After evacuation to $\sim 10^{-4}$ torr, the furnace was back filled with purified argon, the glass batch lowered into the hot zone and held in static argon for 12 hours at 1000°C. Upon quenching, the resulting glass was characteristically blue at low total FeO concentrations and greenish-grey with higher ($\sim$30 weight %) amounts. There was also a trace of residual Fe metal on the surface, as would be expected from the reaction

$$Fe + Fe_2O_3 \rightarrow 3Fe_{.95}O + .15\ Fe\ . \qquad (35)$$

All glasses were ground to powder in an Al_2O_3 mortar just prior to use in the individual cell experiments.

---

* Trade designation: SS-C (powder).

B. Cell Construction

A schematic diagram of the experimental set-up is illustrated in Fig. 1. The outer electrode was formed by a twisted single wrap of 20 mil Pt wire around the outside of the calcia stabilized zirconia tube;* the inner electrode was formed by wrapping 20 mil wire in helical fashion (2 times) around a glass rod to form a coil slightly larger than the inside diameter of the CSZ tube. This was then bent so that the free end extended out along the center line of the tube. The coil was then "spring-fitted" on the inside and forced to the bottom with a piece of glass tubing, making a tight fit to the inside. (This snug fit was necessary for successful operation of the cell.) Approximately 1-1/2 grams of glass powder was mixed with about 1/3 gram of the appropriate pure metal powder and put into the tube to a level just above the upper coils. A short piece of mullite thermocouple protection tubing was placed over the exposed electrode inside the tube, resting on a bend in the wire just above the glass level, so as to avoid contact of the CSZ with the wire. A boron nitride plug with a hole just large enough to accommodate the protruding mullite tube was placed over the upper end of the CSZ tube to secure the electrode position and to prevent external material from falling into the glass at any time. The assembly was then seated in a Pt support basket containing a Coors CN-10 cylindrical Al_2O_3 (AD998) crucible containing a mixture of powdered Ni metal (certified chemically pure by the A. J. Mackay Co., Inc.) and NiO powder (Bakers' analyzed reagent). Connection from the 20 mil Pt electrodes to the 20

---

* Obtained from Zircoa, Solon, Ohio.

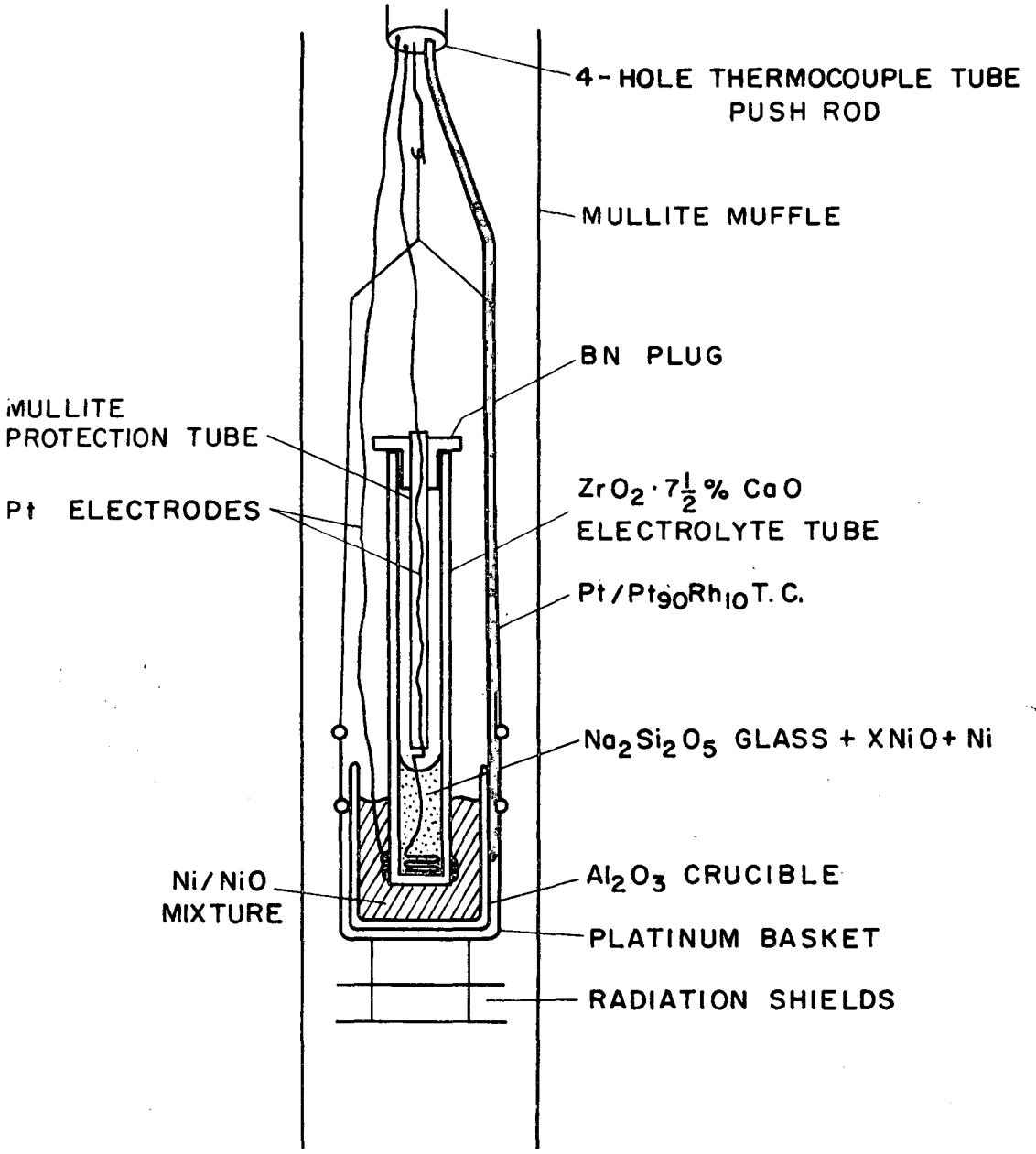

Figure 1. Schematic diagram of the experimental cell assembly.

mil Pt extension leads were made with 8 mil Pt wire. This procedure allowed for easy connection and disconnection without physically upsetting the packed powder. Additional powder was then added and tightly packed around the tube.

After sealing in a resistance wound furnace, the system was evacuated to approximately 10^{-5} torr (2×10^{-8} atm O_2) and filled with argon just before lowering the cell from the cool quench zone into the hot zone. It was found that the duration of evacuation (which varied from 1 hr to 2 days) had no effect on the cell performance. Measurements of cell output were begun about one hour after lowering. This seemed to be sufficient time for thermal equilibration and stabilization of the emf. The cell and thermocouple outputs were recorded on a high impedance Honeywell Electronik 19 potentiometric recorder. The thermocouples were Pt-$Pt_{90}Rh_{10}$. Chromel-alumel couples were tried, but found unsatisfactory in the reducing atmosphere of the cell environment.

The residual oxygen remaining in the furnace after filling with argon almost certainly reacted with the exposed Ni metal of the outer electrode compartment, reducing the O_2 pressure in the system to the equilibrium pressure of an Ni/NiO mixture. Any possible pickup of residual oxygen by the glass in this static environment would result in inconsequential alterations of the metal oxide content of the glass.

Polarization and reversibility of the cell were checked for either by short circuiting the cell for a few seconds with constant emf monitoring or by imposing briefly an emf (with a potentiometer) across the cell. All cells returned promptly to their original emf when the disturbance was eliminated.

Equilibrium was verified both by holding the cells isothermally for long periods of time (2-3 days) without evidence of drift of the emf output and by continuously monitoring the cell voltage as the temperature was raised and lowered. If in a cooling-heating cycle, the electrochemical equilibrium is not achieved as fast as the temperature changes, at any selected temperature one would expect to see higher emf values upon cooling than upon subsequent heating (i.e., a hysteresis effect of emf vs. temperature). Such was not the case with these cells. It was found that continuous cycling gave a reproducibility for any cell to ± 1 mv irrespective of the rate of cycling. The fastest rate of furnace cooling or heating was approximately 1°C/min. At faster rates, it was found that the temperature differences between the cell and furnace wall exceeded ± 1°C. Generally, the cooling rates were of the order of to .5°C/min. All cells were monitored over at least one full cycle of cooling and heating.

At temperatures above 1000°C, stability and reproducibility became difficult to obtain, due to a tendency for downward drift of the emf of all cells. This behavior is characteristic of some side reaction within the cell not associated with the cell reaction. It was not possible to define the specific nature of the drift, but it may be due to attack of the CSZ electrolyte by the glass, thus altering the metal oxide activity in solution. Such a downward drift would be characteristic of the introduction of oxygen into the glass. Since this drift was similarly noticed in a special cell designed to separate completely the electrode compartments from each other, it is felt not to be the result of O_2

transfer from the Ni/NiO reference electrode to the glass through the surrounding atmosphere, but rather to some other undefined reaction. This reaction could be dependent on increased oxygen diffusion through the electrolyte at high temperatures since microscopic examination of a sectioned cell showed no evidence of chemical reactions. Consequently, data reported for 1100°C are taken from extrapolations of ε vs. T curves on the assumption that the partial molar entropy of the dissolved oxide does not change with temperature.

IV. RESULTS

A. The System FeO-NS_2

Experimental studies of the activity of FeO in sodium disilicate glass were made in a cell of the type

$$Ni/NiO \parallel CSZ \parallel Fe/FeO_{a<1} + NS_2.$$

Ni/NiO was used as the reference electrode because its standard free energy of formation, hence its equilibrium oxygen pressure, has been established very accurately. It is perhaps the most common reference electrode used in solid electrolyte galvanic oxygen cells. The standard free energies of formation of both NiO and FeO were taken from the compiled data of Elliot and Gleiser.[21] Ray[22] has reviewed the work of a large number of investigators and concluded that Elliot and Gleiser's tables are more consistent with the accumulated data than values from any one other source and, therefore, should be preferred over others.*

The overall cell reaction may be written

$$Fe + NiO = Ni + FeO_{a<1} . \qquad (36)$$

By adding the free energy of the reaction

$$FeO(s) + Ni(s) = NiO(s) + Fe(s) \qquad (37)$$

---

* A cell of the type Ni/NiO ‖ CSZ ‖ Fe/FeO was also set up, and the output found to agree to ± 1 mv with the theoretical output calculated from the tabulated data of Elliot and Gleiser.

to the measured free energy ($-nF\varepsilon$) of the cell reaction, one obtains the free energy of reaction

$$FeO(s)_{a=1} = FeO(\text{in glass})_{a<1} \tag{38}$$

The activity of the dissolved FeO(a^*_{FeO})† relative to the solid standard state may be calculated from Eq. (17).

The isocompositional cell output (in volts) vs. temperature is presented in Fig. 2. Each line represents an average of at least two trials for the particular glass under investigation. The variation of calculated activity with temperature for each composition is given in Fig. 3. The isothermal dependence of activity (a^*_{FeO}) on composition may be seen in Fig. 4. For the sake of clarity, error limits are not shown in Figures 3 and 4, but they may be readily calculated from Eq. (17), assuming an average uncertainty in cell output of ± 2 mv.

The activity of the oxide relative to the pure liquid standard state may be obtained by multiplying the measured activity by the activity of the pure solid referred to the pure liquid standard state--see Eqs. (33) and (34), and Appendix F. Activities referred to both standard states are listed in Appendix A, and a plot of activity (referred to pure liquid) vs. composition is given in Fig. 5.

---

† a* will be used in the remainder of the text to designate activities of oxides relative to the pure solid standard state; a** will designate activities referred to the pure supercooled liquid standard state.

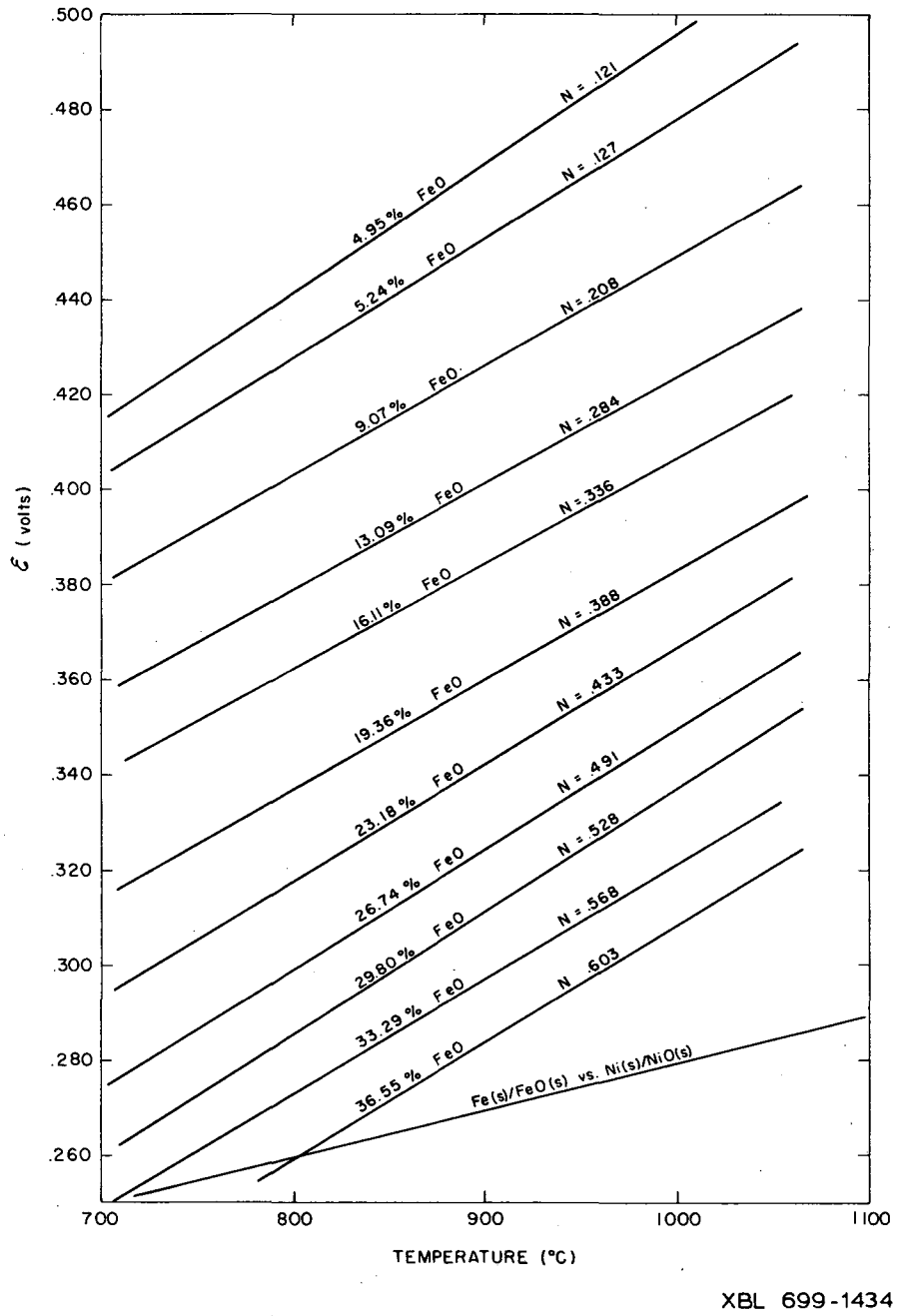

Figure 2. Isocompositional cell output for $FeO-NS_2$ glasses as a function of temperature.

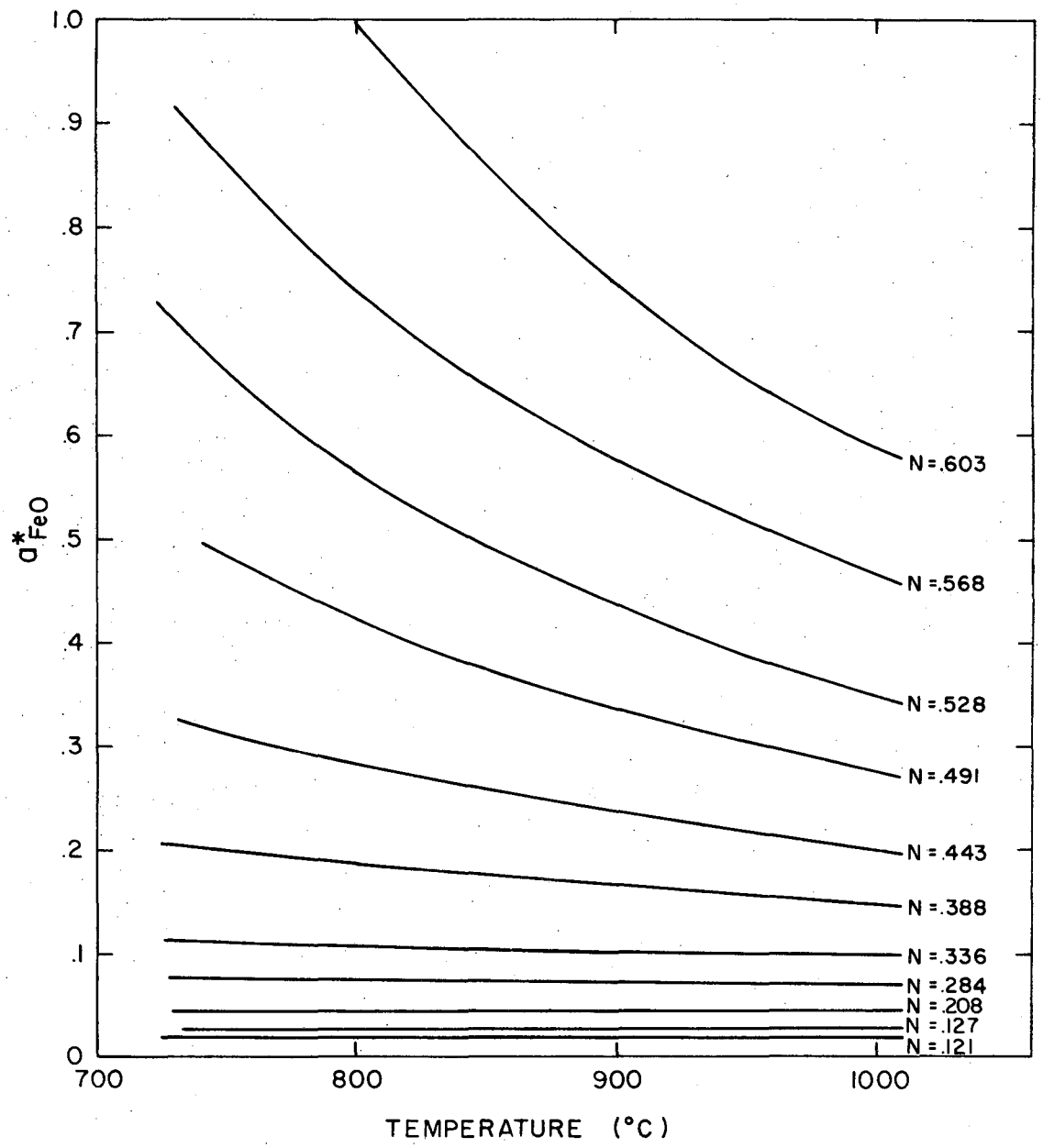

XBL 699-1398

Figure 3. Variation in the activity of FeO (referred to the pure solid standard state) with temperature for each composition studied.

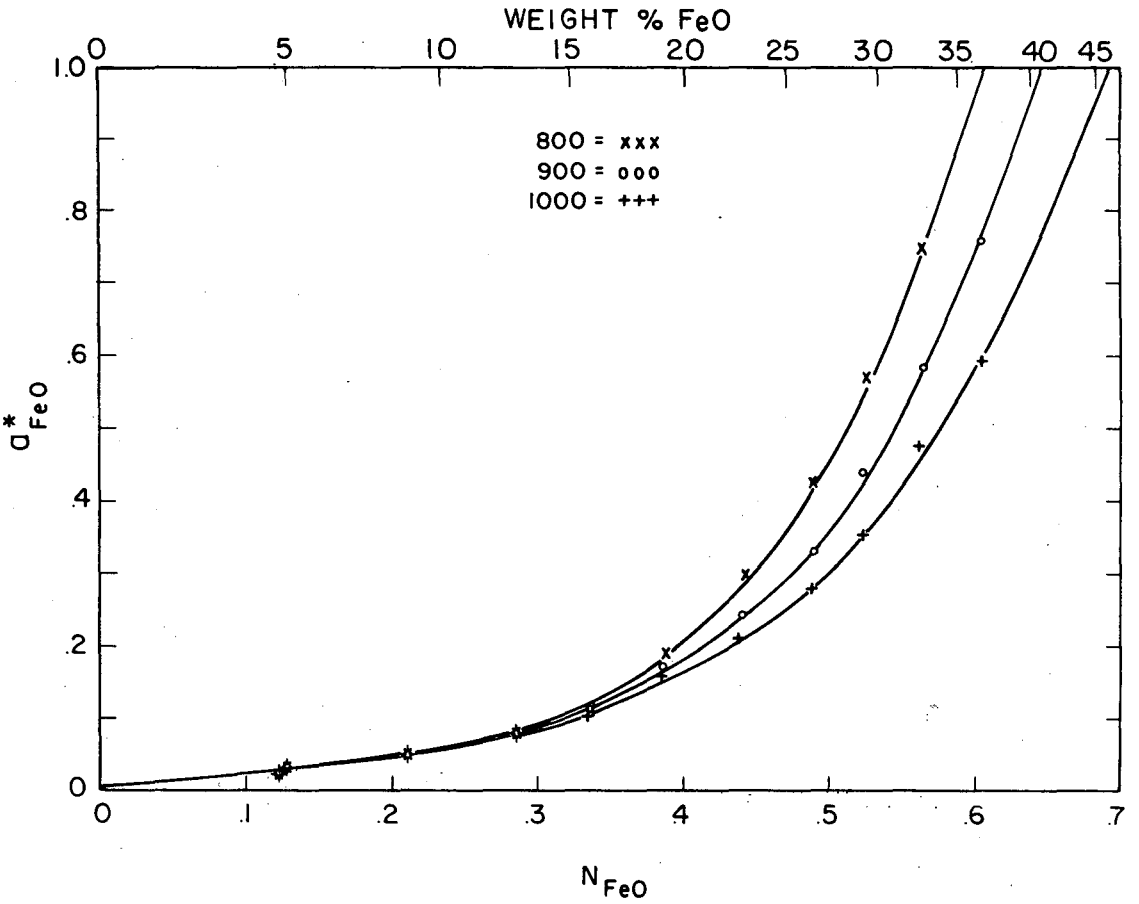

XBL 699-1399

Figure 4. Isothermal dependence of FeO activity (referred to the pure solid standard state) on composition.

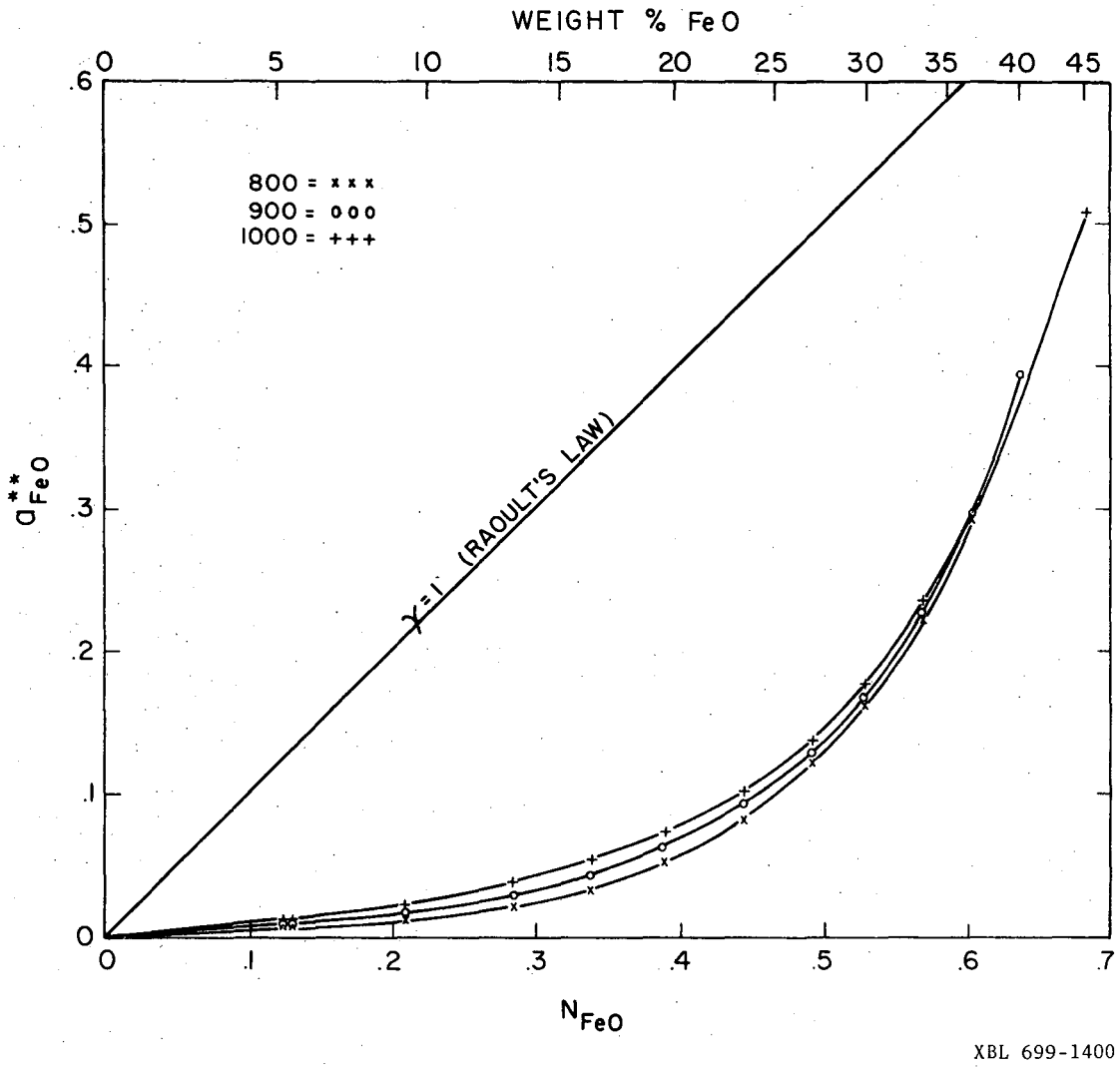

Figure 5. Estimated isothermal dependence of the FeO activity (referred to pure supercooled liquid FeO) on composition.

The activity of NS_2 relative to liquid NS_2 was found by graphical integration of the Gibbs-Duhem equation. A plot of N_{FeO}/N_{NS_2} vs ln γ^*_{FeO} is given in Fig. 6, and the activities of NS_2 calculated from this method using Eq. (19) are shown in Fig. 7 and tabulated in Appendix A. By determination of the temperature where the activity of the dissolved oxide is equal to the pure oxide (either by measuring directly when the output emf for the cell reaction (37) equals zero, or by extrapolating the activity vs composition curves to the activity of the pure oxide), one can readily ascertain the FeO liquidus line for the binary system. The FeO liquidus obtained in this investigation is shown in Fig. 13 and is seen to be in good agreement with that obtained by quenching methods of Ibrahim and Carter.[11]

The partial molar free energy of the dissolution of solid FeO in NS glass is obtained directly from the temperature variation of the partial molar free energy of the cell reaction by using Eq. (27). The partial molar free energy for the reaction

$$NS_2(\text{pure liquid}) = NS_2(\text{glass}) \qquad (39)$$

may be similarly obtained from Eq. (16d) using activity values calculated from the Gibbs-Duhem integration. The integral free energy of mixing solid FeO with liquid NS_2 according to reaction

$$xFeO(\text{solid}) + yNS_2(\text{liquid}) = xFeO \cdot yNS_2(\text{glass}) \qquad (40)$$

is then calculated from Eq. (24). These data are presented in Appendix A and graphically illustrated in Fig. 8. The partial molar entropies

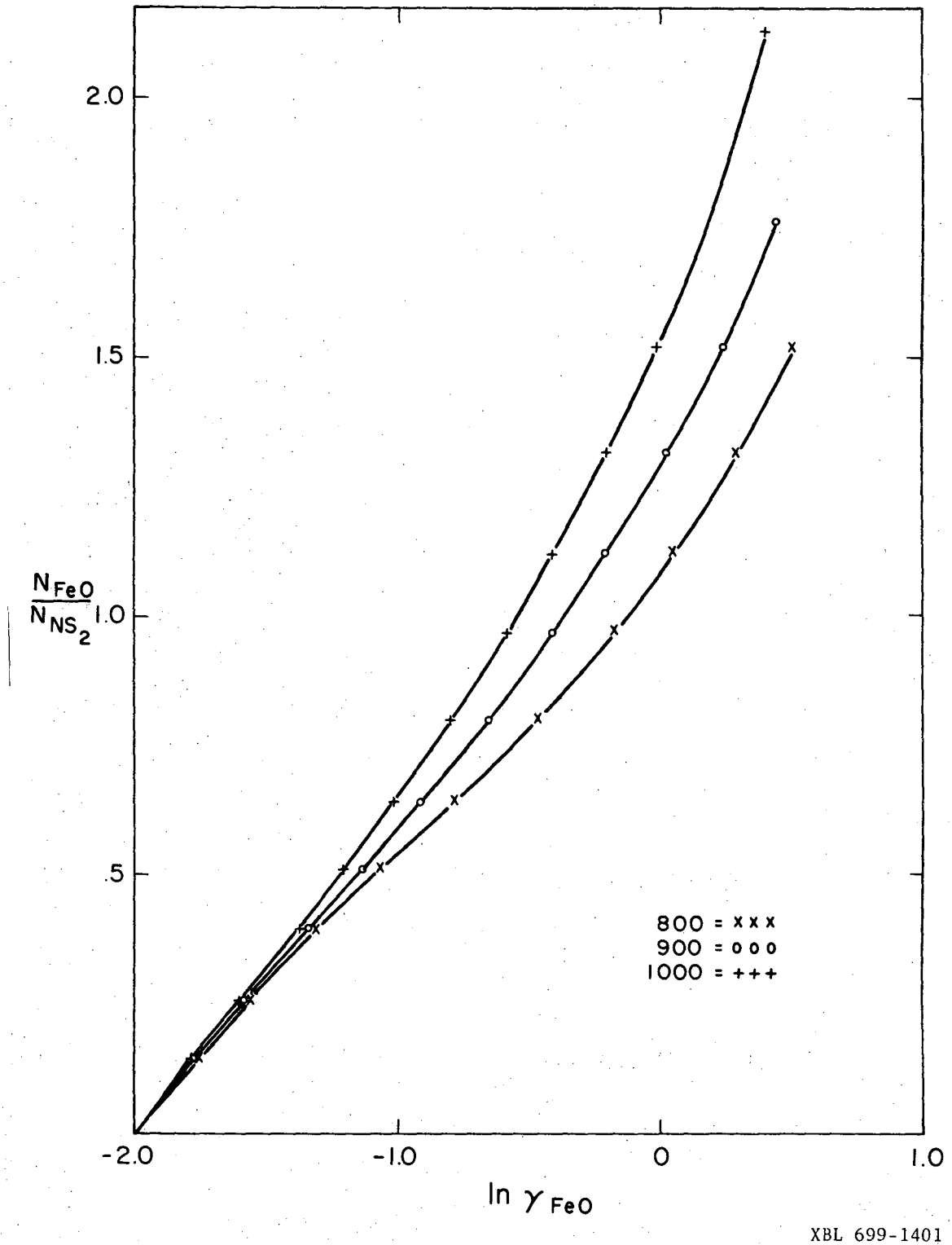

Figure 6. Gibbs-Duhem integration plot for the determination of the activity of NS_2.

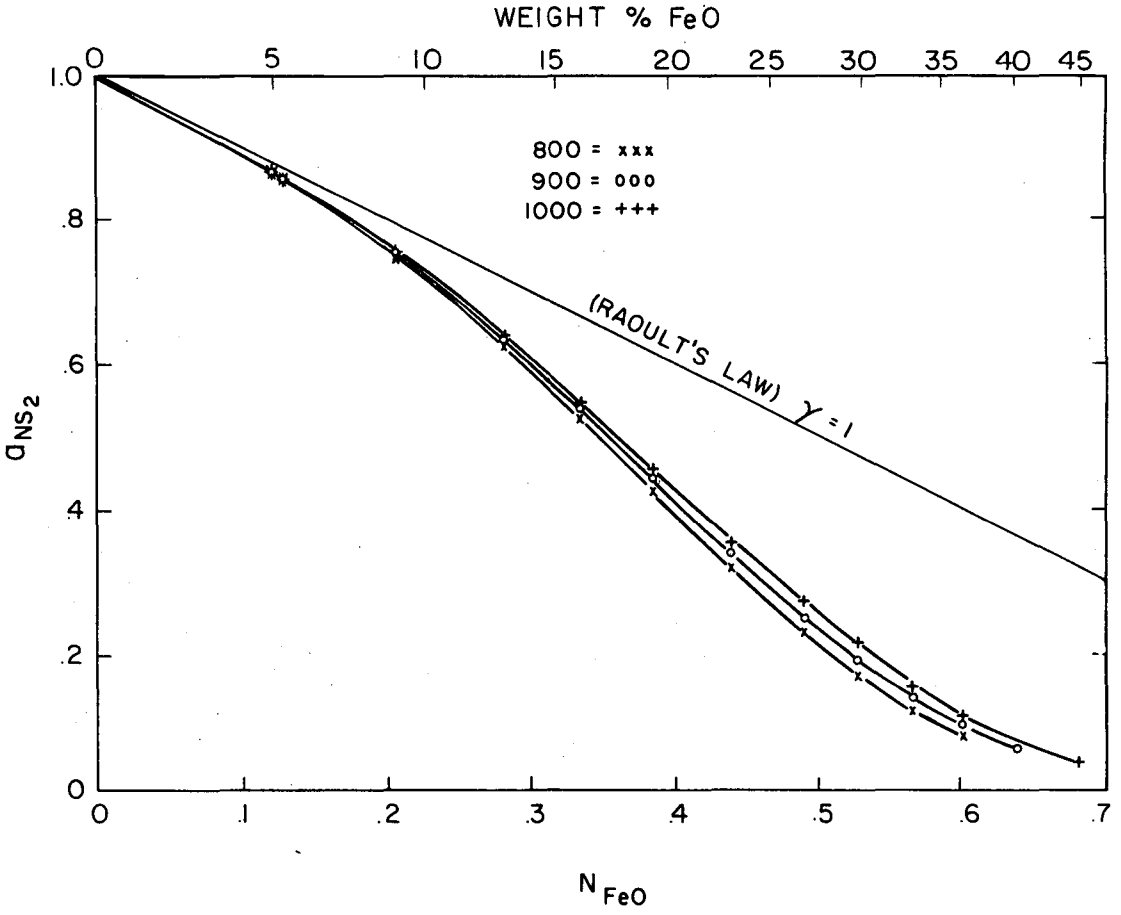

Figure 7. Isothermal activities of NS_2 (referred to liquid standard state) calculated from Gibbs-Duhem integration.

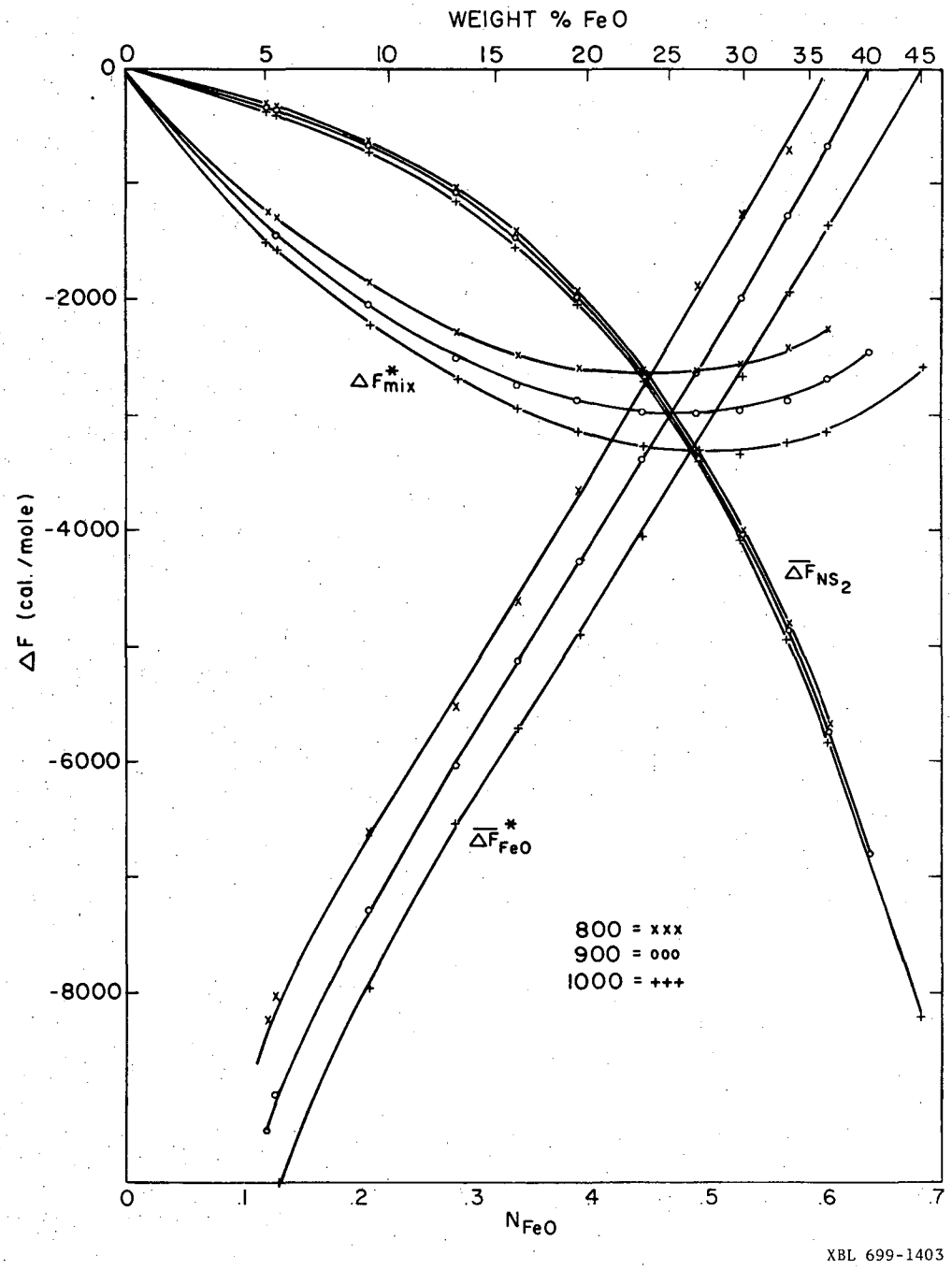

Figure 8. Free energy plots for FeO (referred to the pure solid standard state); NS_2 (referred to the pure liquid).

($\overline{\Delta S}^{*}_{FeO}$, $\overline{\Delta S}_{NS_2}$) and the integral entropy of mixing (ΔS^{*}_{mix}) as well as the partial molar enthalpies ($\overline{\Delta H}^{*}_{FeO}$, ΔH_{NS_2}) and the enthalpies of mixing (ΔH^{*}_{mix}, ΔH^{**}_{mix}) are given in Figs. 9 and 10.

The thermodynamic functions pertaining to the mixing of the supercooled hypothetical liquid with pure liquid NS_2 must take into account the reaction

$$FeO(\text{supercooled liquid}) = FeO(\text{solid}) \qquad (41)$$

by adding the partial molar functions for the above reaction to those calculated for reaction (40).

Since the heat capacity data for the supercooled liquid FeO is not available, the activity of the pure solid FeO relative to the pure liquid standard state was estimated from the relation

$$-\ln(a_s/a_l \equiv 1) = \frac{\Delta H_f}{RT}\left(1 - \frac{T}{T_f}\right) \qquad (34)$$

where H_f = 8500 cal/mole and T_f = 1367°C (1650°K). Eq. (34) results from integration of the van't Hoff equation

$$\frac{d \ln K}{dT} = \frac{\Delta H}{RT} \qquad (42)$$

where K is the equilibrium constant ($a_{solid}/a_{liquid} \equiv 1$) for reaction (41), by assuming that the heat capacities of the solid and supercooled liquid are equal over the temperature interval of consideration, partial and

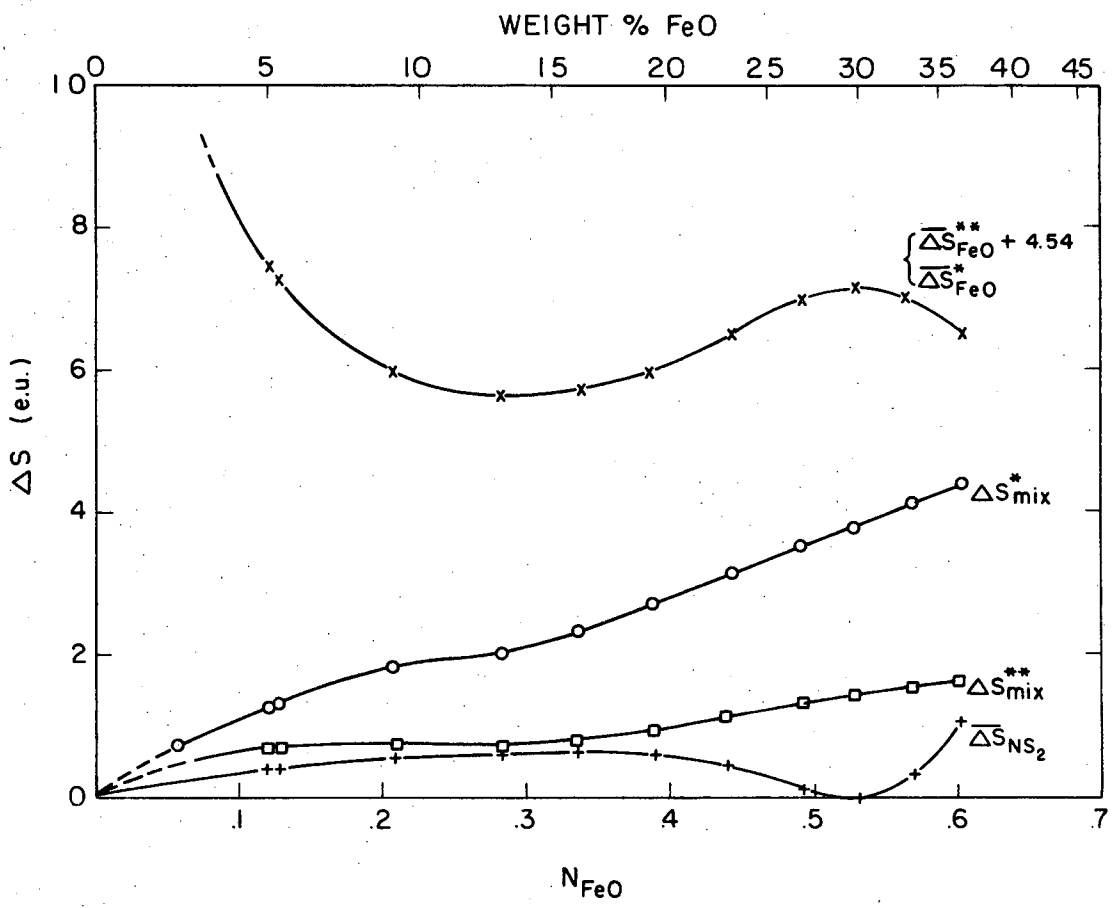

XBL 699-1404

Figure 9. Entropy plots for FeO and NS_2.

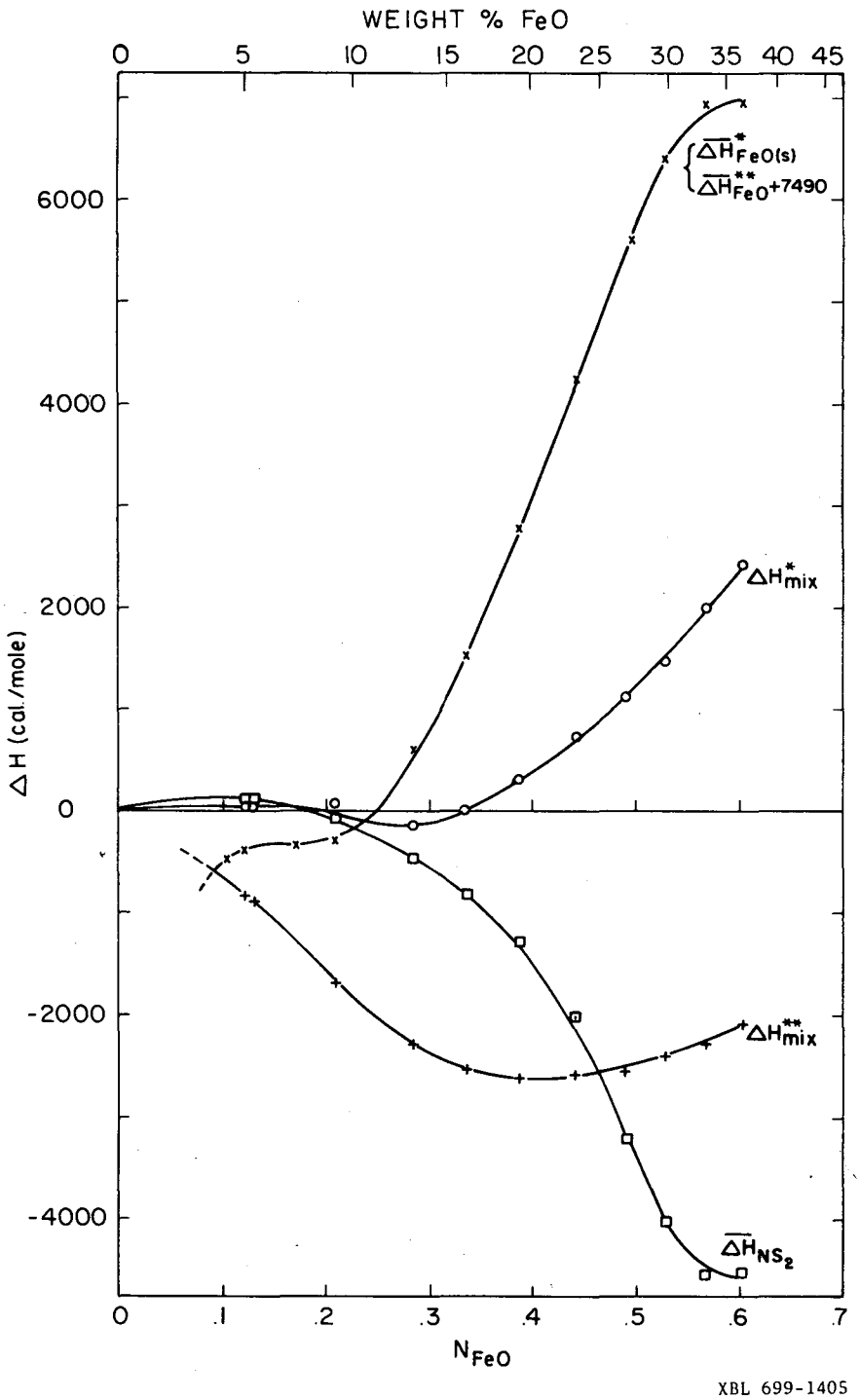

Figure 10. Enthalpy plots for FeO and NS_2.

integral thermodynamic functions for the reaction

$$xFeO(\text{supercooled liquid}) + yNS_2(\text{liquid}) = xFeO \cdot yNS_2(\text{liquid glass}) \quad (43)$$

may be calculated from the combination of the measured data with that data calculated for reaction (41). These ($\overline{\Delta F}^{**}_{FeO}$, ΔS^{**}_{mix}; $\overline{\Delta H}^{**}_{FeO}$, ΔH^{**}_{mix}; $\overline{\Delta F}^{**}_{FeO}$, ΔF^{**}_{mix}) are presented in Figs. 9, 10, and 11 respectively.

The NS_2 liquidus was found by determining the temperature of intersection of the NS_2 activity vs temperature lines for each glass composition with plots of the activity of solid NS_2 (referred to pure liquid) vs temperature calculated from the free energy change of the reaction

$$NS_2(\text{solid}) = NS_2(\text{liquid}) \quad (44)$$

by integrating the heat capacity data of Kelley, according to Eq. (33). These data are presented in Fig. 12, and both liquiduses are plotted on a proposed phase diagram in Figs. 13 and 38. (See page 69 for a discussion of Fig. 38.)

B. The System CoO-NS_2

Experimental determinations of the activity of CoO in NS_2 glass were made in a cell of the type

$$Ni/NiO \parallel CSZ \parallel Co/CoO_{a<1} + NS_2 \ .$$

Initially, a mixture of Co/CoO was tried as the reference electrode

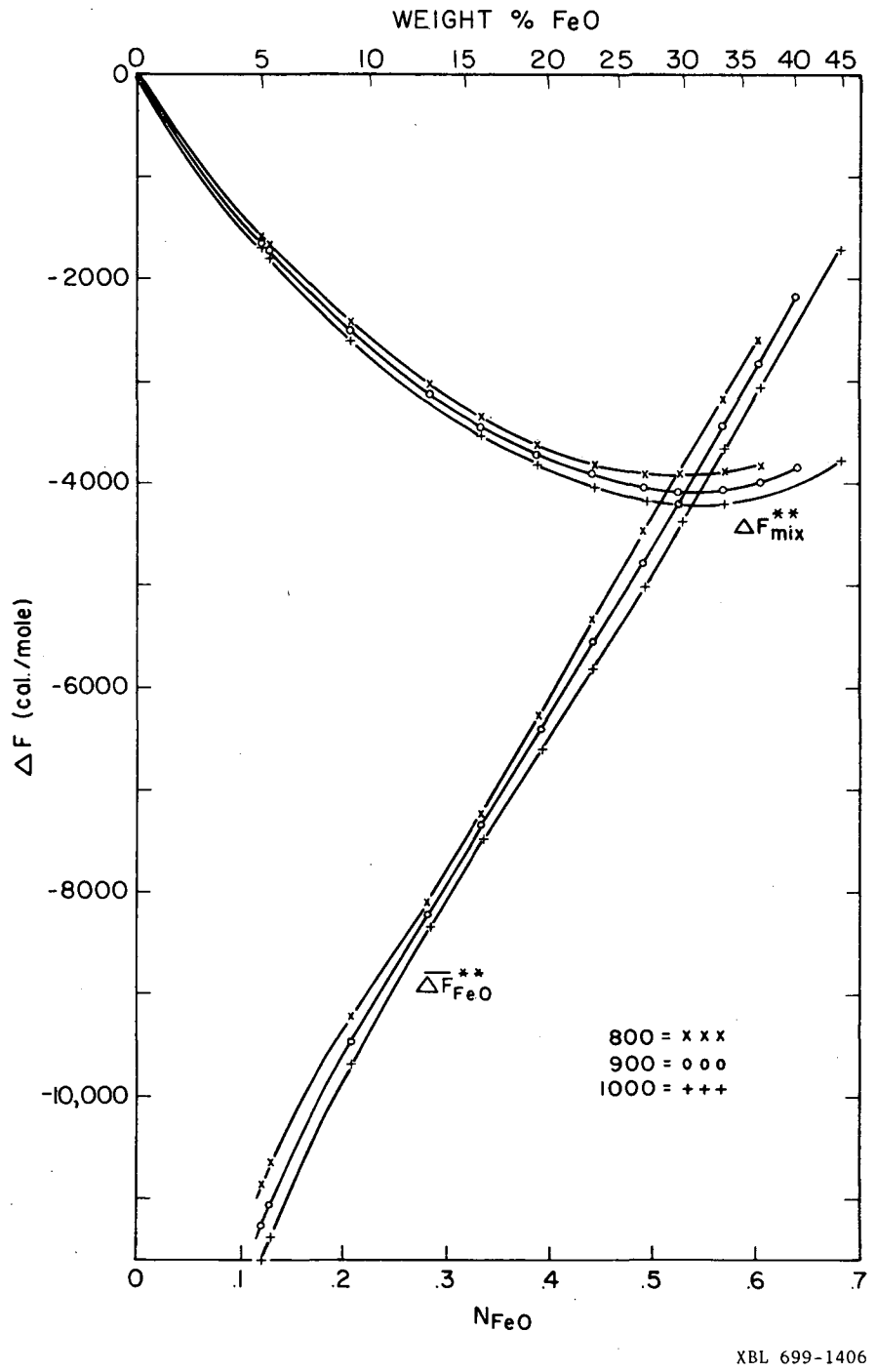

Figure 11. Estimated free energy plots for FeO (referred to the pure supercooled liquid standard state).

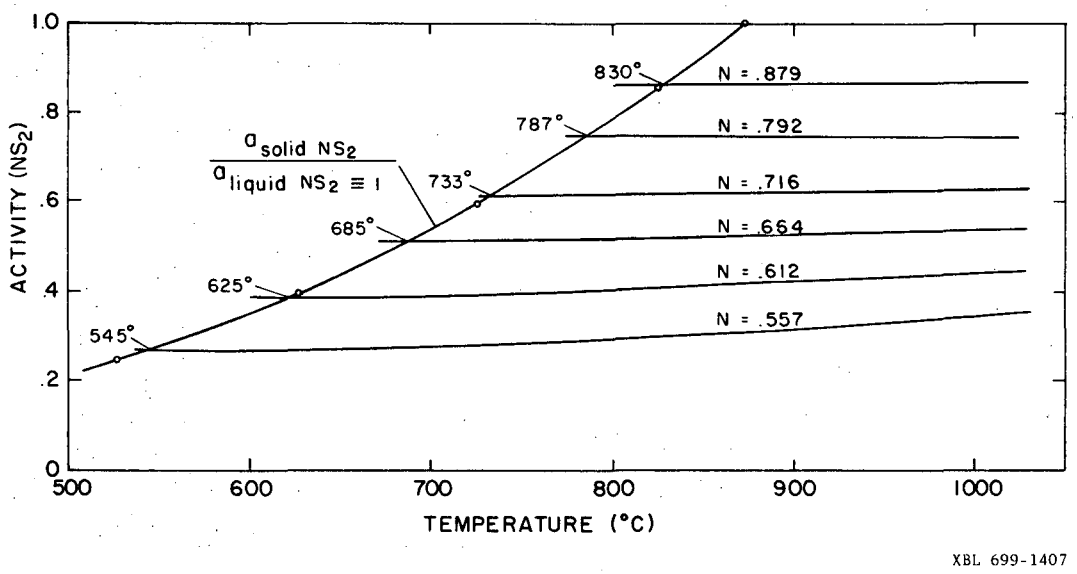

Figure 12. Isocompositional activity plots for NS_2 for determination of the NS_2 liquidus in the FeO-NS_2 system.

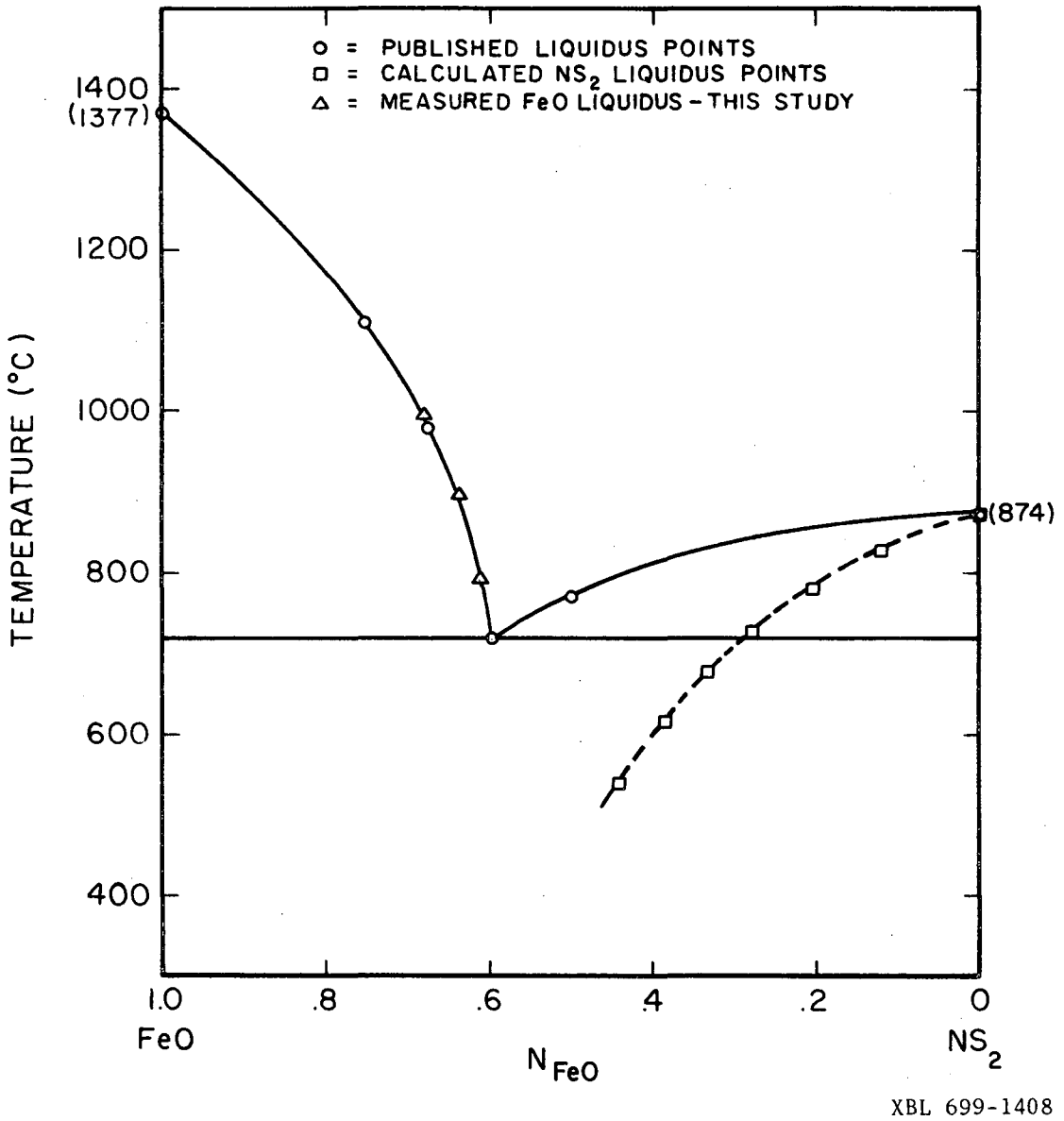

Figure 13. Comparison of the calculated NS_2 and FeO liquiduses with the published phase diagram of Ibrahim and Carter.[11]

rather than Ni/NiO, but it was found that this mixture caused the Pt electrodes to become brittle, and was, therefore, unsatisfactory for extended cell runs. As with the $FeO-NS_2$ study, the data of Elliot and Gleiser[21] was used to calculate the standard free energy for the reaction

$$CoO(s) + Ni(s) = Co(s) + NiO(s).^{*} \tag{45}$$

Adding this to the overall cell reaction

$$Co(s) + NiO(s) = CoO_{a<1} + Ni, \tag{46}$$

one obtains

$$CoO(s) = CoO(\text{in glass})_{a<1}, \tag{47}$$

to which Eq. (17) may be applied for activity determination.

The isocompositional cell output (in volts) vs temperature is shown in Fig. 14. Each line represents the average of two or more trials and the uncertainty is ±2 mv. The variation in activity of CoO with temperature for each composition is presented in Fig. 15, and the isothermal activity-composition plots are given in Fig. 16. In both figures, the activity of CoO is presented relative to pure solid CoO. The activity of solid CoO relative to the pure supercooled liquid CoO

---

* As with the FeO experiments, output of a cell of the type Ni/NiO ‖ CSZ ‖ Co/CoO agreed well with the data of Elliot and Gleiser.[21]

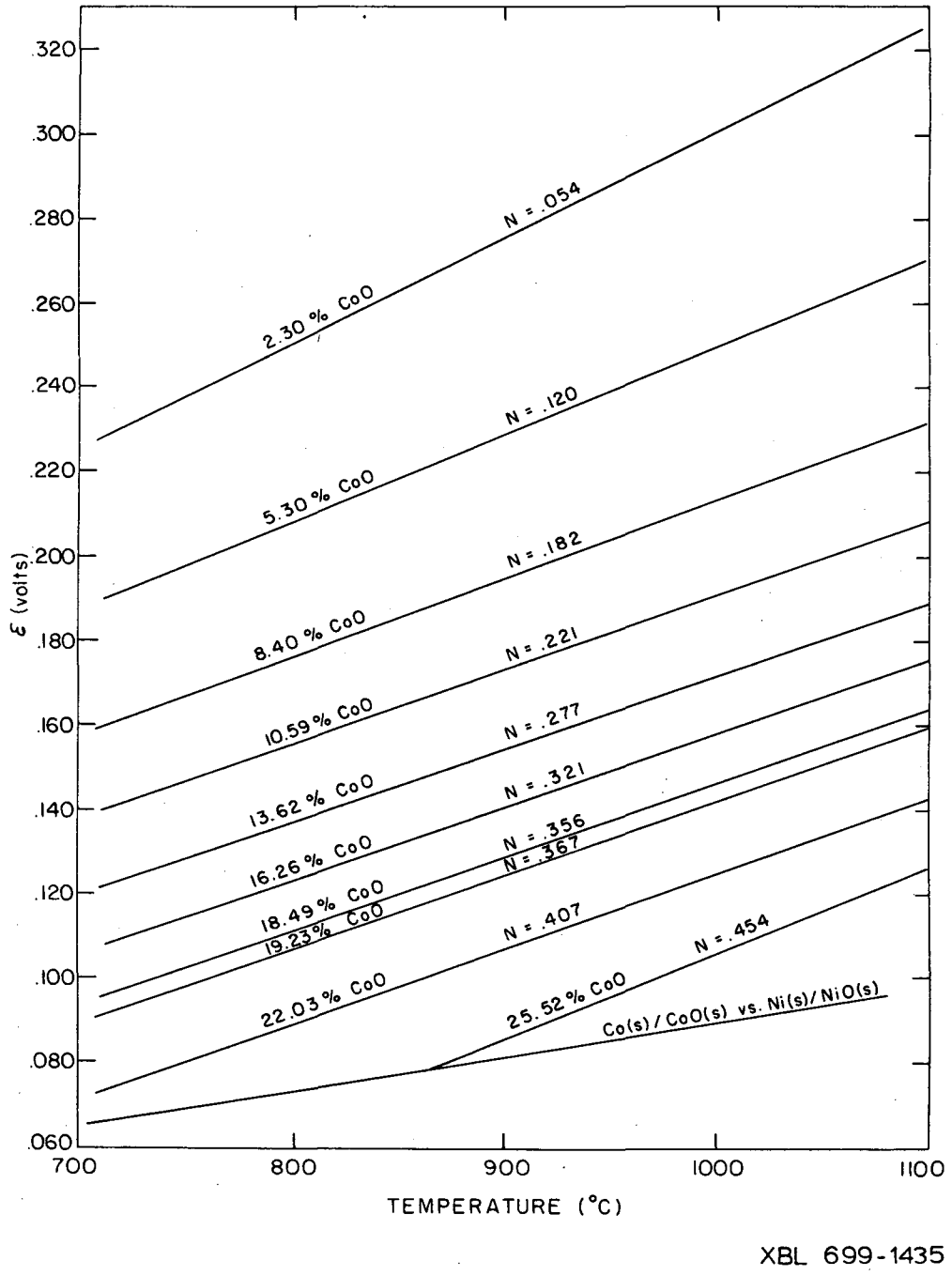

Figure 14. Isocompositional cell output for CoO-NS_2 glasses as a function of temperature (±2 min).

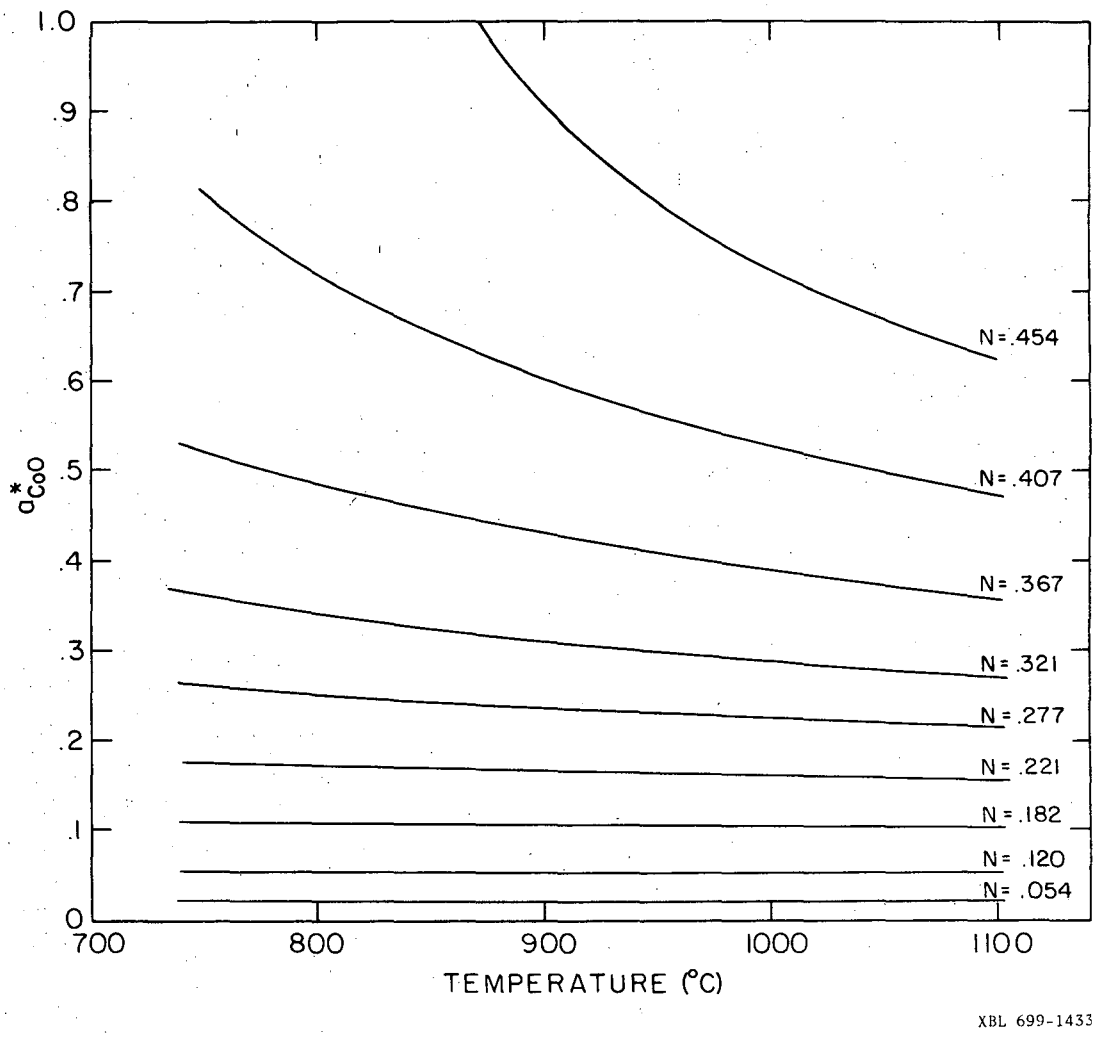

Figure 15. Variation in the activity of CoO (referred to the pure solid standard state) with temperature for each composition studied.

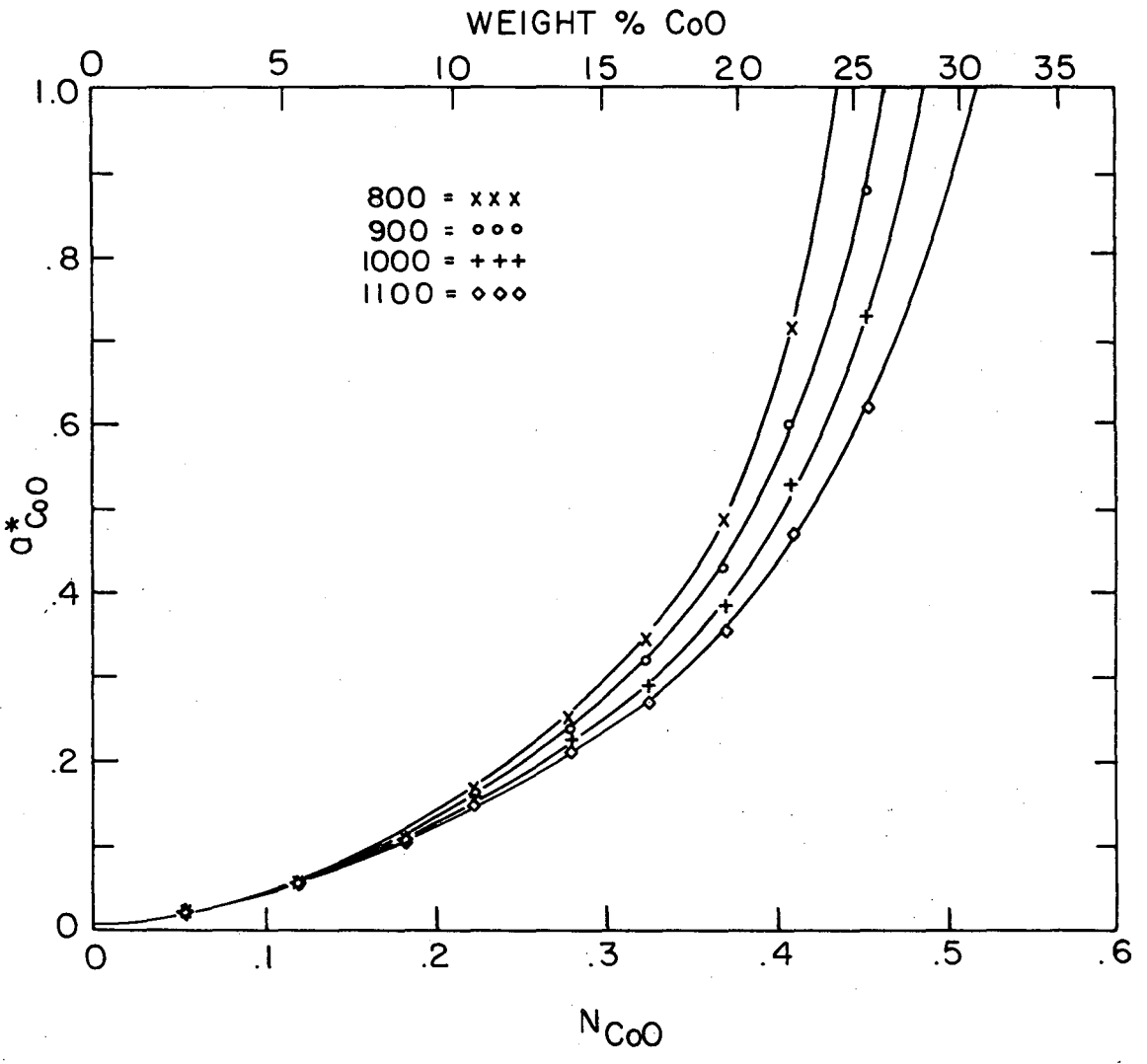

Figure 16. Isothermal dependence of CoO activity (referred to the pure solid standard state) on composition.

was estimated from Eq. (34). The entropy of fusion (ΔS_f) was assumed to be the same as for FeO (4.54 cal/mole°C), and the heat of fusion (ΔH_f) was found from the product $T_f \Delta S_f$, (T_f=2078°K), giving ΔH_f = 9434 cal/mole. The estimated activities of solid CoO relative to the pure liquid CoO standard state, and the approximate free energies for the reaction

$$CoO(solid) = CoO(supercooled\ liquid) \qquad (48)$$

are presented in Appendix F. Activities of CoO in NS_2 glass solution referred to both standard states are listed in Appendix B, and isothermal plots of a^{**}_{CoO} vs composition are given in Fig. 17.

The activity coefficient of NS_2 relative to pure liquid NS_2 was found from graphical integration of the modified Gibbs-Duhem equation, as presented in Eq. (21). Plots of the alpha-function for four temperatures are given in Fig. 18, and activities calculated from this integration are presented in Fig. 19. They are similarly listed in Appendix B.

The partial thermodynamic functions for CoO and NS_2 were obtained in the same manner as for FeO (see pp. 11-13). The partial molar free energies for CoO and NS_2, and the free energy (ΔF^{*}_{mix}) for one reaction

$$xCoO(s) + yNS_2(liq.) = xCoO \cdot yNS_2(glass) \qquad (49)$$

are plotted in Fig. 20 and listed in Appendix B. The partial molar free energy of CoO ($\overline{\Delta F}^{**}_{CoO}$) and the free energy of mixing (ΔF^{**}_{mix}) for the

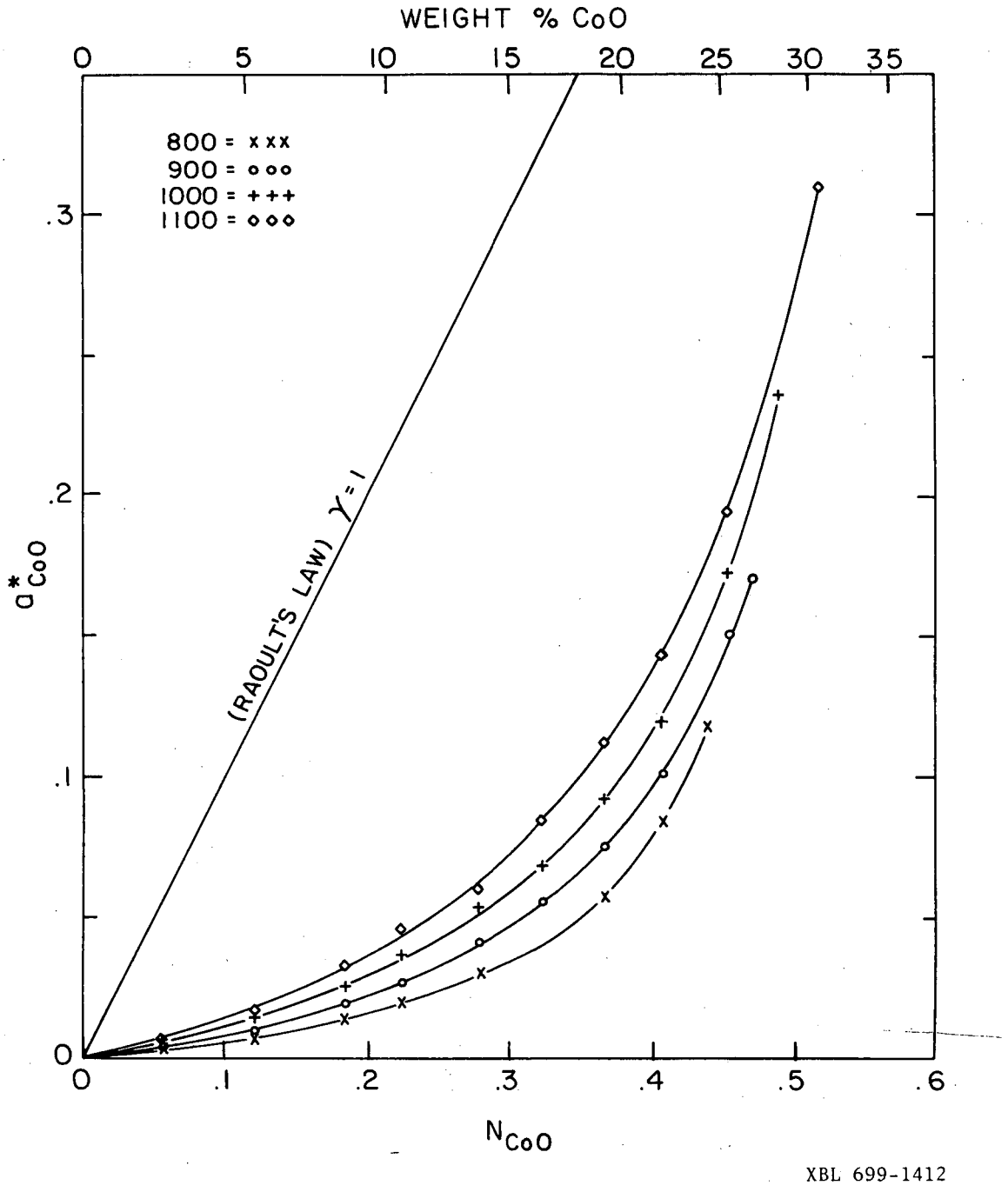

Figure 17. Estimated isothermal dependence of the CoO activity (referred to pure supercooled liquid CoO) on composition.

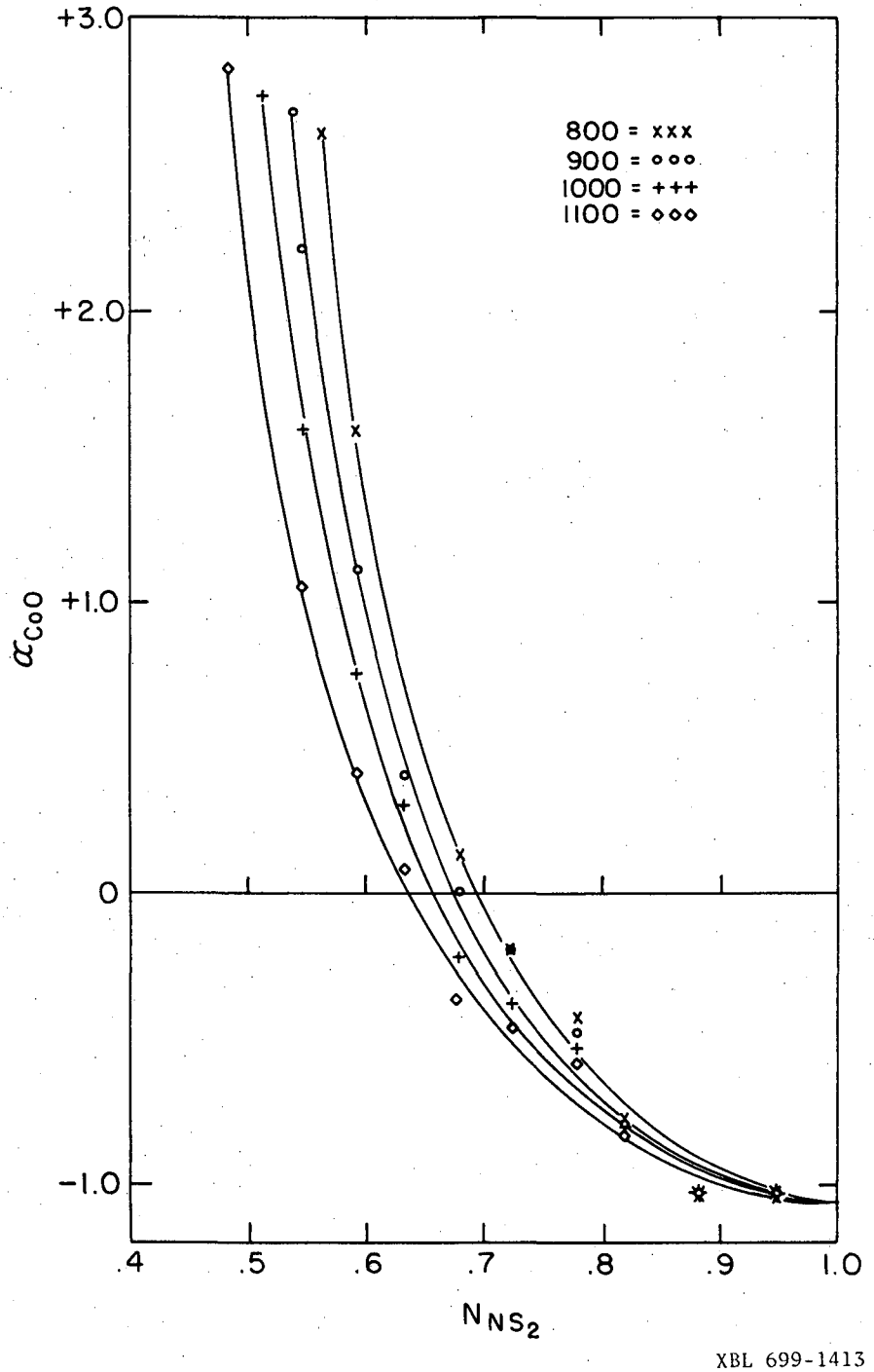

Figure 18. Alpha function plot for determination of the activity of NS_2 in the CoO-NS_2 system by integration of the modified Gibbs-Duhem equation.

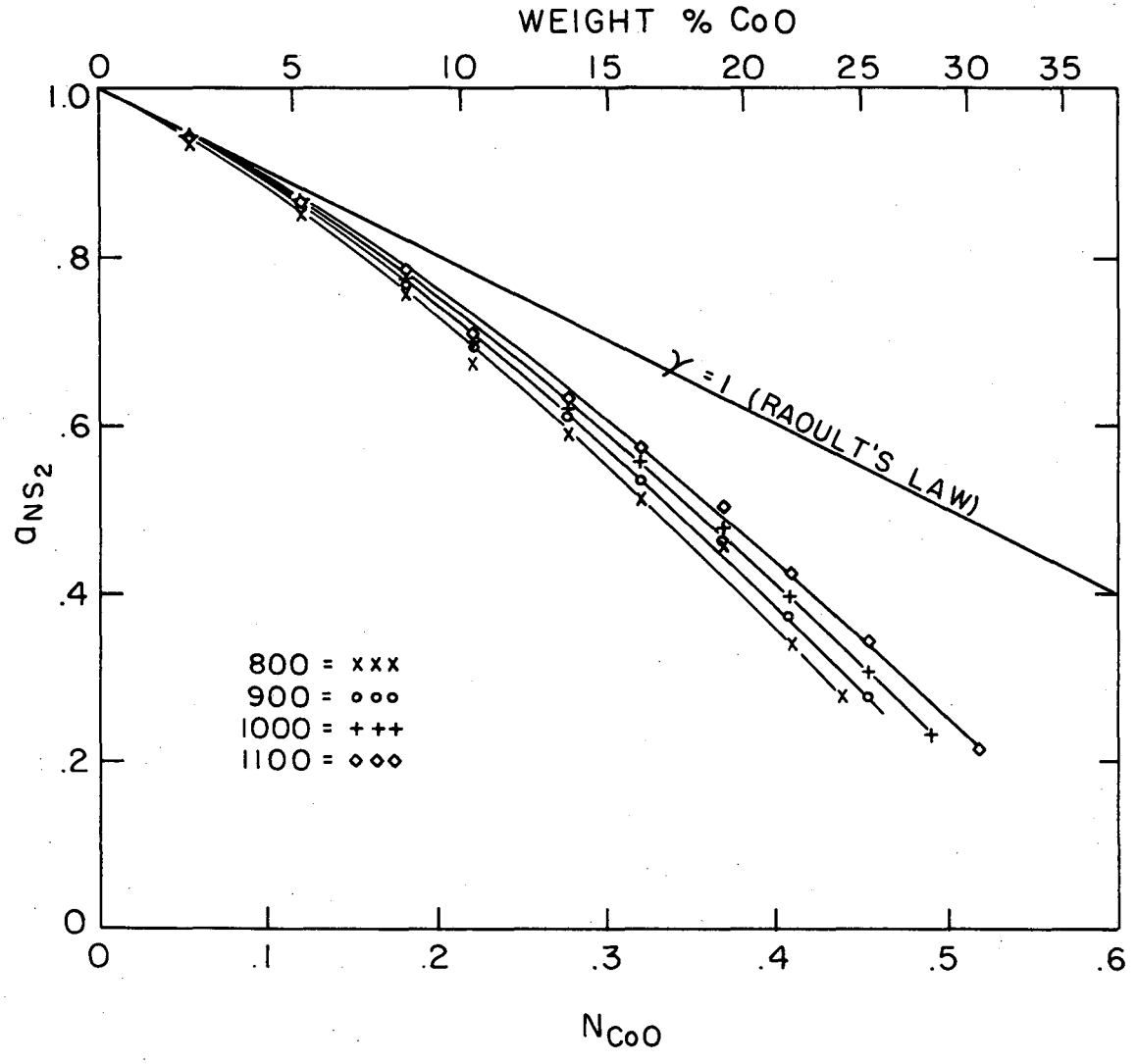

Figure 19. Isothermal activities of NS_2 (referred to the liquid standard state) calculated from integration of the modified Gibbs-Duhem equation.

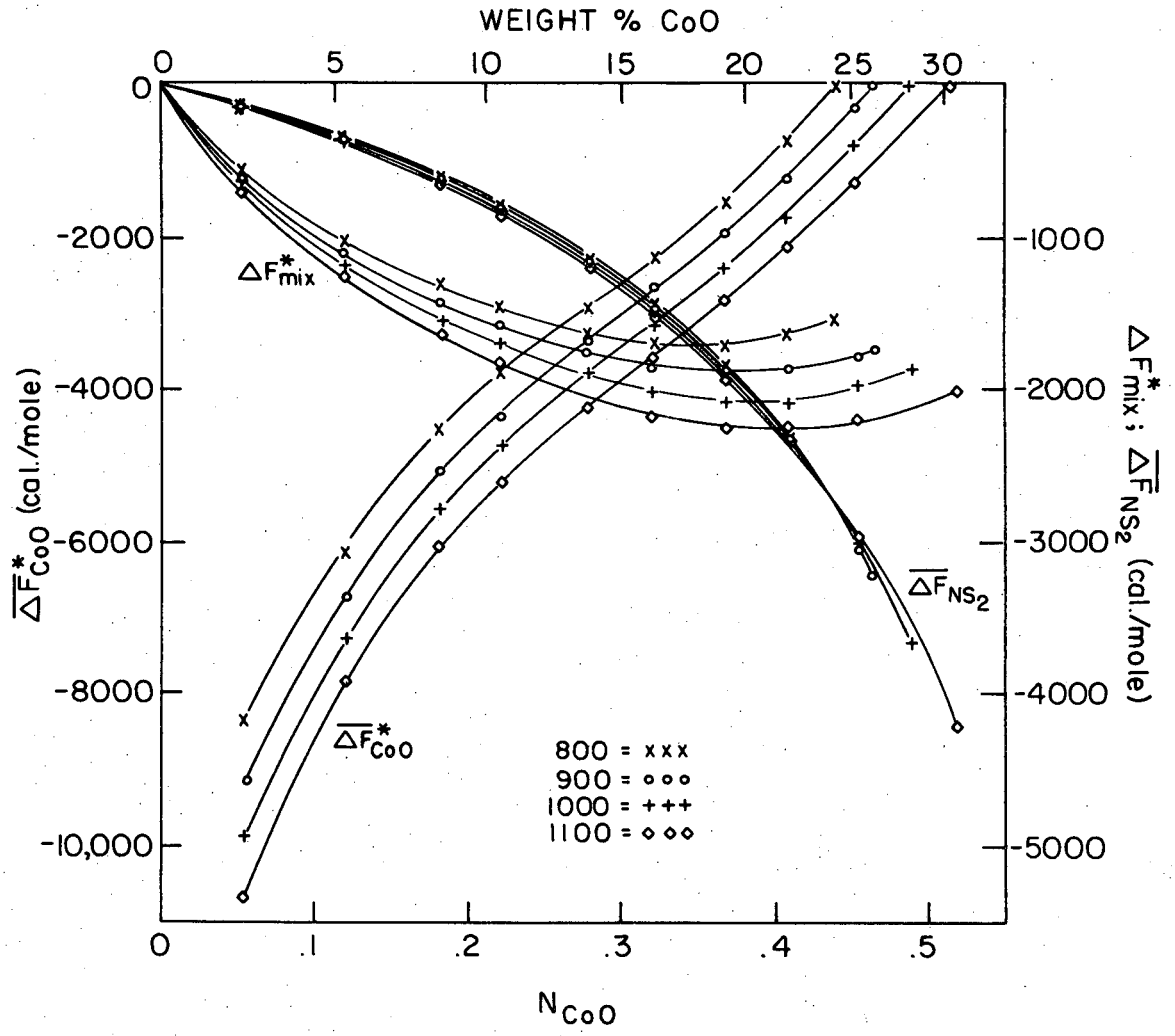

Figure 20. Free energy plots for CoO (referred to the pure solid standard state); NS_2 (referred to the pure liquid).

reaction

$$xCoO(\text{supercooled liquid}) + yNS_2(\text{liq.}) = xCoO \cdot yNS_2(\text{glass}) \qquad (50)$$

are plotted in Fig. 21 and listed in Appendix B. The partial molar entropies ($\overline{\Delta S}^{*}_{CoO}$, $\overline{\Delta S}^{**}_{CoO}$, $\overline{\Delta S}_{NS_2}$) and the integral entropies of mixing (ΔS^{*}_{mix}, ΔS^{**}_{mix}); partial molar enthalpies ($\overline{\Delta H}^{*}_{CoO}$, $\overline{\Delta H}^{**}_{CoO}$, $\overline{\Delta H}_{NS_2}$) and the enthalpies of mixing (ΔH^{*}_{mix}, ΔH^{**}_{mix}) for reactions (49) and (50) are given in Figs. 22 and 23 respectively.

The NS_2 liquidus was determined from the intersection of plots of the measured activity of NS_2 with a plot of the activity of pure solid NS_2 relative to the pure liquid standard state. This is presented in Fig. 24. This solubility data, combined with the CoO liquidus data, determined by intersection of the a^{*}_{CoO} curves with $a^{*}_{CoO}=1.0$, allows a tentative phase diagram for the pseudobinary system $CoO-NS_2$ to be proposed. This is illustrated in Fig. 25.

C. The System $NiO-NS_2$

Activity measurements were made in the $NiO-NS_2$ system by means of a cell of the type

$$Ni/NiO \parallel CSZ \parallel Ni/NiO_{a<1}+NS_2 \ .$$

Since Ni/NiO is used as the reference electrode, the overall cell reaction simply becomes

$$NiO(\text{solid})_{a=1} = NiO(\text{glass})_{a<1}. \qquad (51)$$

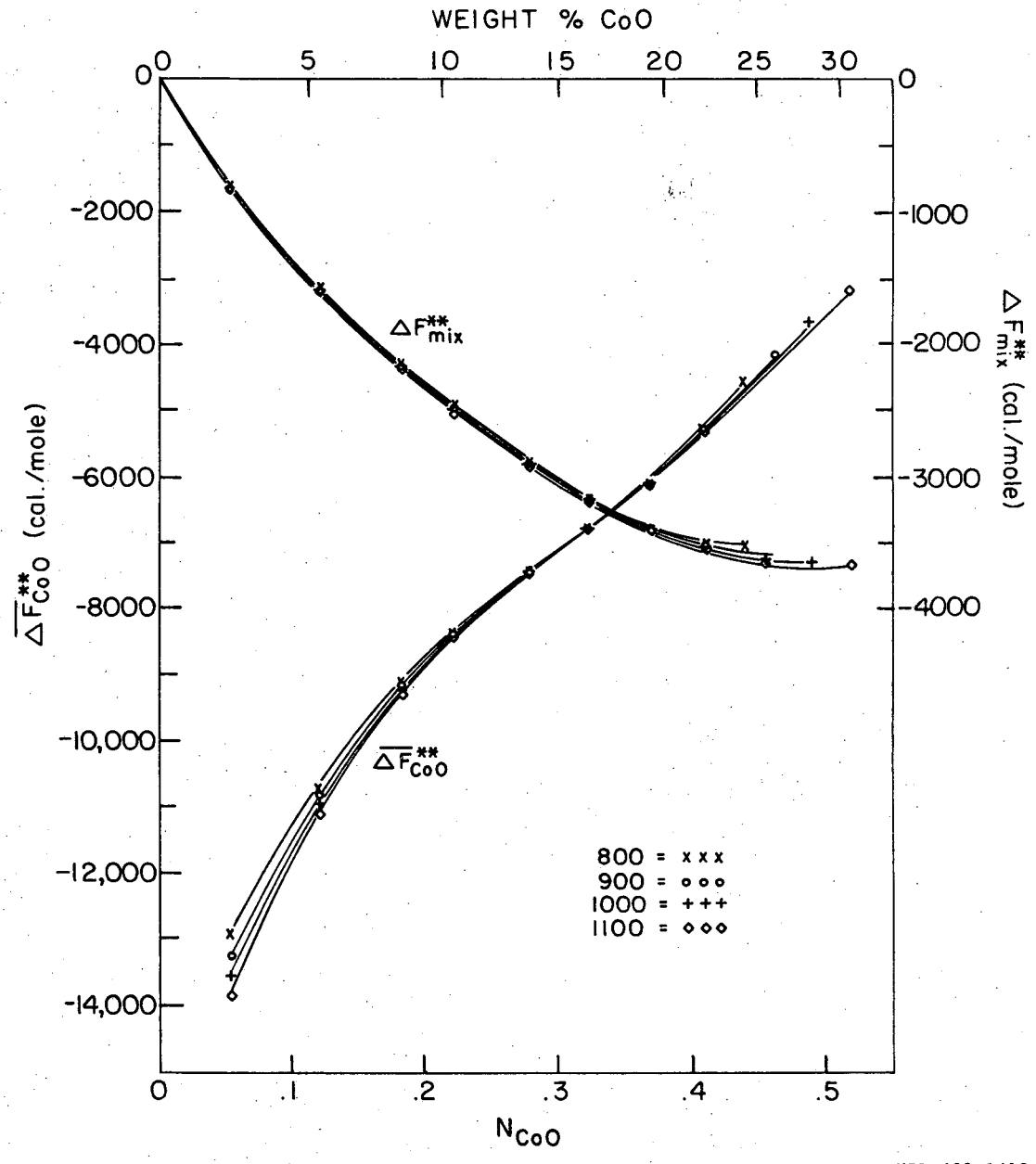

XBL 699-1418

Figure 21. Estimated free energy plots for CoO (referred to the pure supercooled liquid standard state).

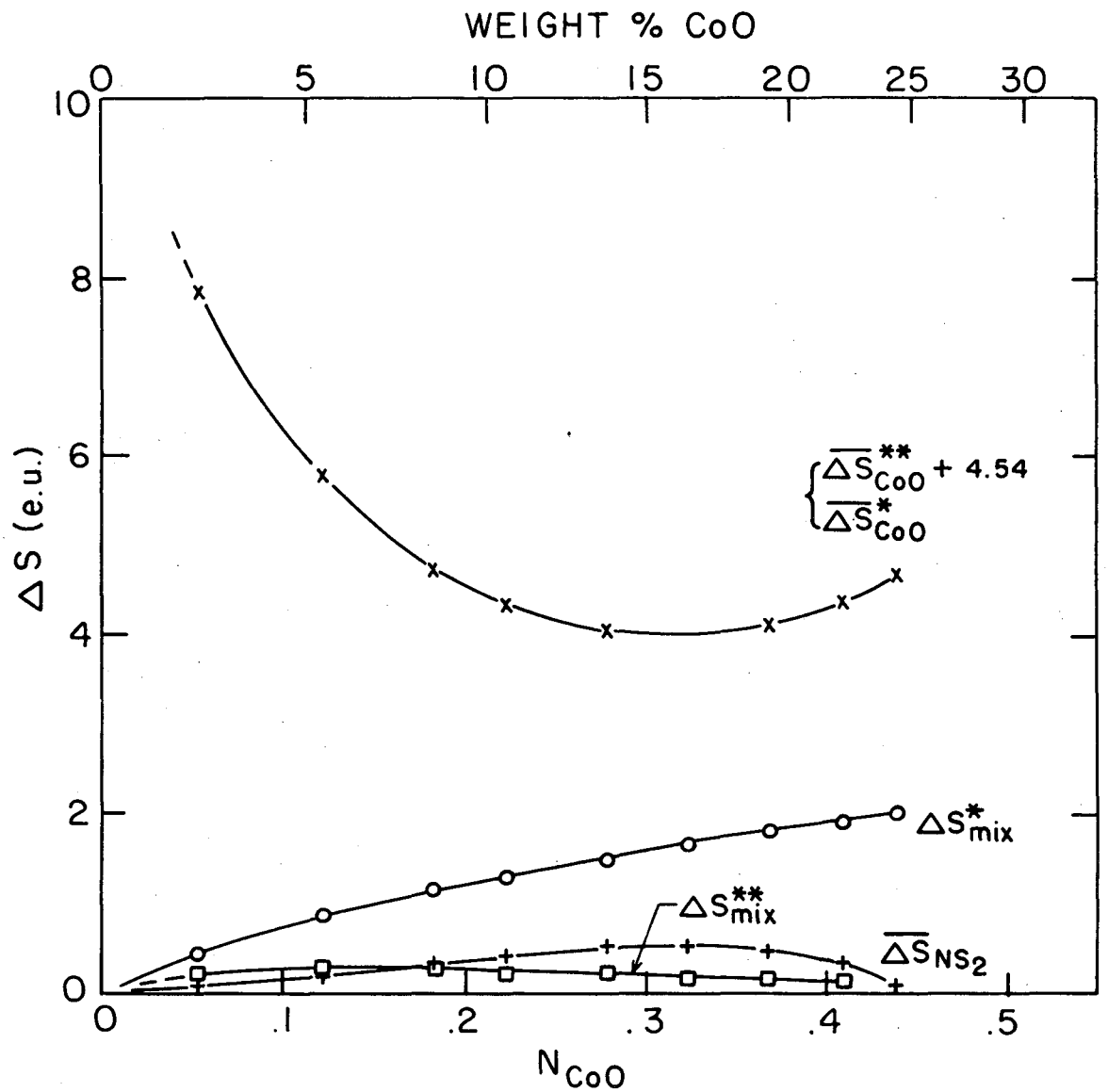

XBL 699-1416

Figure 22. Entropy plots for CoO and NS_2.

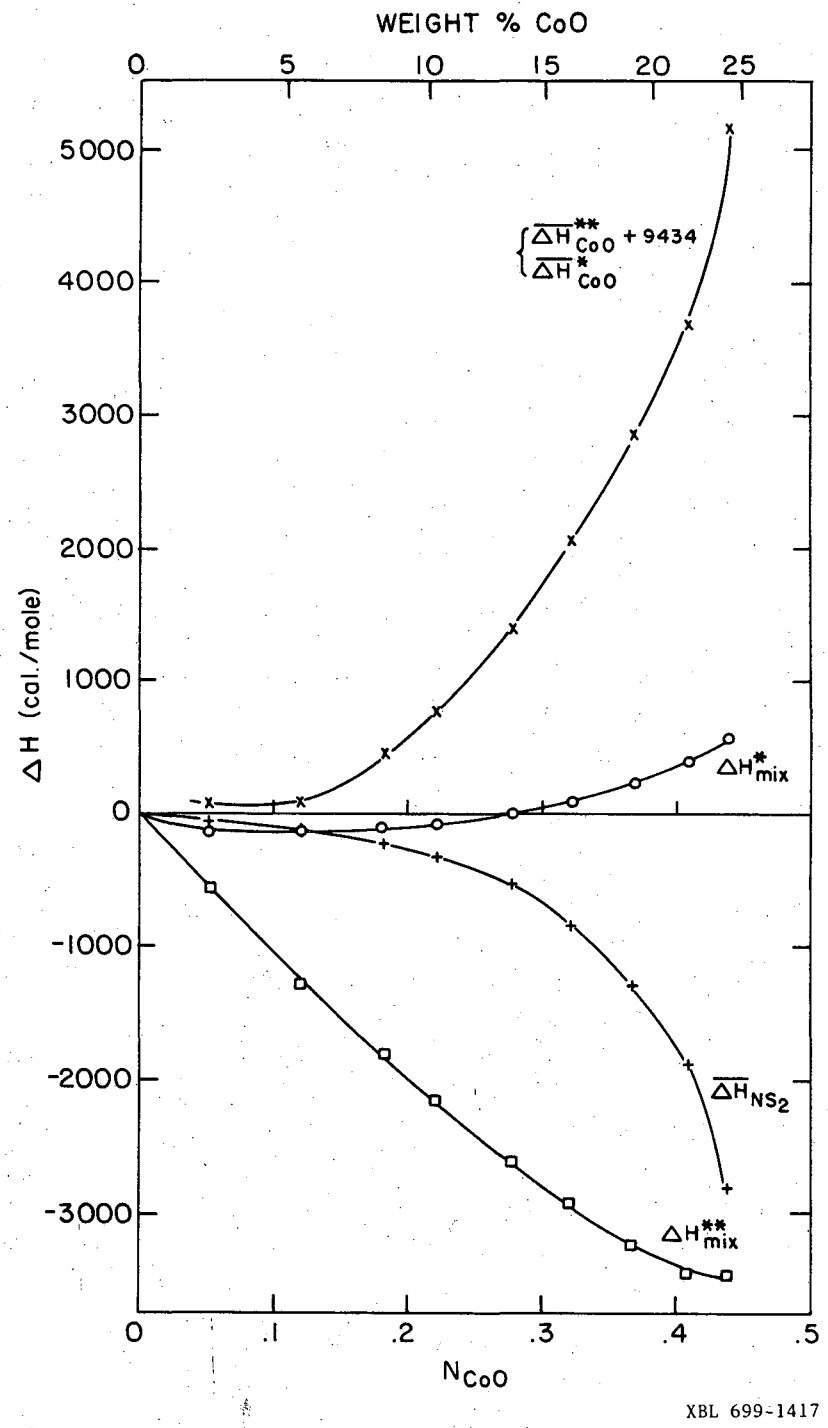

Figure 23. Enthalpy plots for CoO and NS_2.

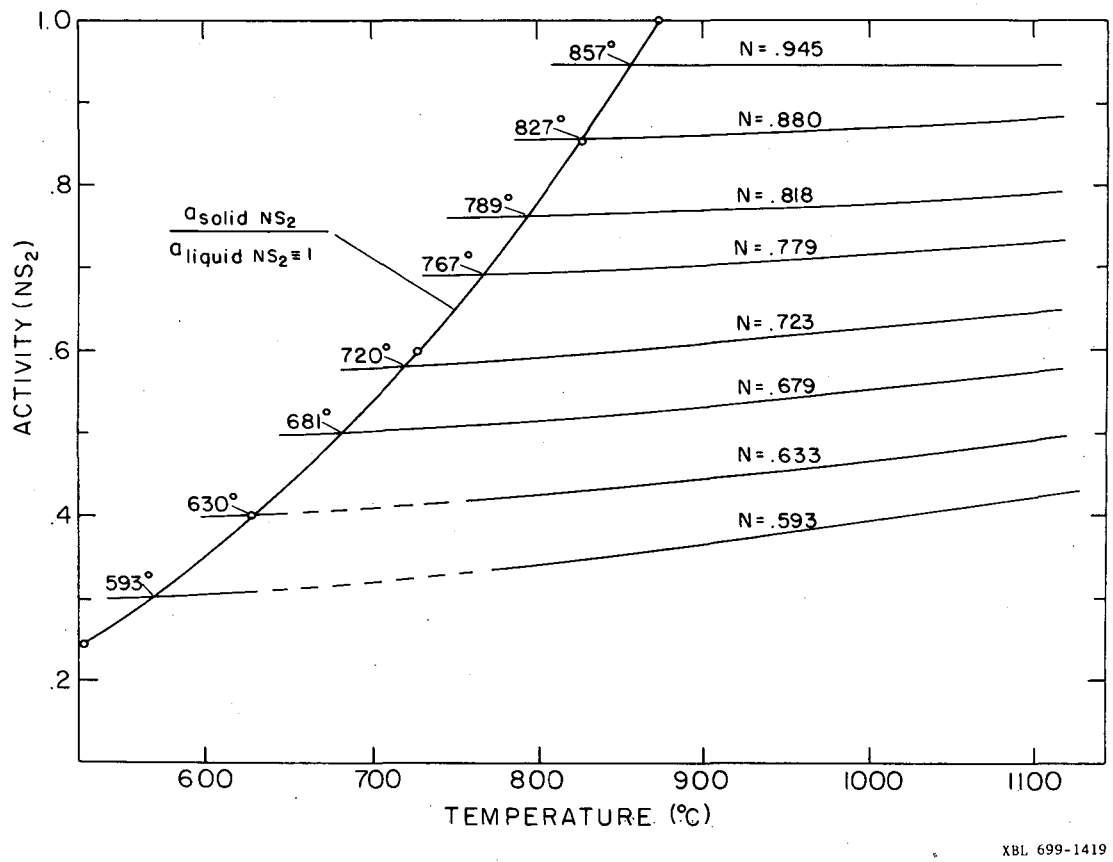

Figure 24. Isocompositional activity plots for NS_2 for determination of the NS_2 liquidus in the $CoO-NS_2$ system.

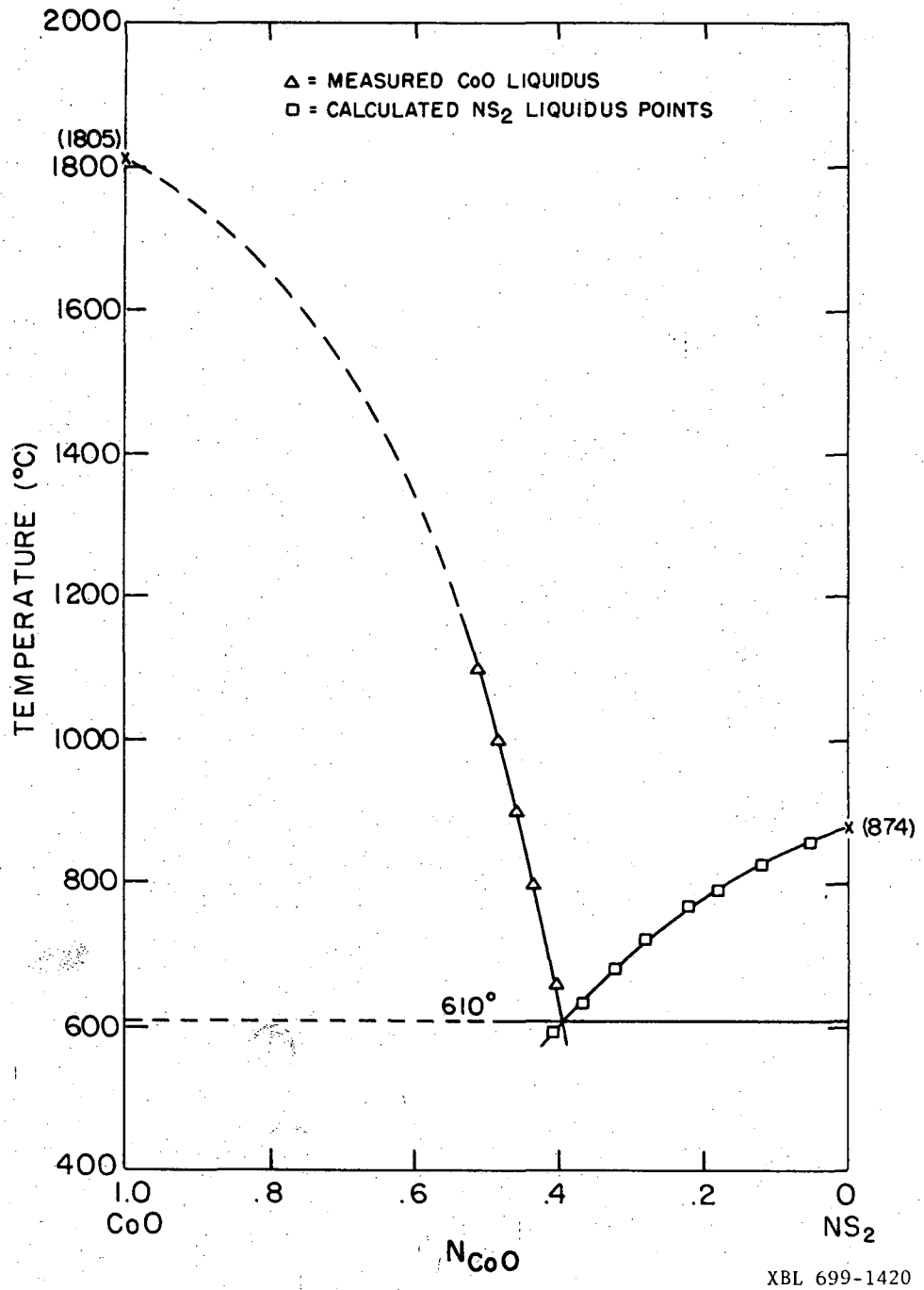

Figure 25. Proposed phase diagram for the CoO-NS_2 system.

Equation (17) is thus applicable for determination of a^{*}_{NiO}.

The isocompositional cell output (in volts) vs temperature is shown in Fig. 26. As with the CoO and FeO studies, each line represents the average of a minimum of two experimental determinations for each composition. The uncertainty is ±2 mv. The variation of a^{*}_{NiO} with temperature for each composition is shown in Fig. 27, and the isothermal activity-composition plots are given in Fig. 28. Assuming an entropy of fusion of 4.54 e.u. (the reported value for FeO), and enthalpy of fusion (ΔH_f) of 10161 cal/mole was estimated at T_f(NiO)=2238°K. The activity of pure solid NiO relative to the hypothetical supercooled liquid NiO was estimated between 800° and 1100°C from Eq. (34). These activities and the free energies for the reaction

$$NiO(solid) = NiO(supercooled\ liquid) \qquad (52)$$

are presented in Appendix F. The estimated activities of NiO referred to this supercooled liquid NiO (a^{**}_{NiO}) are given in Appendix C and graphically presented in Fig. 29.

The activity of NS_2 relative to the pure liquid was calculated from integration of Eq. (21). Plots of the alpha functions for the temperatures of consideration are given in Fig. 30, and the calculated activities are plotted vs. composition in Fig. 31.

The partial molar thermodynamic functions were calculated in the same manner as for the FeO and CoO systems. The partial molar free energies ($\overline{\Delta F}^{*}_{NiO}$, $\overline{\Delta F}_{NS_2}$) and the free energy ($\Delta F^{*}_{mix}$) for the reaction

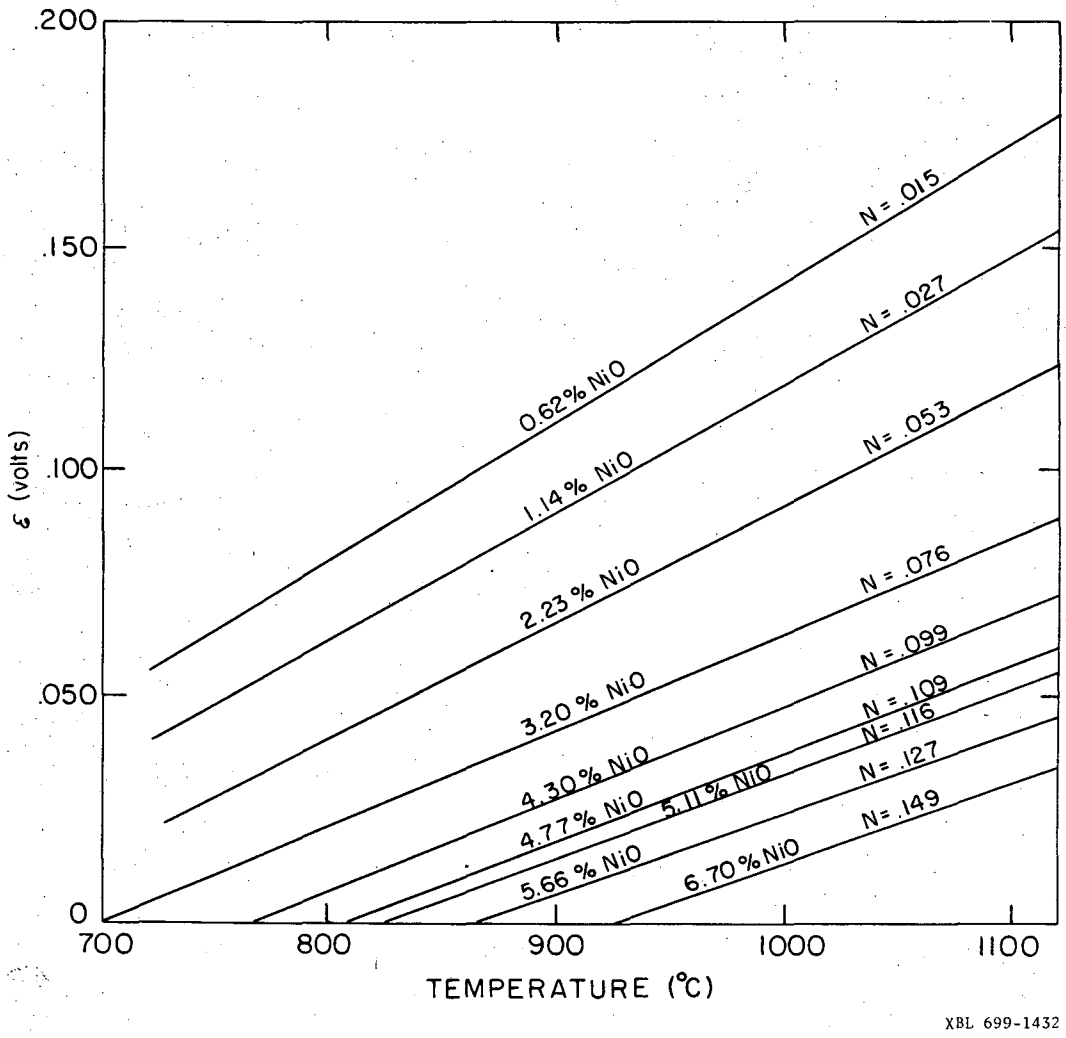

Figure 26. Isocomposition cell output for NiO-NS_2 glasses as a function of temperature (±2 mv).

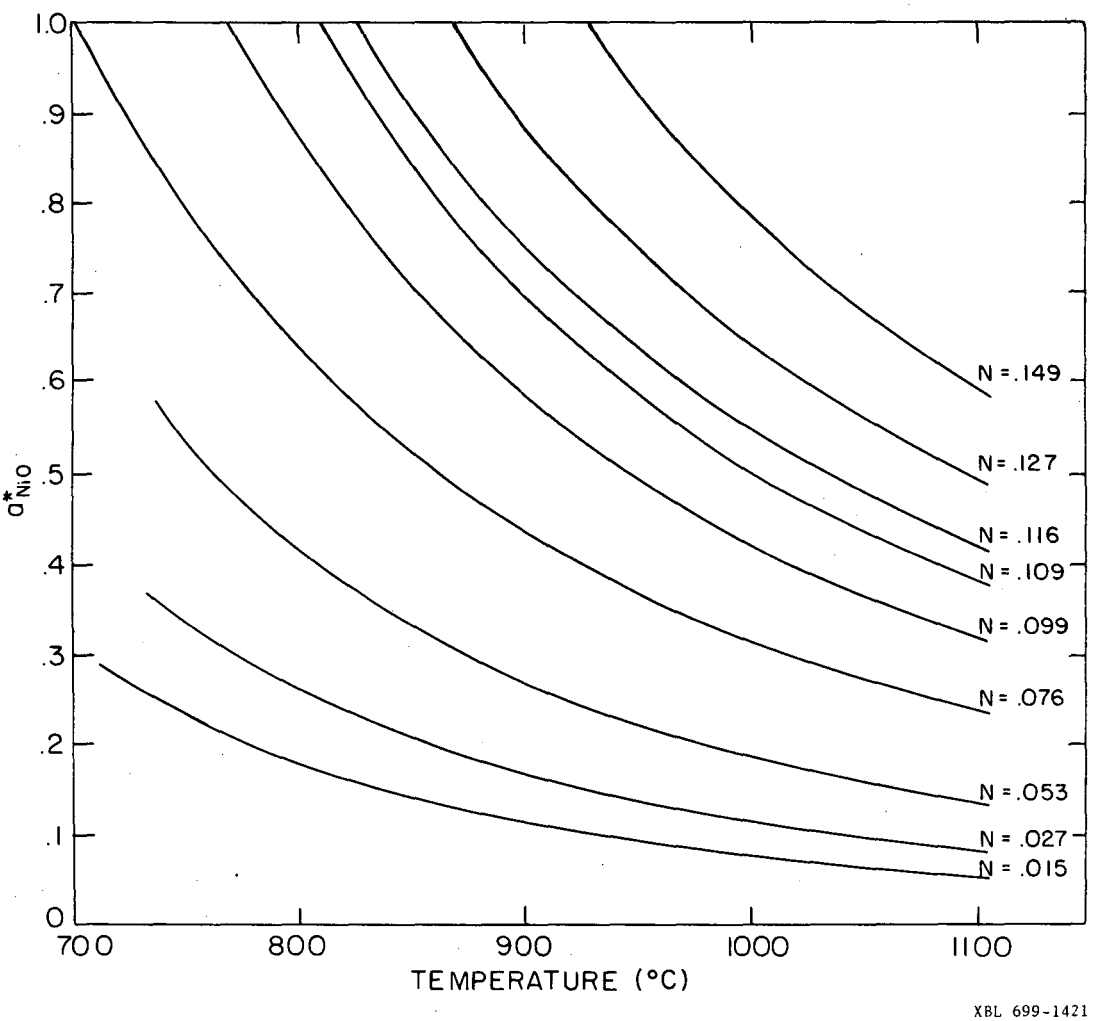

Figure 27. Variation in the activity of NiO (referred to the pure solid standard state) with temperature for each composition studied.

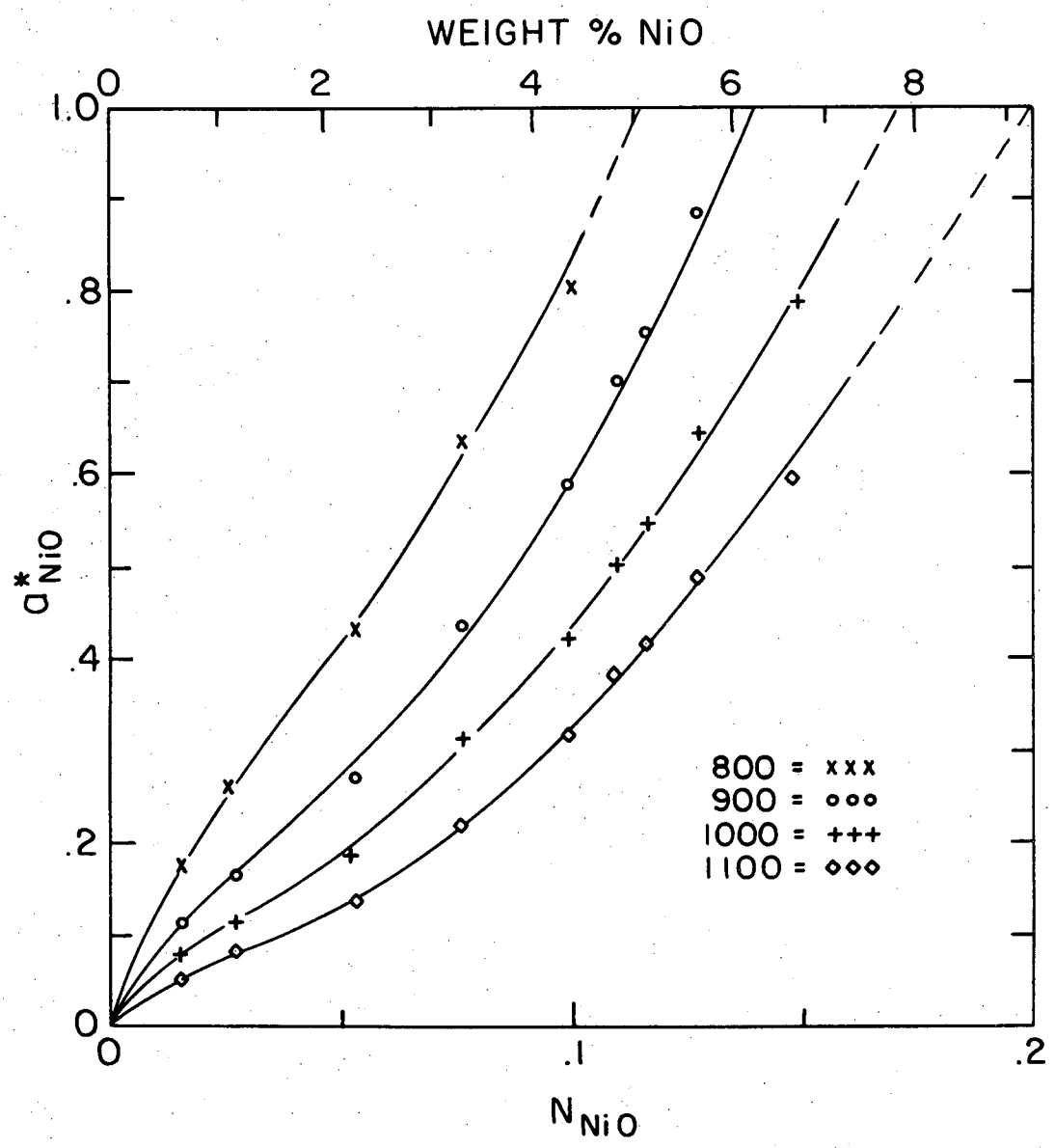

Figure 28. Isothermal dependence of NiO activity (referred to the pure solid standard state) on composition.

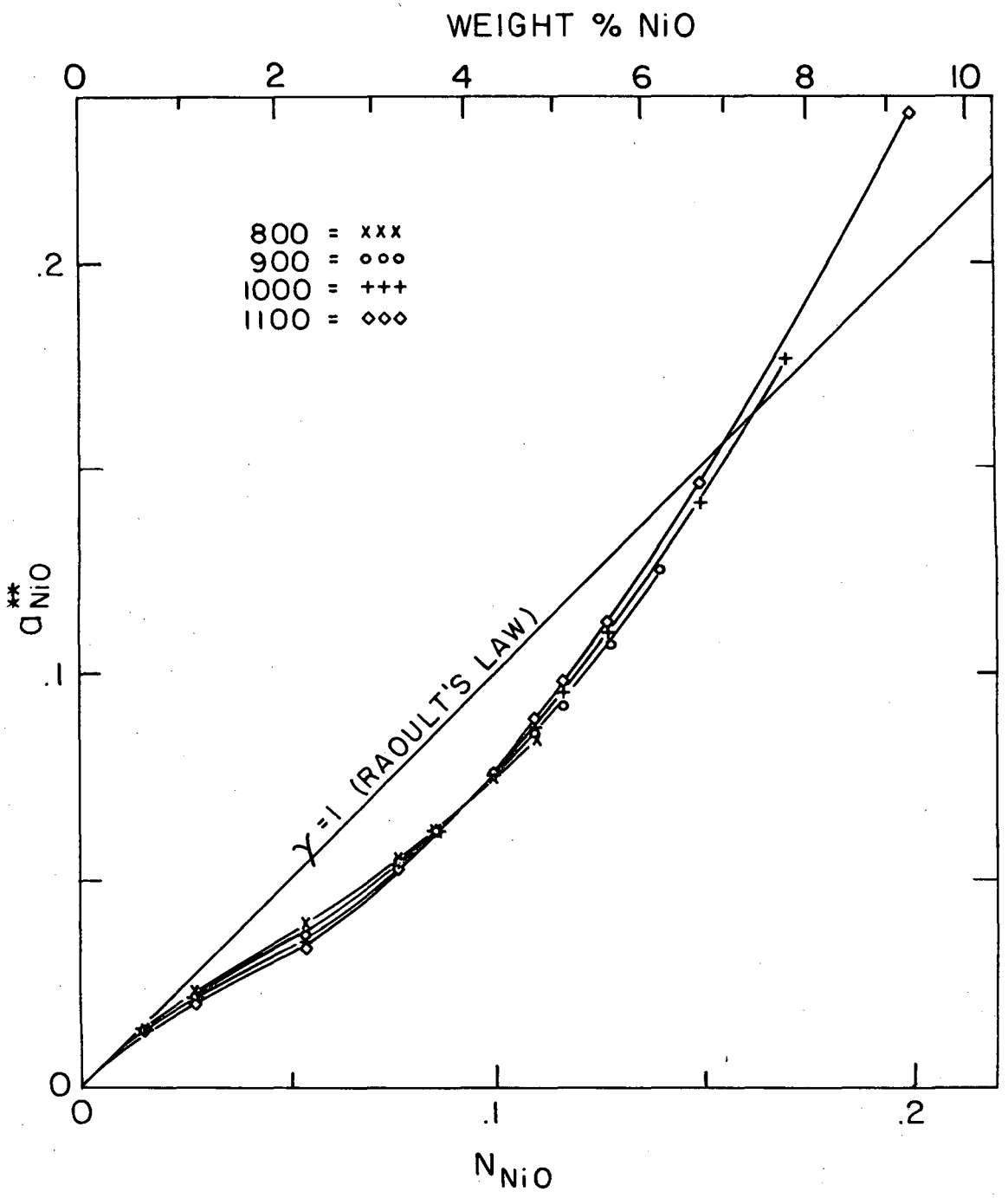

Figure 29. Estimated isothermal dependence of the NiO activity (referred to pure supercooled liquid NiO) on composition.

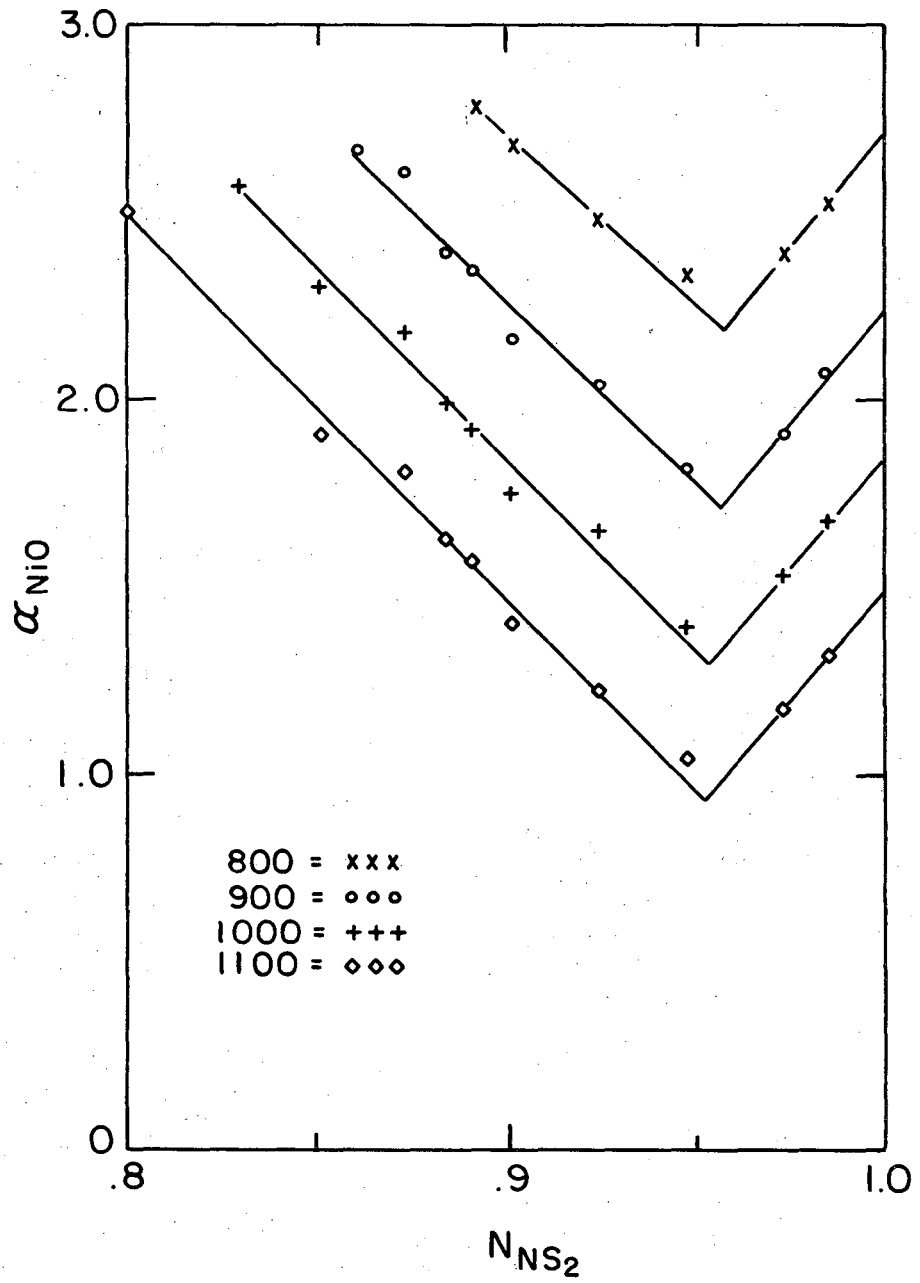

Figure 30. Alpha function plot for determination of the activity of NS_2 in the NiO-NS_2 system by integration of the modified Gibbs-Duhem equation.

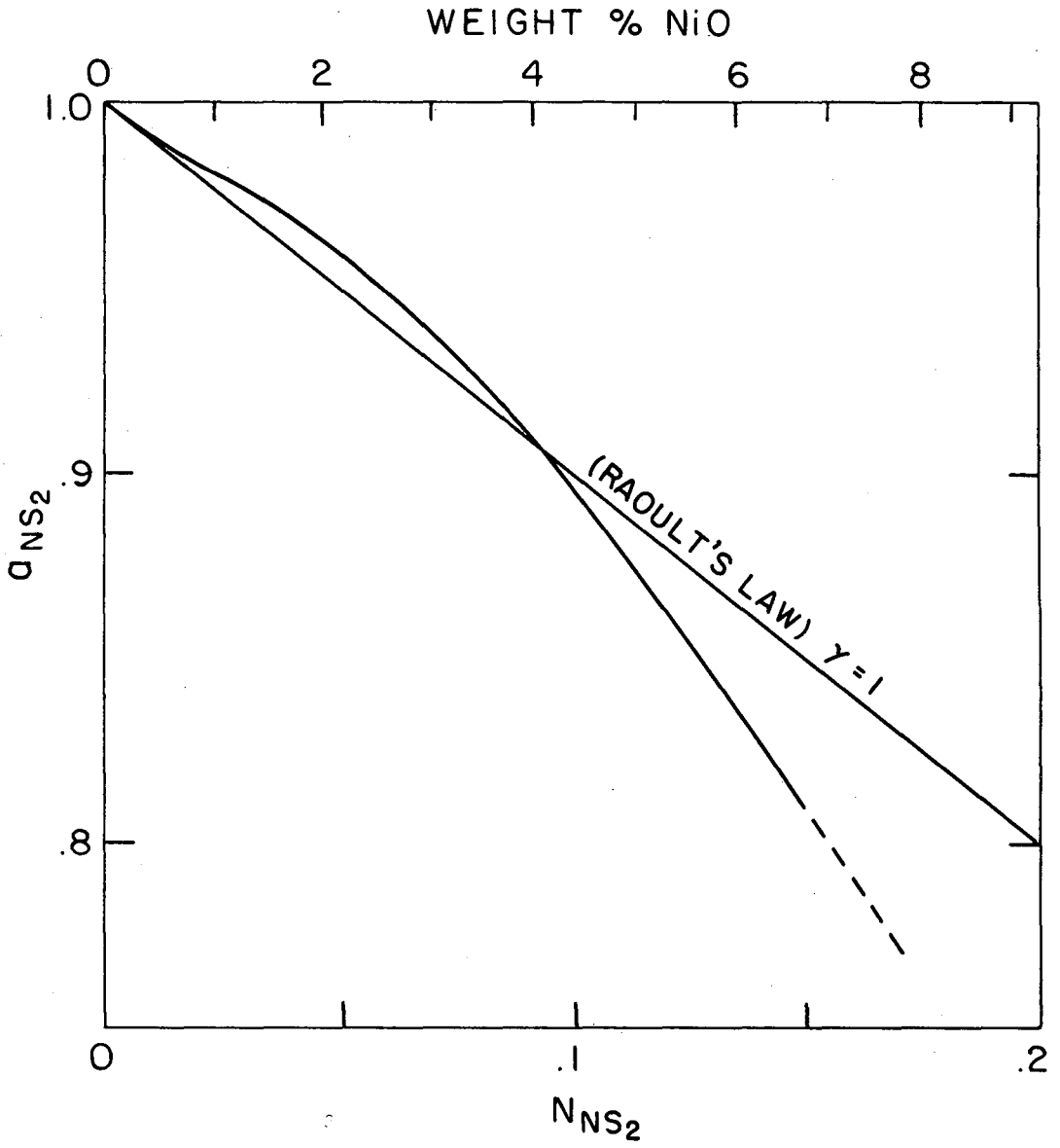

XBL 699-1425

Figure 31. Activity of NS_2 (referred to the liquid standard state) calculated from integration of the modified Gibbs-Duhem equation. (One curve is drawn to represent all temperatures between 800° and 1100°C. Over this small range of concentration, the experimental uncertainty is too large to distinguish precisely the temperature variation on activity of NS_2). The estimated uncertainty in these data is 2%.

$$xNiO(solid) + yNS_2(liquid) = xNiO \cdot yNS_2(glass) \qquad (53)$$

are plotted in Fig. 32 and listed in Appendix C. The partial molar free energy of NiO ($\overline{\Delta F}^{**}_{NiO}$) and the free energy of mixing (ΔF^{**}_{mix}) for the reaction

$$xNiO(supercooled\ liquid) + yNS_2(liquid) = xNiO \cdot yNS_2(glass) \qquad (54)$$

are plotted in Fig. 33 and also listed in Appendix C. The partial molar entropies ($\overline{\Delta S}^{*}_{NiO}$, $\overline{\Delta S}^{**}_{NiO}$, $\overline{\Delta S}_{NS_2}$) and the integral entropies of mixing (ΔS^{*}_{mix}, ΔS^{**}_{mix}); partial molar enthalpies ($\overline{\Delta H}^{*}_{NiO}$, $\overline{\Delta H}^{**}_{NiO}$, $\overline{\Delta H}_{NS_2}$) and the enthalpies of mixing (ΔH^{*}_{mix}, ΔH^{**}_{mix}) for reactions (53) and (54) are given in Figs. 34 and 35 respectively.

The NS_2 liquidus was determined by the intersection of the experimentally calculated a_{NS_2} vs temperature plots, with the plot of the activity of pure solid NS_2 relative to the pure liquid standard state. This graph is presented in Fig. 36. The solubility data for NiO was determined either by intersection of the a^{*}_{NiO} curves with $a^{*}_{NiO}=1$ (Fig. 27) or by intersection of ε_{cell} vs temperature with $\varepsilon_{cell}=0$. These liquidus data allow one to construct a tentative phase diagram for the NiO-rich end of the pseudobinary NiO-NS_2 system. This is given in Fig. 37.

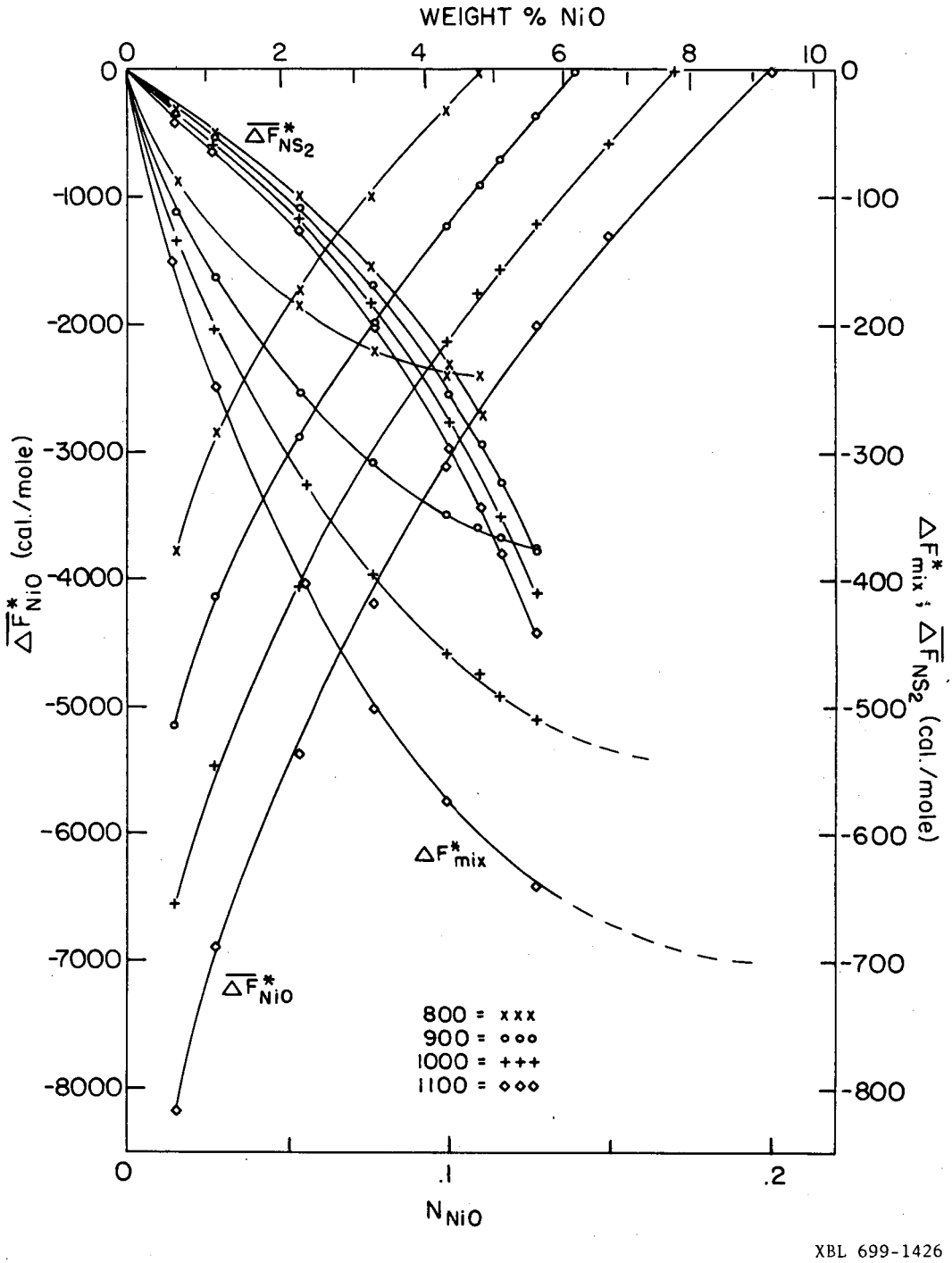

Figure 32. Free energy plots for NiO (referred to the pure solid standard state); NS_2 (referred to the pure liquid).

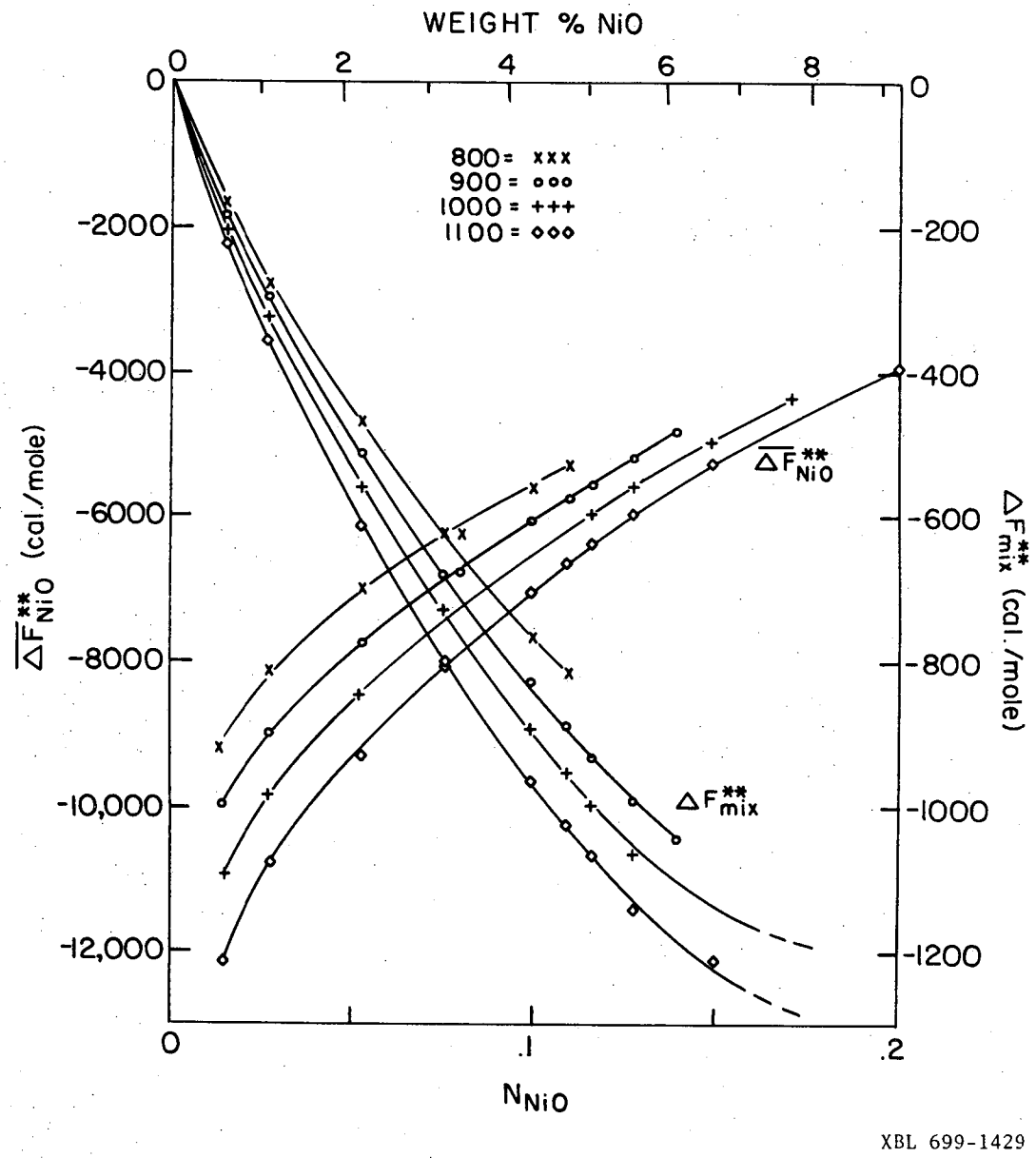

Figure 33. Estimated free energy plots for NiO (referred to the pure supercooled liquid standard state).

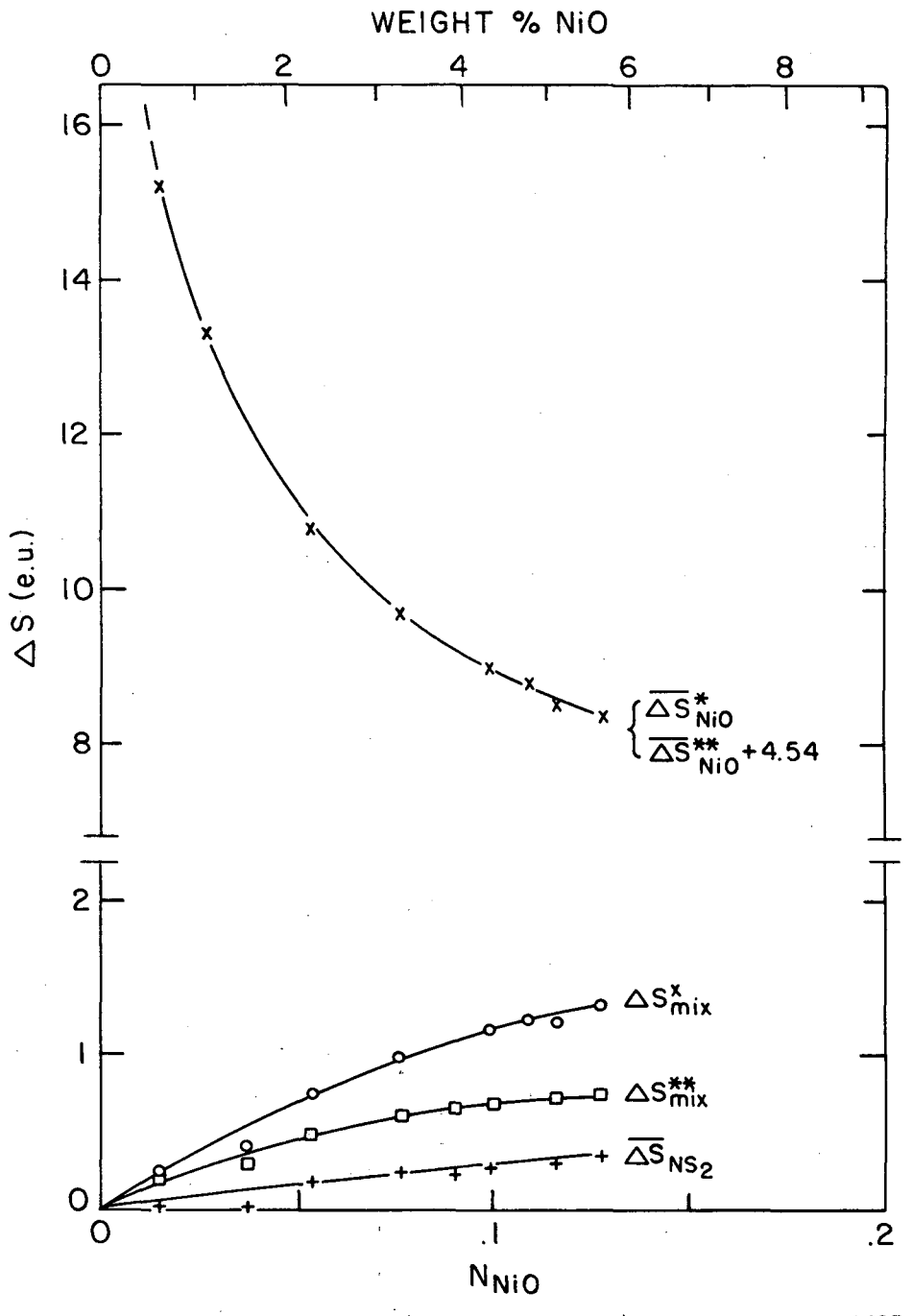

Figure 34. Entropy plots for NiO and NS_2.

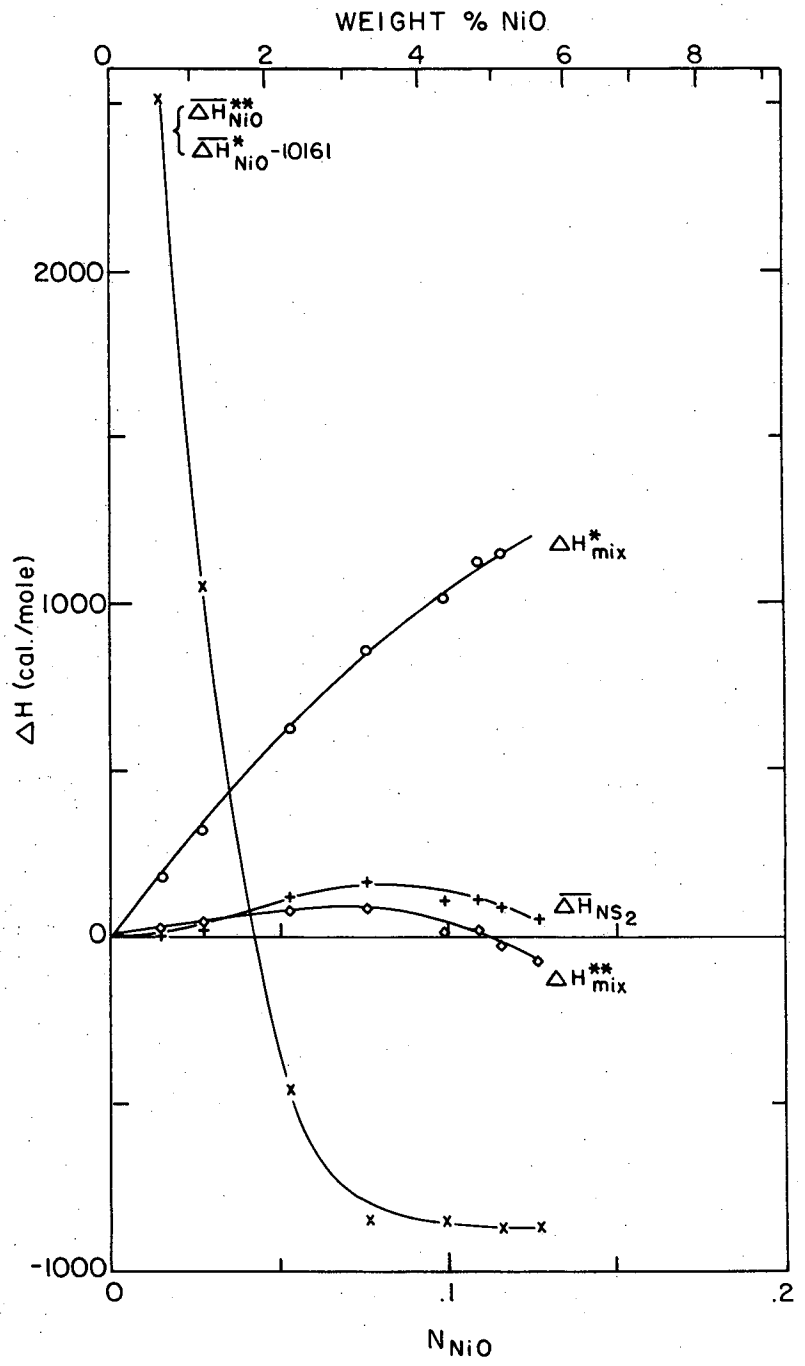

Figure 35. Enthalpy plots for NiO and NS_2.

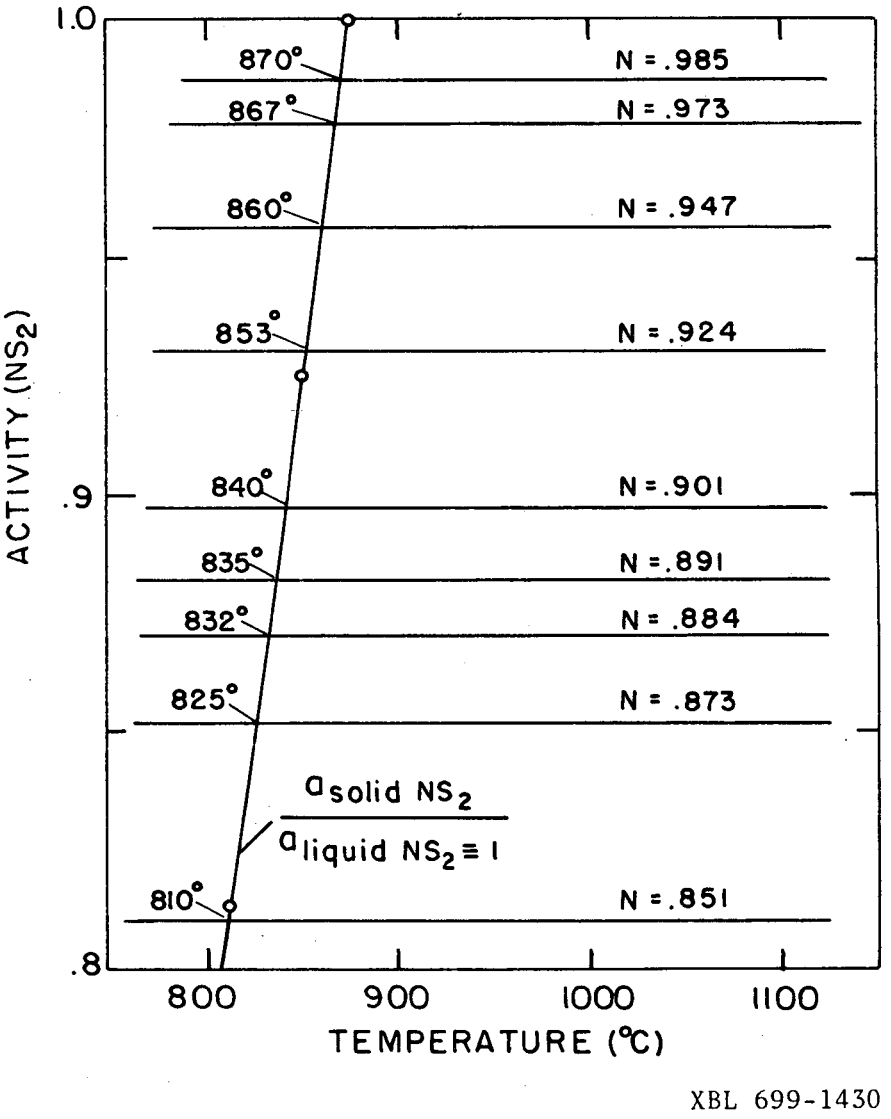

Figure 36. Isocompositional activity plots for NS_2 for determination of the NS_2 liquidus in the NiO-NS_2 system.

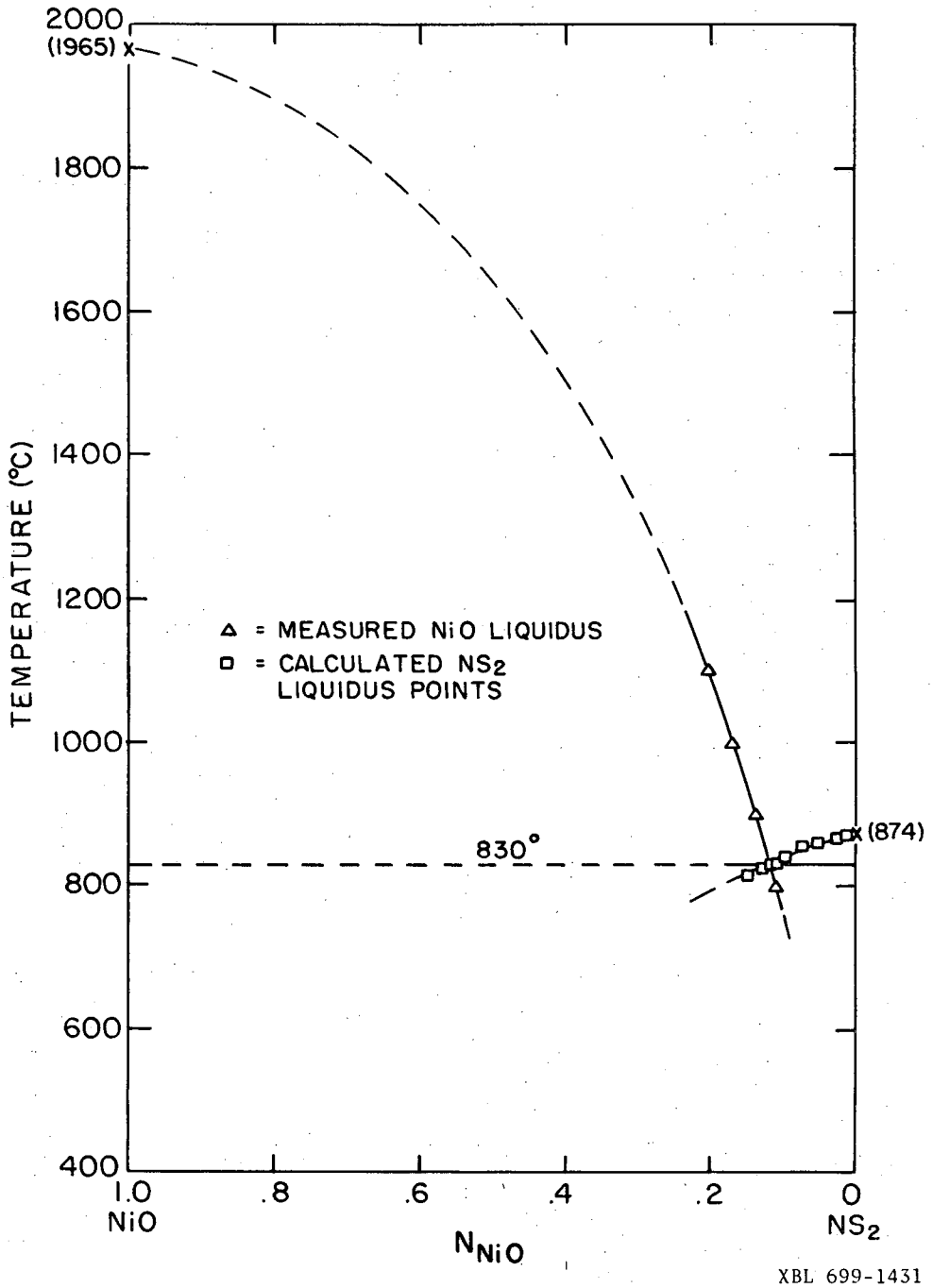

Figure 37. Proposed phase diagram for the NiO-NS_2 system.

V. DISCUSSION OF RESULTS

A. The System FeO-NS_2

1. Phase Relations

A plot of the experimentally determined liquiduses for the precipitation of crystalline FeO and NS_2 is given in Fig. 13, superimposed on the published binary diagram of Ibrahim and Carter.[11] It is seen that there is good agreement between their FeO liquidus, determined by quench methods, and the liquidus found in this study by intersection of the measured activity curves with the activity line for pure solid FeO. The NS_2 liquidus calculated from this study does not agree at all with that of Ibrahim and Carter;[11] the calculated curve being much lower than the published one. In fact, the freezing point depression of the NS_2 by the addition of FeO is so severe that extension of the FeO liquidus to a point of intersection (assuming a simple binary eutectic diagram) would result in a eutectic at an unreasonably low temperature. A freezing point depression of the magnitude proposed by Ibrahim and Carter[11] could result only if the FeO in solution exhibited a positive deviation from ideality.

There is little question as to the reality of the negative deviation indicated by these emf experiments, since this phenomenon has been qualitatively demonstrated by two other independent methods of investigation:

(1) The melting of FeO glasses containing 26.74 weight % FeO (N_{FeO}=.491) and 29.80 weight % FeO (N_{FeO}=.528) was at one time attempted in an atmosphere of CO/CO_2 at a ratio of 10:1 at 1000°C. The results indicated that the 26.74% glass melted satisfactorily, but there was

definite evidence of decomposition of the 29.80% glass. Calculation of the maximum activity of FeO which is stable according to the reaction

$$Fe + CO_2 = CO + FeO \qquad (55)$$

at a 10:1 CO/CO_2 ratio at 1000°C yielded a value of $a_{FeO}=0.233$ (see Appendix E). The successful formation of the 26.74% glass is indication that the activity of FeO in this composition is very near the maximum value of 0.233. This is in accordance with the overall data which has been obtained by emf measurements.

(2) Guiot[23] has also investigated the activities of FeO in NS_2 glass by use of the formation cell

$$Fe \parallel FeO + NS_2(glass) \parallel O_2(Pt). \qquad (56)$$

Although the results of this independent experiment are not quantitative, due to the unknown magnitude of the electronic transference in the glass, they compare qualitatively with these data, indicating an even stronger negative deviation than this study indicates. The possibility of any positive deviations of FeO activity from ideality is then ruled out by the coincidence of the results of these three independent observations.

Carter and Ibrahim's[11] NS_2 liquidus is not thermodynamically possible. However, the experimental data of both Carter and Ibrahim[11] and this study can be resolved by reconstruction of the binary phase diagram as presented in Fig. 38. This may be done by postulating the existence of a previously unreported compound of the formula $FeNa_2Si_2O_6$ (alternately

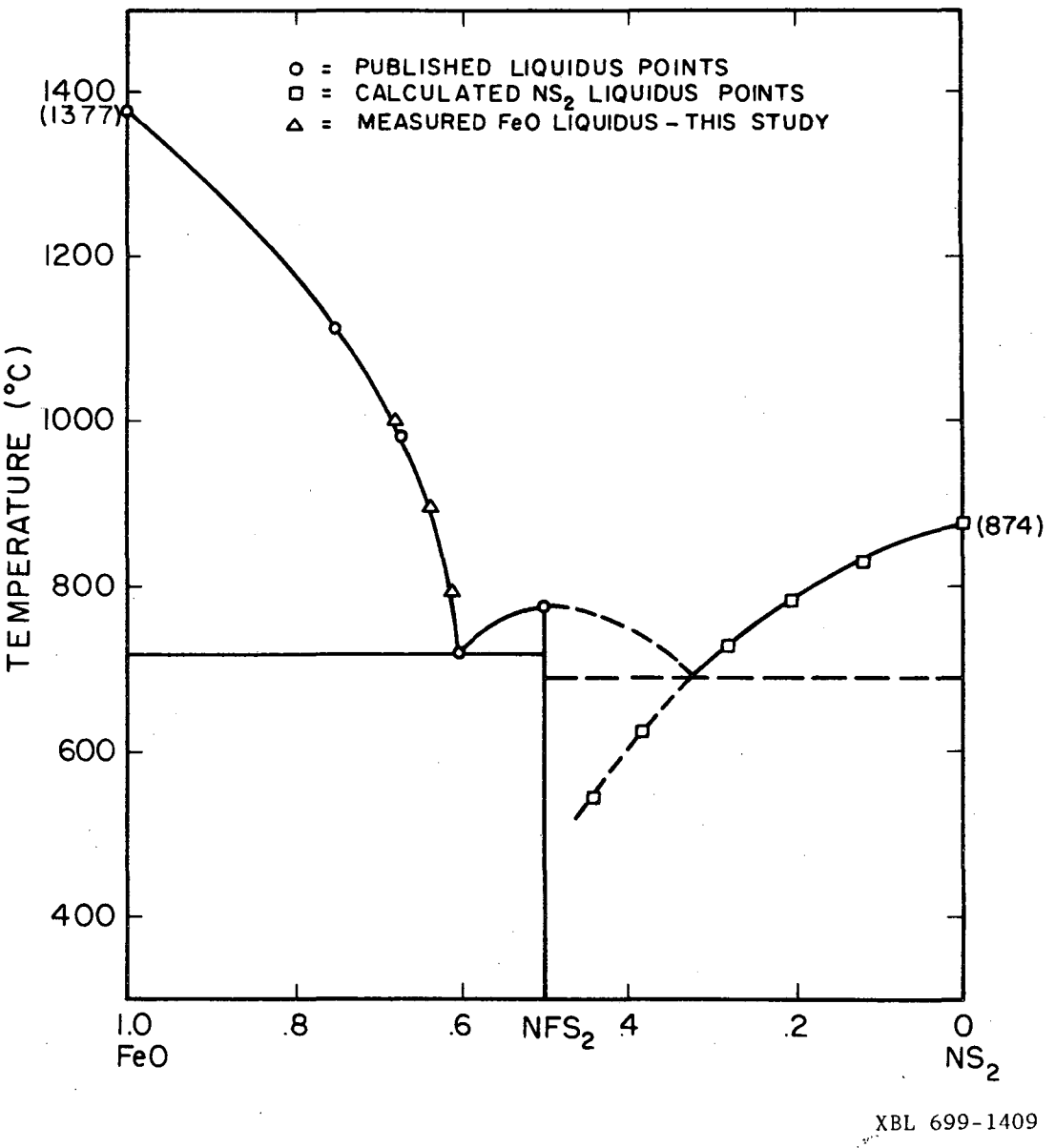

Figure 38. Proposed phase diagram of the FeO-NS_2 system incorporating the postulated compound NFS_2.

$FeO \cdot Na_2O \cdot 2SiO_2$), and concurrently suggesting that the experimental data of Ibrahim and Carter is too incomplete to warrant the construction of the binary diagram $FeO-NS_2$ as they have presented it.

They do not exclude this possibility in the text of their publication by saying on page 149 "...(Melts along the join $2FeO \cdot SiO_2-Na_2O \cdot 2SiO_2$) did not crystallize easily, and certain of them required three or four days' heat treatment before the initial crystals appeared..." On page 152 they report, "...Greatest difficulty was experienced in crystallizing compositions (along the $2FeO \cdot SiO_2-Na_2O \cdot 2SiO_2$ join) between 50 and 60 (weight) percent NS_2. (These compositions are slightly richer in iron than the postulated compound $FeO \cdot Na_2O \cdot 2SiO_2$). Thus only one or two crystals were seen after heating the 47/53 melt for one week at 610°C. The same specimen heated for 125 hours at 590°C developed (a fine structure) resembling a eutectic, although the (matrix) was glassy..." Further, on page 155 they state "...Melts (along the join $FeO \cdot SiO_2-Na_2O \cdot SiO_2$) containing 35 and more (weight) percent NS_2 were completely glassy after furnace cooling..." The postulated compound composition occurs at the 50/50 point along this join.

Although they present one experimental point for the liquidus at 50 mole percent FeO in the $FeO-NS_2$ binary, no other experimental points for definition of this curve are given. If one accepts the validity of this point on the assumption that they may have been incorrect in discerning the nature of the crystalline products resulting, it becomes easy to incorporate all their observations into the modified diagram in Fig. 14. It is not possible by these experiments to ascertain the liquidus between the 50 mole percent composition and the calculated NS_2

liquidus. A possible liquidus has been drawn in with dashed lines to illustrate the qualitative shape of the diagram. Schairer, Yoder and Keene[24] have also presented a preliminary ternary diagram for the system Na_2O-FeO-SiO_2, which differs from that of Ibrahim and Carter.[11] These diagrams are presented in Fig. 39. Schairer, et al.[24] have broken up the primary phase field of NS_2 into two divisions with a speculative eutectic (indicated by the dashed line) at approximately 16 weight percent FeO (N_{FeO}=0.324) on the FeO-NS_2 join. Assuming the eutectic as this composition, the results of this study indicate the eutectic temperature to be ∿685°C. Schairer et al.[24] show another eutectic at about 35 weight percent FeO (N_{FeO}=0.59) which corresponds to that of Ibrahim and Carter.[11] Between these points, they have suggested "several fields."

They have, however, indicated the 800°C isotherm intersecting the FeO-NS_2 join at approximately 14 weight percent FeO (N_{FeO}=0.30). This is not in agreement with either Ibrahim and Carter[11] (who establish the 800° liquidus point at 23 weight percent FeO), or this study (which fixes the 800° NS_2 liquidus point at approximately 8 weight percent).

Alternatively, a liquidus of the shape indicated in Fig. 14 may be explained by assuming that the FeO-NS_2 system is not a true binary (as stated by Ibrahim and Carter[11]). This would require that the join FeO-NS_2 extend across the primary phase field of some other compound (not NFS) in the FeO-Na_2O-SiO_2 ternary system. To do this, either the boundaries of the primary phase fields shown in the diagrams of Schairer et al.[24] and Ibrahim and Carter[11] must be reconstructed; or one must propose the existence of some compound other than NFS, whose primary phase field will encompass the region between the two eutectics in Fig. 14. Likely

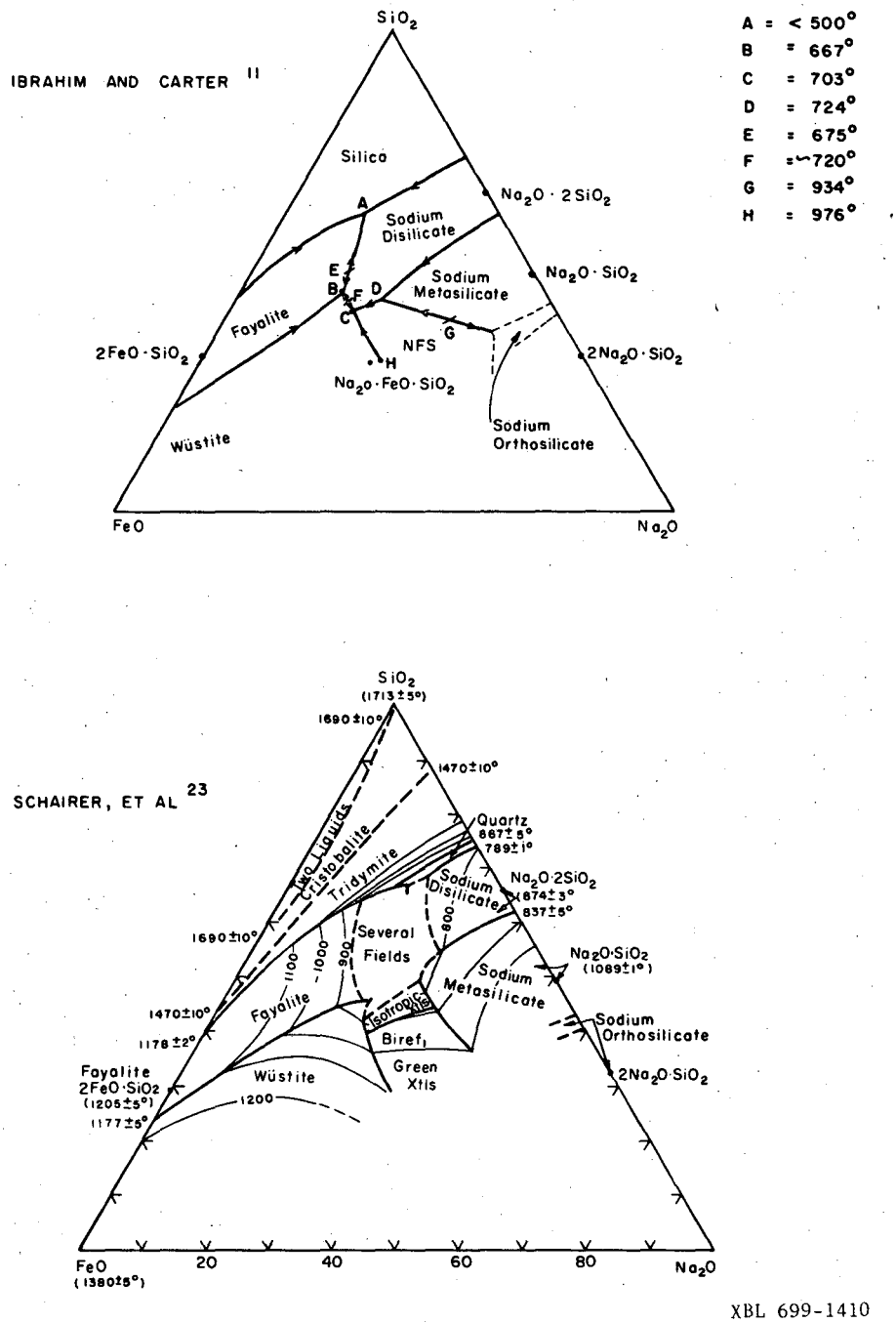

Figure 39. Two ternary diagrams for the FeO-Na_2O-SiO_2 system taken from published literature.

candidates are NFS_4, N_2FS_3, NFS_3 and/or NF_2S_3. None of these compounds have been identified, but would be found within the region designated "several fields" by Schairer et al.[24] Confirmation of this will have to await direct observation of these compounds.

The results of this investigation indicate the value and utility of thermodynamic studies in providing information about phase diagrams. It is a tool which can be used to particular advantage in glass systems which tend to supercool readily and crystallize slowly, thus circumventing the difficulties inherent in quenching techniques.

2. Structure

Any interpretation of the structure of molten silicates based solely upon thermodynamic studies must be made with great reservation. Bockris[25] has pointed out that thermodynamic properties do not give direct information on problems of structure, but rather act as an important check on structural theories derived from other data, such as electrical conductivity, viscosity, etc. Flood and Knapp[26] have developed models for the structure of borosilicate melts containing a single network modifying cation, based solely upon the thermodynamic properties of the pure components involved and the shapes of the liquidus curves. Such models are of limited applicability, and are not particularly definitive even for selected systems. In general, however, large negative deviations from ideality may be interpreted as a tendency toward complex ion formation by the individual components, and positive deviations indicate tendencies toward exsolution of the particular component. The extremely negative deviations found in the $FeO-NS_2$ system are then taken as evidence that FeO is readily incorporated into the structure of the solvent NS_2.

Additional evidence of structural changes in the glass may be seen from the variation of the entropy of mixing and the partial molar entropy of solution of the components. This study indicates that the $\overline{\Delta S}_{FeO}$ tends to a minimum at approximately $N_{FeO}=0.3$ and goes through a maximum at $N_{FeO}=0.5$. This is taken as a qualitative indication of a disordering process with respect to the distribution of FeO in the atomic lattice between $N_{FeO}=0.3$ and $N_{FeO}=0.5$. The partial molar entropy of NS_2 falls to zero at $N_{FeO}=0.5$. Since this is the composition of the proposed compound $FeO \cdot Na_2O \cdot 2SiO_2$, this might be interpreted as a partial ordering of the soda-silica lattice as would be necessary for nucleation of a crystalline phase. Richardson[27] has pointed out that liquid compounds are probably structurally similar to the solid phase, except that they are lacking in the long range order of the crystalline structure.

B. The System CoO-NS_2

1. Phase Relations

From the experimentally determined liquidus lines and the known melting points of CoO and NS_2, a simple eutectic phase diagram has been constructed in Fig. 27. There is no known published information on phase relations in either this pseudo-binary system or in the ternary system CoO-Na_2O-SiO_2. The solubility limits of CoO in NS_2 are, however, in qualitative agreement with interface compositions for CoO-NS_2 diffusion couples.[8] Because of the general chemical similarity between Fe^{2+} and Co^{2+} in silicate systems Co-silicates analagous to the postulated Fe-silicates may also exist in the system CoO-Na_2O-SiO_2. The displacement of the CoO and FeO liquiduses as functions of composition and

temperature indicate, however, that analagous compounds may have differing stabilities at high temperatures. For example, Figs. 14 and 27 suggest that $Na_2O \cdot FeO \cdot 2SiO_2$ may melt congruently, whereas $Na_2O \cdot CoO \cdot 2SiO_2$ (if it exists) may melt incongruently. This is speculation, and confirmation rests with further investigation of the phase relations in this system.

2. Structure

It may be seen from comparison of Figs. 5 and 19 that CoO exhibits strong negative deviations from ideality in the same manner as FeO in NS_2 solvent. Figures 9 and 23 further indicate practically parallel variation of the partial molar entropy of the metal oxide with composition up to the solubility limit of CoO. This suggests that CoO and FeO are isostructural on an atomic scale. The negative slope of the partial molar entropy curve of CoO and FeO is the result of a reduction in the available sites for distribution of the CoO and FeO within the NS_2 matrix as the oxides are added. As original sites are filled, however, the addition of oxygen increases the O/Si ratio above the initial 2.5, thus breaking down the atomic network structure by increasing the number of unshared oxygens. This structural disruption thus provides additional sites for incorporation of the metal oxide cations. The result of these two opposing factors--the filling of the matrix with oxide cations and the structural randomization resulting from an increasing O/Si ratio--is a minimum in each partial molar entropy curve for CoO and FeO.

C. $NiO-NS_2$

1. Phase Relations

As with CoO, there are no reported studies of phase relations in the systems $NiO-NS_2$ or $NiO-Na_2O-SiO_2$. The solubility data determined here enables one to construct a simple eutectic diagram as shown in Fig. 37. The NiO liquidus has been extended to the melting point of pure NiO, since no compounds other than the pure end members have been identified in this system. The eutectic determined from intersection of the liquidus lines occurs at $N_{NiO}=0.12$ at 830°C.

2. Structure

Due to the estimation of the heat of fusion of NiO at temperatures far below its melting point, it is not possible to obtain quantitative values of a^{**}_{NiO} from Eq. (34). The curves presented in Fig. 31 are therefore semiquantitative, based upon the assumption that the heat capacity of the solid NiO and the supercooled liquid NiO are equal--that is, the heat of fusion is constant at all temperatures. At temperatures far below the normal fusion temperature, the assumption may not be valid. For this reason, one cannot say with certainty that the a^{**}_{NiO} curves of Fig. 31 <u>really</u> extend above the Raoult's Law line, thus indicating a positive deviation from ideality. No interpretation of structure based on such a deviation can be made. Qualitatively, NiO appears to show less negative deviation than either CoO or FeO in NS_2 solution, indicating that it is not as readily incorporated into the glass structure, and probably has less tendency for form complex ionic species with the solvent than do either CoO or FeO. Further structural interpretation requires other non-thermodynamic data.

VI. SUMMARY

The solid electrolyte galvanic cell method has been adapted to the measurement of thermodynamic properties of FeO, CoO and NiO in sodium disilicate glass solutions over the temperature interval 700°-1100°C. Activities of these oxides (relative to the pure solid oxides) have been determined as a function of composition and temperature, and thus provide a more substantial basis for predicting and interpreting chemical reactions between these glasses and metals or other oxides. It may now be possible, for example, to relate the degree of wetting and chemical bond formation to the glass composition in a more general way than before these studies were carried out. Similarly, these data are fundamental in defining conditions under which metallic dendrites will form in glass-metal systems.

The oxides of iron, cobalt, and nickel all show negative deviations from Raoult's Law with iron being the most negative, and nickel the least. These are interpreted to mean that the oxides are incorporated readily into the glass structure, possibly forming complex ionic species with the silicate solvent. The partial molar entropies of solution for these oxides indicate that definite structural changes in the glass occur as the oxides are added--changes which manifest themselves in an increase in the number of atomic sites available to accommodate additional network modifying ions. This is in agreement with the Zachariason concept of glass structure based on O/Si ratios.

Calculation of a partial phase diagram for the pseudobinary system $FeO-NS_2$ indicates discrepancies between this study and published studies

of the $FeO-NS_2$ system. These discrepancies are resolved by the author by postulating the existence of one or more unreported compounds in the ternary system $FeO \cdot Na_2O \cdot 2SiO_2$. Such compounds have not been previously identified because of the difficulties involved in getting glasses of approximately that composition to crystallize within reasonable periods of time. It has been further speculated on structural grounds than analagous compounds in the system $CoO \cdot Na_2O \cdot 2SiO_2$ may also exist; but if so, probably have stabilities different from their FeO counterparts. Simple eutectic phase diagram for the $CoO-NS_2$ and $NiO-NS_2$ systems have been proposed, based upon limited data available from this study.

ACKNOWLEDGMENTS

The author wishes to express his appreciation to Dr. Prodyot Roy for his encouragement in the early stages of this investigation, and to Professors Leo Brewer, Ralph Hultgren and John Chipman for their advice. Special thanks to Professor Joseph A. Pask under whose direction this work was carried out.

I am also grateful to Kelly Radmilovic, Gloria Pelatowski, Rieda Officer, George Dahl, Bill Bullis and Dr. Bernard Evans for their technical assistance. Finally, I am especially indebted to my wife, Carolyn, for both her editorial and clerical assistance, and her prolonged moral support.

This work was carried out under the auspices of the U. S. Atomic Energy Commission.

BIBLIOGRAPHY

1. J. A. Pask and R. M. Fulrath, "Fundamentals of Glass to Metal Bonding: VIII, Nature of Wetting and Adherence," J. Am. Ceram. Soc. 45 (12) 592-96 (1962).

2. F. D. Gaidos and J. A. Pask, "Effect of Glass Composition on the Glass-Iron Interface," Advances in Glass Technology, pp. 548-65, (Plenum Press, New York, 1962).

3. M. P. Borom and J. A. Pask, "Reactions Between Metallic Iron and Cobalt Oxide-Bearing Sodium Disilicate Glass," J. Am. Ceram. Soc. 49 (1) 1-6 (1966).

4. M. P. Borom, J. A. Longwell, and J. A. Pask, "Role of 'Adherence Oxides' in the Development of Chemical Bonding at Glass-Metal Interfaces," J. Am. Ceram. Soc. 50 (2) 61-66 (1967).

5. I. A. Aksay, "Factors Controlling Wetting of MgO by Silicate Liquids," Lawrence Radiation Laboratory Report UCRL-18766 (M.S. Thesis) p. 19 (March 1969).

6. M. Humenick, Jr. and W. D. Kingery, "Metal-Ceramic Interactions: III, Surface Tension and Wettability of Metal-Ceramic Systems," J. Am. Ceram. Soc. 37 (1) 18-23 (1954).

7. M. P. Borom and J. A. Pask, "The Kinetics of the Dissolution and Diffusion of the Oxides of Iron in Sodium Disilicate Glass," J. Am. Ceram. Soc. 51 (9) 490-498 (1968)

8. A. M. Lacy - unpublished experimental results.

9. K. K. Kelley and E. G. King, U. S. Bureau of Mines Bulletin 592, "Contributions to the Data on Theoretical Metallurgy, XIV: Entropies of the Elements and Inorganic Compounds," (1961).

10. K. K. Kelley, U. S. Bureau of Mines Bulletin 584, "Contributions to the Data on Theoretical Metallurgy, XIII: High Temperature Heat Content, Heat Capacity, and Entropy Data for the Elements and Inorganic Compounds," (1960).

11. P. T. Carter and M. Ibrahim, "The Ternary System Na_2O-FeO-SiO_2," J. Soc. Glass Technol. 36 142-63 (1952).

12. A. P. Herring, "Electrochemical Determination of Activities in Sodium Oxide-Silica Melts," given at the 68th annual meeting of the Glass Division of the American Ceramic Society, Washington, D.C. (1966).

13. R. Didtshenko and E. G. Rochow, "Electrode Potentials in Molten Silicates," J. Am. Chem. Soc. 76 3291 (1954).

14. Esin and Lepinskikh, Izv. Akad. Nauk. S.S.S.R., Otd. Tekh. Nauk, 60 (1954); see - J. W. Tomlinson, "Electrochemical Measurements," Physicochemical Measurements at High Temperatures, Sec. 4, Ch. 11, p. 268.

15. K. K. Kiukolla and C. Wagner, "Measurements on Galvanic Cells Involving Solid Electrolytes," J. Electrochem. Soc. 104 (6) 379-87 (1957).

16. B. C. H. Steele, "High Temperature Thermodynamic Measurements Involving Solid Electrolyte Systems," in Electromotive Force Measurements in High Temperature Systems, Proceedings of a Symposium, Nuffield Research Group, Imperial College, London, April 13-14, 1967, pp. 3-27, edited by C. B. Alcock, American Elsever Publishing Company (1968).

17. Y. Matsushita and K. Goto, "The Application of Oxygen Concentration Cells with the Solid Electrolyte $ZrO_2 \cdot CaO$ to Thermodynamic Research, Thermodynamics, IAEA Symposium, Vienna, pp. 111-129, Vol. 1 (1965).

18. H. S. Ray, "Thermodynamic and Structural Properties of Silicate Melts," Ph.D. Thesis, University of Toronto (1967); see - Dissertation Abstracts 28 (4) 1544-B (October 1967).

19. G. G. Charette and S. N. Flengas, "Thermodynamic Properties of $PbO-SiO_2$ Slags by emf Measurements, Canadian Metallurgical Quarterly, 7 (4) 191-200 (1968).

20. F. D. Richardson and L. E. Webb,"Oxygen in Molten Lead and Thermodynamics of Lead Oxide-Silica Melts," Trans. Inst. Mining and Metallurgy, 64 529 (1955).

21. Elliot and M. Gleiser, Thermochemistry for Steelmaking, Vol. 1 (Addison-Wesley Publishing Co. Inc., New York), 1960.

22. H. S. Ray, "Electrochemical Measurements in Molten Oxides and the Role of Free Energy Data in Activity Calculations," Indian J. Chem. Vol. 6, 732-35 (1968).

23. J. Guiot - private communication.

24. J. F. Schairer, H. S. Yoder and A. G. Keene, Carnegie Inst. Washington, Yearbook, 53, 126 (1954); see - Phase Diagrams for Ceramists, 1969 Supplement, Fig. 2432, ed. by E. M. Levin, C. R. Robbins and H. F. McMurdie.

25. J. O'M. Bockris, general discussion, Disc. Faraday Soc., 4 p. 320 (1948).

26. W. J. Knapp and H. Flood, "Activities in Borosilicate Melts; I, Some Melts in the System $CaO-B_2O_3$," J. Am. Ceram. Soc., 40 (7) 246-49 (1957).

27. F. D. Richardson, "The Constitution and Thermodynamics of Liquid Slags," Disc. Farad. Soc., 4 p. 247 (1948).

Appendix A: Tabulation of thermodynamic data for the FeO-NS_2 system

N_{FeO}	a^{*}_{FeO}	$\ln a^{*}_{FeO}$	a^{**}_{FeO}	$\ln a^{**}_{FeO}$	N_{NS_2}	a_{NS_2}	$\ln a_{NS_2}$	$\overline{\Delta F}^{**}_{FeO}$	$\overline{\Delta F}^{*}_{FeO}$	$\overline{\Delta F}_{NS_2}$	ΔF^{*}_{mix}	ΔF^{**}_{mix}	γ^{**}_{FeO}
Temperature 800°C													
.121	.021	-3.863	.006	-5.093	.879	.866	-.1439	-10858	-8236	-307	-1266	-1583	.050
.127	.023	-3.772	.007	-5.002	.873	.858	-.1532	-10664	-8042	-327	-1307	-1639	.055
.208	.045	-3.101	.013	-4.331	.782	.747	-.2917	- 9233	-6611	-622	-1808	-2413	.063
.284	.075	-2.590	.022	-3.820	.716	.619	-.4797	- 8144	-5522	-1023	-2301	-3045	.077
.336	.115	-2.163	.034	-3.393	.664	.518	-.6578	- 7234	-4612	-1402	-2481	-3362	.101
.388	.180	-1.715	.053	-2.945	.612	.405	-.9039	- 6278	-3656	-1927	-2598	-3616	.137
.443	.280	-1.273	.082	-2.503	.557	.295	-1.2208	- 5336	-2714	-2602	-2652	-3814	.185
.491	.415	- .879	.121	-2.109	.509	.207	-1.5750	- 4496	-1874	-3358	-2629	-3917	.246
.528	.555	- .589	.162	-1.819	.472	.153	-1.8773	- 3878	-1256	-4002	-2552	-3979	.307
.568	.765	- .268	.223	-1.498	.432	.105	-2.2538	- 3193	- 571	-4805	-2400	-3890	.392
.603	1.000	0	.292	-1.230	.397	.070	-2.6593	- 2622	0	-5670	-2251	-3832	.484
Temperature 900°C													
.121	.020	-3.912	.008	-4.841	.879	.867	-.1427	-11283	-9118	- 333	-1396	-1658	.066
.127	.022	-3.817	.009	-4.746	.873	.859	-.1520	-11061	-8896	- 394	-1439	-1716	.071
.208	.044	-3.124	.017	-4.053	.792	.748	-.2904	- 9446	-7281	- 677	-2051	-2501	.082
.284	.075	-2.590	.030	-3.519	.716	.625	-.4700	- 8202	-6037	-1095	-2499	-3114	.106
.336	.108	-2.226	.043	-3.155	.664	.530	-.6349	- 7353	-5188	-1480	-2726	-3453	.128
.388	.160	-1.833	.063	-2.762	.612	.428	-.8486	- 6437	-4272	-1978	-2868	-3708	.162
.443	.235	-1.448	.093	-2.377	.550	.324	-1.1270	- 5540	-3375	-2627	-2958	-3899	.210
.491	.325	-1.124	.128	-2.053	.509	.240	-1.4271	- 4785	-2620	-3326	-2979	-4042	.261
.528	.427	- .851	.167	-1.780	.472	.178	-1.7260	- 4148	-1983	-4023	-2946	-4089	.316
.568	.577	- .550	.228	-1.479	.432	.124	-2.0875	- 3447	-1282	-4865	-2830	-4060	.401
.603	.750	- .288	.296	-1.217	.397	.085	-2.4651	- 2836	- 671	-5745	-2685	-3991	.491
.638	1.000	0	.395	-0.929	.362	.054	-2.9188	- 2165	0	-6803	-2463	-3844	.619

Note: a* refers to the solid st. state for FeO.
a** refers to the liquid st. state for FeO.
ΔF and ΔH data are listed in terms of cal/mole.
ΔS data is given in cal/mole °K.

Appendix A: Tabulation of thermodynamic data for the FeO-NS_2 system (continued)

N_{FeO}	a^{*}_{FeO}	$\ln a^{*}_{FeO}$	a^{**}_{FeO}	$\ln a^{**}_{FeO}$	N_{NS_2}	a_{NS_2}	$\ln a_{NS_2}$	$\overline{\Delta F}^{**}_{FeO}$	$\overline{\Delta F}^{*}_{FeO}$	$\overline{\Delta F}_{NS_2}$	ΔF^{*}_{Mix}	ΔF^{**}_{mix}	γ^{**}_{FeO}
Temperature 1000°C													
.121	.020	-3.912	.010	-4.587	.879	.867	- .1427	-9895	-11602	- 361	-1515	-1721	.083
.127	.022	-3.817	.011	-4.492	.873	.860	- .1508	-9655	- 1136	- 381	-1559	-1776	.087
.208	.043	-3.147	.022	-3.822	.792	.751	- .2864	-7960	- 9667	- 724	-2229	-2585	.106
.284	.076	-2.577	.039	-3.252	.716	.632	- .4589	-6518	- 8225	-1161	-2682	-3167	.137
.336	.105	-2.254	.053	-2.929	.664	.542	- .6125	-5701	- 7408	-1549	-2944	-3518	.158
.388	.144	-1.938	.073	-2.613	.612	.449	- .8007	-4902	- 6609	-2025	-3141	-3804	.188
.443	.201	-1.604	.102	-2.279	.557	.349	-1.0527	-4057	- 5764	-2663	-3281	-4037	.230
.491	.271	-1.306	.138	-1.981	.509	.765	-1.3280	-3303	- 5010	-3359	-3332	-4170	.281
.528	.350	-1.050	.178	-1.725	.472	.204	-1.5896	-2656	- 4363	-4021	-3300	-4202	.337
.568	.465	- .766	.237	-1.441	.432	.144	-1.9379	-1937	- 3644	-4902	-3218	-4188	.417
.603	.585	- .536	.298	-1.211	.397	.101	-2.2926	-1356	- 3063	-5799	-3120	-4149	.494
.683	1.000	0	.509	- .675	.317	.039	-3.2442	0	- 1707	-8206	-2601	-3767	.745

$\overline{S}^{*}_{FeO}$	$\overline{S}^{**}_{FeO}$	$\overline{S}_{NS_2}$	$\overline{H}^{*}_{FeO}$	$\overline{H}^{**}_{FeO}$	$\overline{H}_{NS_2}$	S^{*}_{mix}	S^{**}_{mix}	H^{*}_{mix}	H^{**}_{mix}
7.40	2.86	.40	-403	-7893	+ 135	1.25	.70	75	- 836
7.25	2.71	.40	-360	-7850	+ 115	1.27	.69	55	- 897
5.95	1.41	.52	-305	-7795	- 64	1.81	.71	74	-1672
5.65	1.11	.55	603	-6887	- 448	2.00	.71	-155	-2277
5.70	1.16	.61	1519	-5971	- 761	2.32	.79	8	-2512
6.00	1.46	.61	2761	-4729	-1261	2.70	.94	299	-2610
6.50	1.96	.49	4243	-3247	-2056	3.15	1.14	728	-2584
7.00	2.46	.12	5612	-1878	-3206	3.50	1.27	1126	-2554
7.15	2.61	-.05	6422	-1068	-4074	3.75	1.40	1472	-2487
7.0	2.46	.29	6948	- 542	-4517	4.10	1.52	1999	-2259
6.50	1.96	1.08	6949	- 541	-4417	4.35	1.61	2416	-2080

Appendix B: Tabulation of thermodynamic data for the CoO-NS_2 system

N_{CoO}	a^{*}_{CoO}	$\ln a^{*}_{CoO}$	a^{**}_{CoO}	$\ln a^{**}_{CoO}$	N_{NS_2}	a_{NS_2}	$\ln a_{NS_2}$	$\overline{\Delta F^{*}}_{CoO}$	$\overline{\Delta F^{**}}_{CoO}$	ΔF_{NS_2}	ΔF^{*}_{mix}	ΔF^{**}_{mix}	γ^{**}_{CoO}
Temperature 800°C													
.054	.020	-3.912	.002	-6.053	.946	.945	- .0566	-8340	-12904	- 121	- 565	- 811	.037
.120	.056	-2.882	.007	-5.023	.880	.855	- .157	-6144	-10708	- 334	-1032	-1579	.058
.182	.120	-2.120	.014	-4.261	.818	.760	- .274	-4519	- 9083	- 584	-1300	-2131	.077
.221	.170	-1.772	.020	-3.913	.779	.690	- .371	-3778	- 8342	- 791	-1451	-2460	.090
.277	.255	-1.366	.030	-3.502	.723	.590	- .528	-2912	- 7476	-1126	-1621	-2885	.108
.321	.345	-1.064	.041	-3.205	.679	.515	- .664	-2268	- 6832	-1416	-1689	-3155	.128
.367	.485	- .724	.057	-2.865	.633	.425	- .854	-1543	- 6107	-1821	-1722	-3394	.155
.407	.715	- .335	.084	-2.476	.593	.340	-1.074	- 714	- 5278	-2290	-1655	-3506	.206
.437	1.000	0	.118	-2.141	.563	.280	-1.273	0	- 4564	-2714	-1528	-3522	.270
Temperature 900°C													
.054	.020	-3.912	.003	-5.677	.946	.945	-.0566	-9119	-13233	- 131	- 617	- 839	.056
.120	.056	-2.882	.010	-4.647	.880	.862	-.149	-6718	-10832	- 347	-1112	-1605	.083
.182	.115	-2.163	.020	-3.928	.818	.772	-.259	-5042	- 9156	- 604	-1411	-2160	.110
.221	.160	-1.833	.027	-3.598	.779	.710	-.342	-4389	- 8503	- 797	-1565	-2500	.122
.277	.240	-1.427	.041	-3.192	.723	.610	-.404	-3326	- 7440	-1152	-1754	-2894	.148
.321	.325	-1.124	.056	-2.889	.679	.530	-.635	-2620	- 6734	-1480	-1846	-3167	.175
.367	.440	- .821	.075	-2.586	.633	.447	-.805	-1914	- 6028	-1876	-1890	-3400	.204
.407	.590	- .528	.101	-2.293	.593	.370	-.994	-1231	- 5345	-2317	-1875	-3549	.248
.454	.885	- .122	.151	-1.887	.546	.270	-1.309	- 284	- 4398	-3051	-1795	-3663	.333
.462	1.000	0	.171	-1.765	.538	.252	-1.378	0	- 4114	-3212	-1728	-3628	.370

Note: a* refers to the solid st. state for CoO.
a** refers to the liquid st. state for CoO.
ΔF and ΔH data are listed in terms of cal/mole.
ΔS data is given in cal/mole °K.

Appendix B: Tabulation of thermodynamic data for the CoO-NS_2 system (continued)

N_{CoO}	a^{*}_{CoO}	$\ln a^{*}_{CoO}$	a^{**}_{CoO}	$\ln a^{**}_{CoO}$	N_{NS_2}	a_{NS_2}	$\ln a_{NS_2}$	$\overline{\Delta F}^{*}_{CoO}$	$\overline{\Delta F}^{**}_{CoO}$	F_{NS_2}	ΔF^{*}_{mix}	ΔF^{**}_{mix}	γ^{**}_{FeO}
Temperature 1000°C													
.054	.020	-3.912	.005	-5.356	.946	.946	- .0555	- 9893	-13545	- 140	- 667	- 864	.093
.120	.056	-2.882	.013	-4.326	.880	.870	- .139	- 7289	-10941	- 352	-1184	-1623	.108
.182	.110	-2.207	.026	-3.651	.818	.780	- .248	- 5582	- 9234	- 627	-1529	-2193	.143
.221	.155	-1.864	.037	-3.308	.779	.720	- .329	- 4714	- 8366	- 832	-1690	-2497	.167
.277	.225	-1.492	.053	-2.936	.723	.630	- .462	- 3773	- 7425	-1168	-1890	-2901	.191
.321	.290	-1.238	.068	-2.682	.679	.555	- .589	- 3131	- 6783	-1490	-2016	-3189	.212
.367	.390	- .942	.092	-2.386	.633	.470	- .755	- 2382	- 6034	-1909	-2083	-3423	.251
.407	.505	- .683	.119	-2.127	.593	.396	- .926	- 1727	- 5379	-2342	-2092	-3578	.292
.454	.730	- .315	.172	-1.759	.546	.310	-1.171	- 797	- 4449	-2961	-1979	-3637	.379
.488	1.000	0	.236	-1.444	.512	.235	-1.448	0	- 3652	-3662	-1875	-3657	.484
Temperature 1100°C													
.054	.020	-3.912	.006	-5.084	.946	.946	- .0555	-10673	-13870	- 151	- 720	- 892	.111
.120	.056	-2.882	.017	-3.054	.880	.880	- .128	- 7863	-11063	- 349	-1251	-1634	.142
.182	.107	-2.235	.033	-3.407	.818	.790	- .236	- 6097	- 9294	- 644	-1636	-2218	.181
.221	.147	-1.917	.046	-3.089	.779	.730	- .315	- 5230	- 8427	- 859	-1825	-2532	.208
.277	.210	-1.561	.065	-2.733	.723	.645	- .439	- 4259	- 7456	-1198	-2045	-2932	.235
.321	.270	-1.309	.084	-2.481	.679	.573	- .557	- 3571	- 6768	-1520	-2178	-3205	.262
.367	.355	-1.036	.110	-2.208	.633	.400	- .713	- 2826	- 6023	-1945	-2263	-3442	.300
.407	.460	- .777	.143	-1.949	.593	.425	- .856	- 2120	- 5317	-2335	-2247	-3549	.351
.454	.625	- .470	.194	-1.642	.546	.340	-1.079	- 1282	- 4479	-2944	-2189	-3640	.427
.517	1.000	0	.310	-1.172	.483	.215	-1.537	0	- 3197	-4193	-2025	-3678	.600

Appendix B: Tabulation of thermodynamic data for the CoO-NS_2 system (continued)

N_{CoO}	N_{NS_2}	$\overline{\Delta S}^{*}_{CoO}$	$\overline{\Delta S}^{**}_{CoO}$	$\overline{\Delta S}_{NS_2}$	$\overline{\Delta H}^{*}_{CoO}$	$\overline{\Delta H}^{**}_{CoO}$	$\overline{\Delta H}_{NS_2}$	ΔS^{*}_{mix}	ΔS^{**}_{mix}	ΔH^{*}_{mix}	ΔH^{**}_{mix}
.054	.946	7.83	+3.31	.05	95	-9339	- 75	.40	.23	-144	- 575
.120	.880	5.80	+1.26	.14	90	-9344	- 174	.82	.27	-142	-1274
.182	.818	4.72	+ .18	.32	463	-8971	- 224	1.12	.29	- 99	-1816
.221	.779	4.33	- .21	.41	768	-8666	- 318	1.28	.27	- 68	-2163
.277	.723	4.05	- .49	.52	1386	-8066	- 525	1.50	.24	+ 7	-2614
.321	.679	4.05	- .49	.53	2056	-7378	- 828	1.66	.20	97	-2931
.367	.633	4.18	- .36	.48	2848	-6586	-1301	1.81	.17	233	-3241
.407	.593	4.40	- .14	.36	3689	-5745	-1881	1.92	.16	381	-3454
.437	.563	4.70	+ .16	.10	5157	-4277	-2796	2.00	.13	573	-3443

Appendix C: Tabulation of thermodynamic data for the NiO-NS_2 system

N_{NiO}	a^{*}_{NiO}	$\ln a^{*}_{NiO}$	a^{**}_{NiO}	$\ln a^{**}_{NiO}$	N_{NS_2}	aNS_2	$\ln a_{NS_2}$	$\overline{\Delta F}^{*}_{NiO}$	$\overline{\Delta F}^{**}_{NiO}$	$\overline{\Delta F}_{NS_2}$	ΔF^{*}_{mix}	ΔF^{**}_{mix}	γ^{**}_{NiO}
Temperature 800°C													
.015	.170	-1.772	.015	-4.255	.985	.985	-0.0111	-3778	-9072	- 32	- 88	-168	1.000
.027	.265	-1.328	.023	-3.811	.977	.977	-0.0233	-2831	-8125	- 50	-125	-268	.852
.053	.445	-0.810	.039	-3.293	.955	.955	-0.0460	-1727	-7021	- 98	-184	-465	.736
.076	.630	-0.462	.055	-2.945	.930	.930	-0.0726	- 984	-6278	-155	-218	-620	.724
.099	.860	-0.151	.075	-2.634	.897	.897	-0.1087	- 322	-5616	-232	-240	-765	.758
.109	1.000	0	.087	-2.483	.882	.882	-0.1256	0	-5294	-268	-239	-816	.798
Temperature 900°C													
.015	.110	-2.207	.014	-4.282	.985	.985	-0.0151	-5145	-9981	- 35	-112	-184	.933
.027	.170	-1.772	.021	-3.847	.973	.977	-0.0233	-4131	-8967	- 54	-164	-295	.778
.053	.290	-1.238	.036	-3.313	.947	.955	-0.0460	-2886	-7722	-107	-254	-511	.679
.076	.422	-0.863	.053	-2.938	.924	.930	-0.0726	-2011	-6847	-169	-309	-677	.697
.099	.590	-0.528	.074	-2.603	.901	.897	-0.1087	-1231	-6067	-253	-350	-829	.747
.109	.680	-0.386	.085	-2.461	.891	.882	-0.1256	- 900	-5736	-293	-359	-886	.780
.116	.740	-0.301	.092	-2.376	.884	.870	-0.1393	- 701	-5537	-325	-368	-930	.793
.127	.855	-0.157	.107	-2.232	.873	.850	-0.1625	- 366	-5202	-378	-376	-991	.843
.139	1.000	0	.125	-2.075	.861	.830	-0.1863	0	-4836	-428	-369	-1041	.899
Temperature 1000°C													
.015	.075	-2.590	.013	-4.321	.988	.985	-0.0151	-6550	-10928	- 38	-136	-201	.867
.027	.115	-2.163	.020	-3.894	.973	.977	-0.0233	-5470	-9849	- 59	-205	-323	.741
.053	.200	-1.609	.035	-3.340	.947	.955	-0.0460	-4069	-8447	-116	-326	-558	.660
.076	.307	-1.181	.054	-2.912	.924	.930	-0.0726	-2987	-7365	-184	-397	-730	.710
.099	.430	-0.844	.076	-2.575	.801	.897	-0.1087	-2134	-6512	-275	-459	-892	.768
.109	.500	-0.693	.089	-2.424	.891	.882	-0.1256	-1753	-6131	-318	-474	-952	.817
.116	.540	-0.616	.096	-2.347	.884	.870	-0.1393	-1558	-5936	-352	-492	-1000	.827
.127	.620	-0.478	.110	-2.209	.873	.850	-0.1625	-1209	-5587	-411	-512	-1068	.866
.149	.795	-0.229	.141	-1.960	.851	.820	-0.1985	- 579	-4957	-471	-530	-1139	.946
.170	1.000	0	.177	-1.731	.830	.770	-0.1863	0	-4378	-471	-550	-1200	1.041

Note: a* refers to the solid st. state for NiO.
a** refers to the liquid st. state for NiO.
ΔF and ΔH data are listed in terms of cal/mole.
ΔS data is given in cal/mole °K.

Appendix C: Tabulation of thermodynamic data for the NiO-NS_2 system (continued)

N_{NiO}	a_{NiO}	$\ln a^{*}_{NiO}$	a^{**}_{NiO}	$\ln a^{**}_{NiO}$	N_{NS_2}	a_{NS_2}	$\ln a_{NS_2}$	$\overline{\Delta F}^{*}_{NiO}$	$\overline{\Delta F}^{**}_{NiO}$	$\overline{\Delta F}_{NS_2}$	ΔF^{*}_{mix}	ΔF^{**}_{mix}	γ^{**}_{NiO}
Temperature 1100°C													
.015	.050	-2.996	.012	-4.438	.985	.985	-0.0151	-8173	-12107	- 41	-163	- 222	.800
.027	.080	-2.526	.019	-3.968	.973	.977	-0.0233	-6891	-10825	- 64	-248	- 355	.704
.053	.140	-1.966	.033	-3.408	.947	.955	-0.0460	-5363	- 9297	-125	-403	- 611	.623
.076	.215	-1.537	.051	-2.979	.924	.930	-0.0726	-4193	- 8127	-198	-502	- 801	.671
.099	.320	-1.139	.076	-2.581	.901	.897	-0.1087	-3107	- 7041	-297	-575	- 965	.768
.109	.375	-0.981	.089	-2.423	.891	.882	-0.1256	-2676	- 6610	-343	-597	-1026	.817
.116	.415	-0.879	.098	-2.321	.884	.870	-0.1393	-2398	- 6332	-380	-614	-1070	.845
.127	.480	-0.734	.113	-2.176	.873	.850	-0.1625	-2002	- 5936	-443	-641	-1141	.890
.149	.620	-0.478	.146	-1.920	.851	.830	-0.1863	-1304	- 5238	-508	-680	-1213	.980
.200	1.000	0	.236	-1.442	.800			0	3934		-700	-1320	1.180

N_{NiO}	N_{NS_2}	$\overline{\Delta S}^{*}_{NiO}$	$\overline{\Delta S}^{**}_{NiO}$	ΔS_{NS_2}	$\overline{\Delta H}^{*}_{NiO}$	$\overline{\Delta H}^{**}_{NiO}$	ΔH_{NS_2}	$\overline{\Delta S}^{*}_{mix}$	$\overline{\Delta S}^{**}_{mix}$	ΔH^{*}_{mix}	ΔH^{**}_{mix}
.015	.985	15.2	10.7	.03	12678	2517	-9	.25	.19	181	29
.027	.973	13.3	8.8	.05	11218	1057	16	.41	.29	319	44
.053	.947	10.8	6.3	.17	9697	-464	113	.73	.49	621	82
.076	.924	9.7	5.2	.23	9319	-842	163	.95	.61	859	87
.099	.901	9.0	4.5	.22	9305	-856	105	1.17	.64	1016	10
.109	.891	8.8	4.3	.25	9430	-731	108	1.24	.69	1124	17
.116	.884	8.5	4.0	.29	9282	-879	82	1.24	.72	1149	-30
.127	.873	8.2	3.7	.32	9290	-871	48	1.32	.75	1222	-69

Appendix D: Comparison of values obtained for the activity of pure solid NS_2 relative to the supercooled liquid standard state when (1) the free energy of fusion is known for all temperatures below the normal melting point and (2) when the heat of fusion is assumed invariant with temperature.

Kelley[10] has given heat capacity data for both the crystalline solid sodium disilicate and the supercooled liquid. By integration of the expression for the heat capacity change for the reaction

$$NS_2(\text{supercooled liquid}) = NS_2(\text{solid}) \qquad (44b)$$

according to Eq. (33), and taking the heat of fusion of NS_2 as 8500 cal/mole at 1147°K, one obtains the following expression for the free energy of reaction (44b)

$$\Delta F = 11.47T\ln T - 8.23\times10^{-3}T^2 - 4.515\times10^{5}T^{-1} - 81.234T + 11696$$

From the expression

$$\Delta F = RT \ln \frac{a_{NS_2(\text{solid})}}{a_{NS_2(\text{liquid})} \equiv 1} \qquad (33)$$

the activity of the solid NS_2 may be readily calculated.

In the event that free energy data are not available for the solid and supercooled liquid states, Eq. (34) may be used to estimate the activity of the solid referred to the pure supercooled liquid standard state. Following is a table listing the activity values calculated

for solid NS_2 by the methods of Eq. (33) and Eq. (34).

Temperature (°C)	Calculated a_{NS_2}(solid) - Eq.(33)	Estimated a_{NS_2}(solid) - Eq.(34)
800	0.245	0.200
900	0.398	0.358
1000	0.597	0.578
1100	0.854	0.853

Appendix E: Calculation of the maximum activity of "FeO" stable in a 10:1 CO/CO_2 atmosphere at 1000°C

Consider the reaction:

$$Fe + CO_2 = CO + FeO \qquad (55)$$

At 1000°C (from the tables of Elliott and Gleiser)

$$\Delta F^\circ_{CO} = -53676 \text{ cal/mole}$$

$$\Delta F^\circ_{CO_2} = -94687 \text{ cal/mole}$$

$$\Delta F^\circ_{"FeO"} = -43156 \text{ cal/mole}$$

Therefore, $\Delta F^\circ_{reaction} = -2145$ cal/mole. If

$$\Delta F = \Delta F^\circ + RT(2.303)\log \frac{P_{CO} \cdot a_{"FeO"}}{P_{CO_2}}$$

and at equilibrium $\Delta F = 0$, then we may write

$$0 = -2145 + 1.987(1273)(2.303)\log 10 \cdot a_{"FeO"}.$$

Solving for $a_{"FeO"}$,

$$\log a_{"FeO"} = 0.3682 - 1 = -0.6318$$

and

$$a_{\text{"FeO"}} = 0.233$$

An activity of "FeO" larger than 0.233 under these environmental conditions will result in the reaction (55) to proceed to the left as written above, and FeO will decompose in a glass, precipitating metallic Fe.

Appendix F: Estimation of free energies, enthalpies, and entropies of fusion of NiO, CoO, and $Fe._{950}$ at temperatures below their melting points; and estimation of the activity of the pure solid oxide relative to the supercooled liquid (K). (See Eq. (33) and (34).)

T_f = 1650°K (1377°C)

$Fe._{95}O$ ---------- ΔH_f (at 1650°K) = 7490 cal/mole

ΔS_f = 4.54 e.u.

T(°C)	T(°K)	ΔF_f(cal/mole)	K
800	1073	-2622	.292
900	1173	-2165	.395
1000	1273	-1707	.509

T_f = 2078°K (1805°C)

CoO ---------- $\Delta H_f \cong 4.54(2078)$ = 9434 cal/mole

T(°C)	T(°K)	ΔF_f(cal/mole)	K
800	1073	-4564	.118
900	1173	-4114	.171
1000	1273	-3652	.236
1100	1373	-3197	.310

T_f = 2238°K (1965°C)

NiO ---------- $\Delta H_f \cong 4.54(2238)$ = 10161 cal/mole

T(°C)	T(°K)	ΔF_f(cal/mole)	K
800	1073	-5294	.087
900	1173	-4836	.125
1000	1273	-4378	.177
1100	1373	-3934	.236

Appendix G: Conversions of oxide weight percent values to mole fraction

Gram Formula Weights: NiO = 74.71
CoO = 74.933
"FeO" = $Fe_{.95}O$ = 69.055
$Na_2Si_2O_5$ = 182.152

Weight % NiO	N_{NiO}	Weight % CoO	N_{CoO}	Weight % "FeO"	$N_{"FeO"}$
0.62	.015	2.30	.054	4.95	.121
1.00	.024	5.00	.113	5.00	.122
1.14	.027	5.30	.120	5.24	.127
2.00	.047	8.40	.182	9.07	.208
2.23	.053	10.00	.213	10.00	.227
3.00	.070	10.59	.221	13.09	.284
3.20	.076	13.62	.277	15.00	.318
4.00	.092	15.00	.300	16.11	.336
4.30	.099	16.26	.321	19.36	.388
4.77	.109	19.23	.367	20.00	.397
5.00	.114	20.00	.378	23.18	.443
5.11	.116	22.03	.407	25.00	.468
5.66	.127	25.00	.447	26.74	.491
6.00	.135	25.52	.454	29.80	.528
6.70	.149	30.00	.510	30.00	.531
7.00	.155	35.00	.567	33.29	.568
8.00	.175			35.00	.587
9.00	.194			36.55	.603
10.00	.213			40.00	.637
				45.00	.683
				50.00	.725

LEGAL NOTICE

This report was prepared as an account of Government sponsored work. Neither the United States, nor the Commission, nor any person acting on behalf of the Commission:

A. Makes any warranty or representation, expressed or implied, with respect to the accuracy, completeness, or usefulness of the information contained in this report, or that the use of any information, apparatus, method, or process disclosed in this report may not infringe privately owned rights; or

B. Assumes any liabilities with respect to the use of, or for damages resulting from the use of any information, apparatus, method, or process disclosed in this report.

As used in the above, "person acting on behalf of the Commission" includes any employee or contractor of the Commission, or employee of such contractor, to the extent that such employee or contractor of the Commission, or employee of such contractor prepares, disseminates, or provides access to, any information pursuant to his employment or contract with the Commission, or his employment with such contractor.

TECHNICAL INFORMATION DIVISION
LAWRENCE RADIATION LABORATORY
UNIVERSITY OF CALIFORNIA
BERKELEY, CALIFORNIA 94720